Solar Radiation and Artificial Lighting of Controlled Environments with Particular Emphasis on Tomatoes

Craig Bredvold

Miscellaneous Publication 14—1982
Agricultural Experiment Station
University of Minnesota

The University of Minnesota Agricultural Experiment Station paid for the production of this publication. As a miscellaneous publication, it is intended for a very limited audience. Initial distribution was made by the University of Minnesota Department of Agricultural and Applied Economics. Copies of this publication are available from the Department of Agricultural and Applied Economics, 231 Classroom Office Building, University of Minnesota, 1994 Buford Avenue, St. Paul, MN 55108 until the original printing is exhausted.

SOLAR RADIATION AND ARTIFICIAL LIGHTING OF CONTROLLED ENVIRONMENTS WITH PARTICULAR EMPHASIS ON TOMATOES

by
Craig Bredvold

Miscellaneous Publication 14---1982
Agricultural Experiment Station
University of Minnesota

TABLE OF CONTENTS

LIST OF FIGURES

Chapter 1

ARTIFICIAL LIGHTING IN CONTROLLED ENVIRONMENTS

The effects of light (i.e., photosynthetically or physiologically active radiation, hereafter referred to as PAR) as an environmental growth factor for plants is a subject of substantial research interest (see references 5, 9, 61 et al.), but is in its infancy as far as understanding is concerned. A companion Minnesota station study (University of Minnesota Technical Bulletin 326) of a controlled environment vegetable operation shows that variations in photosynthetically active radiation (PAR) cause wide annual yield variations in tomatoes (8). This paper examines solar radiation and artificial lighting for a single controlled environment vegetable firm, hereinafter referred to by the acronym "CEVCO."1/

Evaluation of the use of artificial lighting for controlled environment tomato production requires the consideration of several factors. First, the effects of uncontrolled variables such as quality and quantity of light make the measurement of absolute radiation energy difficult.2/ Second, the extrapolation of phytotron results to plant responses in the external environment is of doubtful accuracy. The estimation of the total cost of supplying an equivalent quantity of radiant energy artificially to generate a measured yield observed under natural solar conditions ignores vital questions of light quality, duration, cycling, and chopping (very short bursts of irradiation and darkness often referred to as sunflecks) differences, which may significantly affect yields. Third, optimum utilization of artificial lighting demands that other environmental factors of less significant cost be optimized to prevent them from limiting production under high lighting intensities. Carbon dioxide (CO_2) and temperature optimization should be possible at little additional expense, but relative humidity (RH) control may be more difficult. Fourth, the question of optimum irradiation distribution within the plant canopy (not considered here) is important. (For some excellent references: 41, 23, 47, 64, 54, 55, 2.) It should be noted that most plants are "under-engineered" for PAR utilization and "over-engineered" for CO_2 utilization at existing natural levels. This implies that cost savings for artificial lighting may occur if the application of artificial light within the crop canopy is optimized over the normal application of sunlight from above the crop. Further, for the wavelength spectrum of light utilized by most higher plants, the light rays within a leaf are almost isotropic (i.e., perfectly diffuse) so the chloroplasts receive a much lower level of radiation energy than that received by the leaf epidermis. Consequently, the photosynthetic systems of many higher plants are not saturated at the levels at which lower plants such as unicellular algae become saturated (41, p. 65), therefore, such comparisons are suspect. Fifth, the effects of different light frequencies upon plant responses vary significantly. Finally, normally the only difficulty with excessive irradiation is the effects of temperature excesses upon fruit quality and plant tissues. Shading and/or misting of crops is frequently done to alleviate this problem.

Notes to Chapter 1

1/ CEVCO produces tomatoes and European cucumbers year round near St. Paul, Minnesota. Reference 8 provides a thorough examination of CEVCO, its houses (standard Hydroculture design), and the economics of its tomato production.

2/ "Many of the published articles...on light studies do not mean a great deal because of the uncontrolled variables--quality and quantity of light, as well as the lack of proper techniques in measuring absolute radiant energy. There have been very few studies conducted on the effects of varying

light intensities and qualities solely on mature plants in their reproductive stages, after they have been grown vegetatively under uniform conditions" (51, p. 1). Much of the current research on artificial lighting of commercial crops is occurring in private industry; the conclusions reached are frequently unavailable to the public.

Chapter 2

PAR AND BASIC PLANT RESPONSES TO RADIANT ENERGY

PAR (also PAI or PhAR), physiologically (including photosynthetically) active radiation (or irradiation), is the irradiation of plants at wavelengths which induce physiological responses. PAR, to date, has not been precisely defined because the exact responses of plants to different wavelengths of radiant energy are not fully known. To define PAR precisely will require radiant energy to be defined in terms of (5, p. 46): the spectral response of the photoreceptor in the effective wavelengths' bands; the flux density received from a radiator in the effective wavelengths' bands; the concentration of the photoreceptors; and the effective irradiance for threshold, optimum, and saturation responses of the photoreceptor.

Figure 1 and Table 1 indicate the known principal photochemical reactions of plants and their related significant wavelength bands. "For practical purposes, the energy content of photosynthetically useful radiation can be taken as one-half the radiative energy recorded with a conventional solarimeter" (41, p. 25; 6, p. 235). The plant radiant energy response band is generally considered to cover 290 nm to 850 nm, although the primary plant functions depend mainly on the narrower band of 380 nm to 780 nm. Suggestions have been made to break the PAR wavelengths into several bands based upon their significance to plant functions, but no standards have been established yet.

Table 1. Principal photochemical reactions of higher plants

Photoprocess	Reaction or Response	Products Energy Conversion	Photoreceptors	Action Spectra Peaks, nm	Approx. Wavelength Band-nm
Chlorophyll synthesis	Reduction of protochlorophyll	Chlorophyll a Chlorophyll b	Protochlorophyll	Blue:445 Red:650	350-470 570-670
Photosynthesis	Dissociation of H_2O into 2(H) and $\frac{1}{2}O_2$ and reduction of (CO_2)	Reductant (H) Phosphorylated compounds	Chlorophylls Carotenoids	Blue:435 Red:675	350-530 600-700
	Enhancement	Phosphorylated compounds	Chlorophylls	Red:650 Far-red:710	630-690 690-730
		Regulation of Growth			
Blue reactions	1 Phototropism 2 Protoplasmic viscosity 3 Photoreactivation	Oxidized auxin, auxin system and/or other components of the cell	1 Carotenoid and/or flavin 2 Unknown 3 Pyridine nucleotide, riboflavin, etc.	1 Near UV:370 Blue:445 & 475 2 Uncertain 3 Uncertain	350-500
Red, far-red reactions	1 Seed germination 2 Seedling and vegetative growth 3 Anthocyanin synthesis 4 Chloroplast responses 5 Heterotrophic growth 6 Photoperiodism 7 Chromosome response	Biochemistry unknown	1-6 Phytochrome	1-6 Induction by red:660; reversal by far-red:710 & 730 7 Far-red induced, red reversed, spectral details uncertain	570-700 680-780

Source: 69, p. 448

Considerable difficulty exists in the analysis of plant radiant energy because most of the terms and standards have been established in relation to visual perception, not PAR. In 1924, the International Commission on Illumination established the response of a typical light-adapted eye. As a consequence, most radiant energy measuring devices and units of illumination are weighted to the distribution shown in Figure 2, where 555 nm arbitrarily equals 1. However, such a response curve does not represent plant response curves to irradiation (Figure 1), therefore, units of illumination such as footcandles, lumens, and candles are not appropriate measures of PAR. It is unfortunate so many scientific studies of plant irradiance have been reported in terms of illumination rather than radiant energy.

Radiant energy is known to affect photosynthesis, chlorophyll synthesis, chloroplast formation, anthocyanin synthesis, seed germination, seedling and vegetative growth, flowering, phototropism, protoplasmic viscosity, photoperiodism, and biological "clocks" (Table 1). The evaluation of such effects has been the subject of intensive research. The objective here is not to detail this knowledge but rather to briefly outline the basic effects and how they can potentially influence the economic optimization of tomato production.

From an economic viewpoint, the ratio of the cost of supplementing another unit of a limiting factor such as PAR divided by its marginal physical product (MPP)1/ will become greater as the factor becomes more limiting; if several factors are limiting, the one with the smallest ratio will provide the greatest return for each additional dollar. Unfortunately, accurate MPP's for inputs are uncertain because the technology and the photosynthetic process are uncertain. However, to the extent that radiant energy is the most expensive factor to supply, per unit of output, then radiant energy becomes the economically limiting factor to the entire photosynthetic process.

The plant leaf is the primary location of photosynthesis and its incidence angle with respect to solar radiation directly affects the level of radiant energy absorbed by the leaf. Further, leaves absorb, transmit, and reflect spectral radiant energy at varying levels. Each photon of absorbed radiant energy adds energy to an electron, according to Planck's law.2/ The energy required for photochemical reactions such as the second subprocess of photosynthesis may range from 20,000 to 100,000 calories per mole of reactant.3/ Also, assimilation of 1 gram of CO_2 requires the transpiration of 90 grams of water on the average, consuming at least another 53,100 calories. The actual synthesis of glucose fron CO_2 requires about 6,700 calories, depending upon the pathway utilized. But typically only 40-80% of the gross assimilation is retained, the rest being consumed in respiration. Thus, greenhouse crops normally have an efficiency of 1% or less in converting radiant energy into a harvestable, energy-rich product (67, p. 9).

The rate of plant energy consumption is dependent upon external factors, such as absolute humidity, air movement, and irradiance (particularly in the infrared waveband), along with plant internal factors.

A basic energy exchange equation for plant leaves includes (13, pp. 273-274)4/:

$$\frac{\text{Energy Gain}}{a_s(I + I_R) + a_t(R_a + R_g)} = \frac{\text{Energy Loss}}{M \pm C + LE}$$

where: a_s = absorptivity of plant to sunlight, I = incident direct solar radiant energy and skylight, I_r = reflected sunlight from floor and surrounding surfaces, a_t = plant absorptivity to long-wave thermal radiant energy, R_a = incident thermal radiant energy from atmosphere; R_g = incident thermal radiant energy from floor, M = radiant exitance from plant, C = net thermal convection to or from

plant, and LE = transpiration. These energy exchanges affect and control photosynthesis, photolysis, transpiration, and water and nutrient uptake, along with other plant processes.

From this description, five important facts stand out:

1. Photosynthesis and photolysis have opposite effects upon the net production of photosynthates. Consequently, net assimilation will increase as the available external energy (proportionally optimum in forms) increases, until that point is reached where the rate of gain in photosynthesis is less than the rate of gain in respiration; until the net photosynthate produced finally declines.
2. A significant amount of interaction exists among the several input factors in their effects upon yields.
3. The understanding of plant processes is already detailed and has been quantified into mathematical models of plants, but many important functions are still not understood.
4. Many of the common measures of inputs currently used are inadequate and must be refined to the point where they identify the significant qualities and/or quantitites distinguished by plants. In this case, radiant energy is the prime example, where one mean measure of irradiance upon a horizontal plane is commonly used to quantify the entire range of spectral radiant energy without distinguishing the important factors of spectral radiant intensity variations, variations in crop canopies and angles of incidence, and variations in patterns of radiation application (e.g., chopped radiant energy).
5. The plant processes form a dynamic system of interrelated subprocesses which requires a complex dynamic model to represent it; probably of simulation form. This will require continuous monitoring of important variables to allow crop control and product optimization with the use of this dynamic model in the future.

In this evaluation of PAR upon a tomato crop three important, and perhaps flagrant, assumptions are made. First, the variations within plants and within the crop canopy are assumed to reach a population mean which is constant across crops (i.e., the law of large numbers operates). Second, in evaluating the substitution of artificial radiant energy for solar radiant energy, an evaluation of light chopping with varying intensities and varying spectral radiant intensities is not considered, but rather, it is assumed that with the proper research an equivalent substitute can be achieved with artificial lighting. Third, it is assumed that other environmental factors can be effectively maintained at levels equal to or better than those which normally exist during peak periods of production. These factors include humidity, CO_2, wind velocity, temperature, etc. Furthermore, the additional expense of this environmental control, except for CO_2, is ignored.

Notes to Chapter 2

1/ The marginal physical product of X_i is the addition of total physical production attributable to the addition of one unit of the variable input X_i to the production process; other inputs remaining fixed.

2/ Planck's law states that the energy of a photon is inversely proportional to wavelength in accordance with: $\varepsilon = h\nu$ where: ε = energy of a photon in ergs·sec^{-1}; h = Planck's constant = 6.62×10^{-27} ergs·sec^{-1}; ν = cycles per second = frequency of electromagnetic wave. Thus, photons of the red end of the PAR spectrum have less energy than those of the blue end.

3/ The second subprocess of photosynthesis refers to the photochemical reaction where: $2H_2O + 2\ ADP + 4\ NADP + 2P_i \xrightarrow[\text{chloroplast}]{\text{radiant energy}} O_2 + 2\ ATP + 4\ NADPH$. Reference 8 outlines this and the other subprocesses of photosynthesis in more detail.

4/ Some conflict exists as to the actual effects of incident solar irradiance upon plant leaf temperature. Some researchers report only a moderate coupling of incident light to the energy content of plants (5, p. 116), while Gates and Benedict have reported that an irradiated leaf temperature may sometimes be as much as 15° C higher than the surrounding ambient temperature in still air (14, pp. 571-572). Such temperature effects are less likely with the use of artificial lights which normally are not significant radiators of infrared radiation. Therefore, to the extent that this factor affects plant processes, temperature adjustments must be made when utilizing artificial lights.

Chapter 3

SOLAR RADIATION

In this paper, a comparison is made between measured solar irradiation, which has been correlated with tomato crop yields at CEVCO in reference 8, and estimated available PAR from artificial lights. Before this comparison is made, however, several important factors must be accounted for. This section identifies some of these factors.

Assuming the sun is the source of radiant energy, the amount occurring at the limits of the earth's atmosphere is dependent primarily upon the distance between the earth and sun (3.3% variation in this distance occurs annually, with the earth being closest about January 1 and farthest away about July 1). The inverse-square law1/ implies that the earth receives about 7 percent more radiant energy in January than in July due to this variation in distance (58, p. 282). At the mean distance between earth and sun, the solar irradiance of a plane normal to the solar rays and at the outer limits of the earth's atmosphere would be 1360 $W \cdot m^{-2}$ (41, p. 23).

As solar radiant energy passes from the limits of the outer atmosphere to a representative horizontal plane at the earth's surface, functioning as a radiant flux recording device (e.g., a Kip and Zonen pyranometer at the University of Minnesota), several modifications of this solar energy occur. Figure 3 depicts the depletion of direct solar radiation intensity across its spectral energy distribution (SED) curve2/ for various lengths of travel of solar rays through the air mass (m)3/. As m increases, the shorter wavelength radiant energy is attenuated relatively more than that of the longer wavelengths resulting in relatively more red radiant energy (occurs at low β angles), while an increase in blue radiant energy occurs as the sun approaches its zenith. The effects of this daily spectral radiant intensity shift upon plant processes may be significant (see reference 60).

The depletion of solar spectral radiant energy due to absorption and scattering follows the relationship (58, pp. 294-295): $I_{N,\lambda} = \tau_{\lambda}^{m} \cdot I_{N_o,\lambda}$ where: $I_{N,\lambda}$ is the monochromatic intensity normal to the sun's rays after passing through m units of atmosphere, $I_{N_o,\lambda}$ is the initial monochromatic intensity, and τ_{λ} is the monochromatic transmissivity for unit depth of atmosphere. Several factors will affect τ_{λ} including atmospheric dust, atmospheric water vapor, atmospheric gases, water droplets, and ice particles in clouds. Following Monteith (41, pp. 26-30), the total solar irradiance of a horizontal surface (I_H) is equivalent to: $I_H = I_N \cdot \sin \beta + I_d$, where: I_N = direct solar irradiance on a plane normal to the solar rays, I_d = diffuse radiation from sky and clouds on a horizontal plane, and β = solar altitude (shown in Figure 14). Ozone in the stratosphere and oxygen in the upper atmosphere absorb a significant portion of ultraviolet radiation, decreasing the ultraviolet percentage of I_H from about 7% outside the atmosphere to about 3% at sea level. Within the 400-700 nm waveband, the most significant effect of the atmosphere is to scatter the radiation as it collides with N_2, O_2, and other molecules. The efficiency of this scattering is approximately proportional to $I \cdot \lambda^{-1}$ (λ is the wavelength of spectral radiant energy and I is the incident total solar radiation upon a surface), indicating that 400 nm radiant energy is dispersed about nine times more effectively than 700 nm radiant energy. Therefore, on a clear day 15-25% of I_H comes from blue skylight. The infrared waveband (λ > 700 nm) is affected by absorption by CO_2 and particularly by water vapor in the 900-3000 nm waveband (41, p. 24). Of the total irradiance reaching the Kip and Zonen pyranometer at the

University of Minnesota, roughly 50% falls within the 380-720 nm waveband, assuming solar altitude angle β exceeds 30^{o} (41, p. 24). This figure is used to estimate the equivalent PAR required from artificial lights (Bond et al. state that 42% of total solar energy falls within 400-700 nm; see reference 6, p. 235). This is recognized as an average value, and not characteristic of solar SED curves during time periods or at locations having significant amounts of dust and/or water vapor. However, "the partitioning of solar radiation between visible and infrared is almost independent of solar altitude (β) because the visible fraction of skylight increases while the visible fraction of direct radiation decreases as the sun approaches the horizon" (41, pp. 24-25). Generally, the effect of clouds is to absorb and scatter the direct solar radiation and skylight, but not to change the spectral radiant energy distribution within the visible spectrum (Figure 4). Thus, the proportion of total solar irradiation within the PAR range remains clearly constant, varying primarily with cloudiness (7, p. 73).

In the 1000-3000 nm waveband, water droplets absorb significant amounts of radiant energy (Figure 4). These effects of water droplets are not only relevant to the atmosphere, but also reflect the effects of a film of moisture on the inside of the house cover (the transparent or translucent cover material of a greenhouse). Heavy condensation during cold weather on single layer glazing materials will cover about 68% of the surface area (about 25% with light condensation), thereby reducing infrared transmission and heat loss, particularly with materials having a high heat (infrared) radiation transparency, such as polyethylene (63, p. 2). Again, however, the effect upon PAR is considered minor, and is nonexistent during warm weather when such condensation does not occur.

The effects of dust particles upon solar radiation scattering is dependent upon particle size relative to the spectral wavelength and requires a complex analysis for evaluation (41, p. 26; 21, pp. 8-11; 8-12, chapter 16). At CEVCO, the dust content within the atmosphere is assumed to be minor and the cause of little distortion in the solar SED curve.

Another factor which does not directly affect the available solar radiation to plants, but which does affect the measurement of solar radiation with a horizontal pyranometer is the measured daylength. A horizontal pyranometer does not measure between 15 and 30 minutes of solar irradiation at sunrise and sunset due to the low solar altitudes (3, p. 3). To the extent that this unmeasured radiation influences plant processes, bias is introduced into comparisons made between such measured solar irradiation and the effectiveness of artificial lighting as a source of irradiation.

The monthly solar irradiance data correlated with CEVCO production constitutes a daily mean of the total irradiance recorded during the month. From similar data recorded at other stations it has been determined that daily radiation data is not normally distributed, but rather is skewed negatively during the summer months (4, p. 10). Winter months show less skewness than summer months except in regions with little cloudiness, which is not the case for CEVCO. The exact effects upon plant processes due to these variations in radiant intensity are uncertain. It is probable that a continuous mean monthly radiant flux level would enhance crop yields and fruit quality and result in some cost reductions due to more consistent production levels. This may not be true, however, in the case of intradaily irradiance fluctuations, which may improve the efficiency of photosynthetic and other plant processes.

Figures 5 and 6 provide average values of solar radiation recorded at the University of Minnesota based upon data collected over 5 years (1965-1969). Note that the average day direct plus diffuse radiation $\overline{(S + D)}$ never exceeds the clear day direct radiation and falls within a range of 100 to 560

langleys per day.4/ The solar noon diffuse radiation has ranged from 30% above to 40% below the .20 $cal \cdot cm^{-2} \cdot min^{-1}$ indicated, but the mean constant value shown reflects the effects of a drier, clearer winter atmosphere compensating for the longer atmospheric paths of winter radiation. Diffuse radiation varies from about 19% to 34% of total daily radiation on clear days during the year (3, p. 19) and implies that a shift occurs in the solar SED curve at CEVCO. If winter solar irradiance is to be supplemented, it requires emphasis upon the blue spectrum in order to return to an identical distribution of the normal mean summer solar SED curve. This is because as the air mass (m) shifts from 1 ($\beta \simeq 11.3^{o}$) to 5 ($\beta \simeq 90^{o}$) (i.e., winter to summer), the wavelength of maximum energy shifts from about 650 nm to 470 nm (5, p. 25), with diffuse solar radiant energy being maximum at about 460 nm (41, p. 25). It may generally be stated that I_d/I_H will decline as β increases on clear days until a minimum is reached, when $\beta > 40^{o}$, of anywhere from .1 to .25 depending upon the amount of dust and other diffracting media in the air (41, p. 30).5/

In relation to this discussion of direct and diffuse radiation, one supposedly significant characteristic of corrugated fiberglass6/ is that it acts as a diffuser of specular radiant energy. However, observation indicates that this diffusion is far from perfect (6, p. 244) and that shading within the tomato rows is significant. Thus, a central location of radiant emittance exists and is dependent upon the sun's position with respect to the greenhouse. Therefore, to the extent that the solar irradiation is diffused more than the radiant emittance of artificial lights, a potentially significant difference in radiant energy effectiveness for plant use may exist. Because of the nondirectional nature of diffuse radiation within the greenhouse, it is more difficult to quantify and evaluate than specular radiant energy. Therefore, it will not be analyzed separately in this paper.

Evaluation of solar radiation within several crop canopies has indicated that the leaf areas do not receive a constant level of irradiance over short periods of time, but rather receive short bursts of significantly lower levels of irradiation. The causes of this fluctuation in irradiation is probably attributable to cloud and wind movement of the crop canopy, although this is not certain (35, p. 21). In any case, studies of the effects of fluctuating PAR levels (i.e., sunflecks or chopping as it is referred to hereafter) done by McCree and Loomis (40, pp. 422-428), Kriedmann, Torokfalvy and Smart, and others indicate that many plants are more efficient at utilizing a given amount of irradiance for photosynthesis if it comes as short bursts of radiation (about .7 seconds duration) separated by short periods of darkness (about 1.3 seconds duration). Figures 7 and 8 compare the adjusted photosynthetic rates of various combinations of light ($250\ W \cdot m^{-2}$) and dark irradiation durations within a 2-second cycle with continuous irradiation ($250\ W \cdot m^{-2}$) on grape leaves. The measured CO_2 uptake (i.e., photosynthetic rate) for cycled irradiation was adjusted so that all cycles and continuous irradiation are valued at an equal quantity of total radiant energy received (i.e., for a 1-second light/dark cycle, observed CO_2 uptake was multiplied by 2). Although the total photosynthate produced is greatest over a given time period under continuous irradiation versus chopped irradiation (i.e., a difference in total radiant energy available exists), the possible savings in energy input when using artificial lighting in a chopping pattern are important. Also, if a similar pattern of chopping does not occur with artificial lighting, as it does with solar irradiation, then a likely difference in yields may be expected. In this study, the question of chopping is assumed to be a technical problem that can be overcome in the designing of artificial lighting systems for plants.

Significance of Solar Altitude Angle (β) upon Crop Intercepted Irradiation

In comparing artificial lighting irradiance with solar irradiance of a crop, the question of the significance of the altitude angle β (or angle of incidence) upon the total irradiance of a crop must be considered inasmuch as the location of the luminaires will frequently have a β angle with respect to the crop significantly different than that of the sun. Also, in order to estimate the amount of radiation intercepted by a crop's surface, the measured irradiance received by a horizontal pyranometer must be multiplied by a shape factor dependent upon the crop's surface geometry and the directional properties of the radiant energy (following Monteith's approach; 41, pp. 39-58). In this case, the cone shape will be used to simulate the crop's shape.

The flux of direct and diffuse solar radiation recorded at the University of Minnesota is measured on a horizontal plane with a pyranometer. Figure 9 depicts the projected area of a solid, with a surface area (A), upon a horizontal surface (A_H): $\bar{S}_b = (\frac{A_H}{A}) \cdot I_{DH}$, where: $\bar{S}_b$ = mean irradiance of a plant, A_H = area of plant's shadow cast upon a horizontal surface, A = surface area of plant, I_{DH} = direct solar irradiation recorded by pyranometer, and $K_s = \frac{A_H}{A}$.

A cone may be used to simulate the distribution of radiant energy upon the leaves of a crop when they are randomly distributed with respect to the points of the compass. Figure 10 depicts the geometry of a cone projected on a horizontal surface. The isosceles sides in the drawing are of unit length and at angle σ with the base. Therefore, base area = $\pi \cdot \cos^2 \sigma$. For the case where direct radiation is incident at an angle $\beta > \sigma$, the walls of the cone are fully irradiated and cast a shadow falling inside the base. The shadow cast upon a horizontal surface (A_H) is then: $A_H = \pi \cdot \cos^2 \sigma$. The wall area (A) is: $A = \pi \cdot \cos \sigma$. Therefore, $K_s = A_H/A = \cos \sigma$ (for $\beta > \sigma$).

The diffuse radiation that strikes leaves is: incoming short- and long-wave radiation, reflected solar radiation, and long-wave radiation emitted by the underlying surface. The analysis of these diffuse components is difficult and the following concerns only the interception of radiation where the intensity of the radiation is assumed to be independent of angle.

For diffuse solar radiation, the proportion which is PAR depends upon the source. PAR to total diffuse radiation is .7 - .8 for radiation from blue sky, .5 for radiation from clouds, and .2 for radiation reflected or transmitted by leaves. With increasing depth into a crop canopy, the downward radiant flux becomes increasingly diffuse and lower in PAR, with the greatest change occurring at about 700 nm. "In principle, the diffuse component of irradiance could be determined in the same way as the direct component, but a rigorous treatment would need to allow for the change of spatial distribution and spectral composition of the diffuse flux at different depths in the canopy" (41, p. 55).

LAI, leaf area index, is the area of leaves above unit area of ground taking only one side of each leaf into account. A small area of LAI has a leaf area index dLAI. The area of shadow cast by dLAI upon a horizontal plane is $(A_H/A) \cdot dLAI$. The intercepted radiation is: $dI_{DH} = -(A_H/A) \cdot I_{DH} \cdot dLAI = -K_s I_{DH} \cdot dLAI$ (- sign indicates LAI is measured downwards from the top of the canopy). Given that the relative solar irradiance of LAI is the ratio I_{LAI}/I_o, the area of sunlit foliage between LAI and (LAI + dLAI) is $(I_{LAI}/I_o)dLAI$; where I_o is the irradiation at the top of the crop canopy and in a crop where: L_t = total leaf area. The leaf area index of sunlit foliage is: $\int_o^{L_t} I_{LAI}/I_o \, dLAI =$

$\int_0^{L_t} e^{-K_s \cdot LAI} \, dLAI = K_s(1 - e^{-K_s \cdot L_t})$ by Beer's Law. At the limit, where L_t is large, the leaf area index of sunlit foliage is: $1/K_s$.

Using the preceding cone analysis approach, where all the leaves are at the elevation $\sigma = 30^o$, but randomly distributed with respect to their azimuth angles, two cases exist: $\beta > \sigma$ (β = solar altitude; see Figure 14) and $\beta > \sigma$. For $\beta > \sigma$, the entire surface of the cone is irradiated and as shown previously.

$K_s = \frac{A_H}{A} = \frac{\pi \cdot \cos^2 \sigma}{\pi} = \cos \sigma$, which is independent of solar altitude angle (β). For $\beta < \sigma$, K_s approaches infinity as β approaches zero. In fact, "most of the measurements that have been made in farm crops show that K_s and s ($s = 1 - K_s$ = sunfleck area) are nearly constant when β exceeds 30^o. Constant values of the coefficients can safely be used in estimates of daily photosynthesis or transpiration rates" (41, pp. 57-58).

Estimating photosynthetic and transpiration rates of leaves in a crop canopy requires the determination of the leaf irradiance, not the irradiance of a horizontal surface. From the preceding discussion, the direct component of irradiance below leaf area index LAI is $I_{DH} \cdot LAI$. And the mean irradiance of the foliage at this depth in the crop canopy is $K_s \cdot I_{DH} \cdot LAI$ in $W \cdot m^{-2}$. At the extremes, if $\sigma = \beta$, the leaf receives no direct irradiation. But if $\sigma = \beta + \pi/2$, the leaf received $I_{DH} \cdot \text{cosec } \beta$ direct irradiation. The modeling of the complete crop canopy requires the division of L_t into n_L layers with each layer, from the top down, receiving the remaining segment of transmitted radiant exitance. For example, the proportion of radiation transmitted to the next layer down would be: $1 - K_s \cdot (1 - \tau) \cdot n_L^{-1}$ of the previous layer's incident radiation where n_L = number of sublayers, $K_s \cdot n_L^{-1} = m^2$ of shadow per m^2 of ground area in a sublayer, τ = transmission coefficient of leaves, $1 - K_s \cdot n_L^{-1}$ = fraction of direct radiation penetrating the layer, and $\tau \cdot K_s \cdot n_L^{-1}$ = diffuse radiation generated by interception and forward scattering. The fraction of transmitted radiation for an entire crop canopy (i.e., $n \cdot L_t$ sublayers) is $(1 - K_s \cdot (1 - \tau)/n_L)^{n_L \cdot L_t}$. If the leaves are randomly distributed, then n_L must go to infinity to prevent overlapping of leaves. The limit of transmitted irradiation through n sublayers of L_t: $\left[(1 - K_s) \cdot (1 - \tau) \cdot n_L^{-1}\right]^{n_L \cdot L_t}$ as $n_L \to \infty$ is: $e^{-K_s \cdot (1 - \tau) \cdot L_t}$, which follows a conventional Beer's Law type of model.

From this discussion, it can be inferred that the solar altitude angle β for artificial lights versus solar radiation with respect to the crop canopy is not as significant a factor as might be first thought. It is probable, however, that with the distribution of artificial lights in a horizontal plane above the work plane (i.e., crop canopy) any advantage due to angle of irradiation would go to the artificial lights over solar radiation because overhead artificial lights will normally utilize reflectors, which limit the angle β to values exceeding σ. On the other hand, with the sun as the course of radiant energy, angle β goes to zero each morning and evening. As shown, when $\beta < \sigma$ and β is approaching 0^o, K_s approaches infinity and the leaf area index of sunlit foliage approaches its limiting value of $1/K_s$, or zero. (It can be assumed that L_t is large.) Thus, the effectiveness of artificial lighting versus solar radiation should increase as solar altitude angle β declines to values below σ for solar irradiation.

A second important point to note is the occurrence of declining PAR levels when going downward into the crop canopy. Transmitted radiation through a crop canopy declines exponentially with respect to increases in K_s and L_t, and decreases in leaf transmissivity τ. Because of this, there would appear to be an advantage in distributing the radiant energy within the crop canopy more effectively. The use of fluorescent lamps allows this by placing them horizontally or vertically between rows of tomato plants.7/ However, the lack of the chopping effect of such irradiation may significantly diminish its photosynthetic effectiveness, as previously discussed. It should also be noted that the older, lower leaves of tomato plants tend to be less efficient photosynthesizers and, therefore, less effective users of PAR.

Derivation of Basic Solar Angles at CEVCO

The following five sections examine several factors which affect the net available radiant energy at the top of a crop canopy within a CEVCO house, including house orientation, reflected radiant energy, house shape factors, and house cover transmissivities. The evaluation of solar irradiation depends upon a basic understanding of fundamental solar geometric relationships. This section will present these relationships. The underlying objectives of these next sections preceding the discussion of artificial lighting are to identify the factors causing variations between external solar irradiation levels and in-house irradiation levels, and to understand the underlying factors affecting in-house solar irradiation levels so owners of greenhouses will be aware of the significance of house design, coverings, spacing, and orientation upon potential crop yields. The completion of the first objective is necessary for a subsequent comparison of in-house artificial lighting with already measured tomato yield responses dependent upon external solar irradiation measurements (recorded with a pyranometer) made near CEVCO.8/ The purpose of the second objective is to help growers become more aware of factors affecting yields, which are frequently being ignored in efforts to conserve energy.

All solar radiation calculations are done in terms of local solar time (LST), with seasonal differences between it and the local standard time at CEVCO depicted in Figure 11. LST = LCT + Equation of Time (Table 2), where LCT (local civil time) is the local standard time adjusted 4 minutes for each degree latitude deviation from the standard meridians, which for the United States are: 75° EST (Eastern Standard Time), 90° CST (Central Standard Time), 105° MST (Mountain Standard Time), and 120° PST (Pacific Standard Time). For CEVCO, at $93^{\circ}11'$ West longitude and 45° North latitude, LCT = CST - (3.167)(4 min) = CST - 12.67 min. The equation of time, shown in Table 2 at weekly values, accounts for irregularities in the earth's rotation, obliquity of the earth's orbit, and other factors.

Calculation of the LST at sunrise at CEVCO on December 22 is: LCT = (3)(4) = -12 min + 0748(CST) = 0736 hours; Equation of Time = 1 min, 47 sec ≃ 2 min; and LST = 0736 + 2 min = 0738 hours. Similarly, for June 22: LST = 412 hours at sunrise.

Three factors must be known to determine the position of a point on the earth's surface with respect to the sun's rays: l = latitude, d = solar declination angle, and h = solar hour angle. Figures 12-13 portray these angles. On December 22, d = -23.45° and on June 22, d = $+23.45^{\circ}$ as shown in Table 2. Hour angle (h) expresses the time of day with respect to solar noon (one hour = 15°). Sunrise occurs on December 22 at 0738 hours; $h = \frac{(262 \text{ min}) \cdot (15^{\circ} \cdot \text{hr}^{-1})}{60 \text{ min} \cdot \text{hr}^{-1}} = -65.5^{\circ}$, and on June 22 at 0412

hours; $h = \frac{(468 \text{ min}) \cdot (15^{\circ} \cdot hr^{-1})}{60 \text{ min} \cdot hr^{-1}} = -11.7^{\circ}$. At solar noon (LST = 1200 hours), h = 0.

From these three basic angles--l, h, d--several other angles are derivable: ψ (solar zenith) angle), β (solar altitude angle), and γ (solar azimuth angle).

Table 2. The sun's declination and equation of time.

Day →	1		8		15		22	
Month	Dec. Deg:Min	Eq. of Time Min:Sec	Dec. Deg:Min	Eq. of Time Min:Sec	Dec. Deg:Min	Eq. of Time Min:Sec	Dec. Deg:Min	Eq. of Time Min:Sec
January	-(23:08)	-(3:16)	-(22:20)	-(6:26)	-(21:15)	-(9:12)	-(19:50)	-(11:27)
February	-(17:18)	-(13:34)	-(15:13)	-(14:14)	-(12:55)	-(14:15)	-(10:27)	-(13:41)
March	-(7:51)	-(12:36)	-(5:10)	-(11:04)	-(2:25)	-(9:14)	0:21	-(7:12)
April	4:16	-(4:11)	6:56	-(2:07)	9:30	-(0:15)	11:57	1:19
May	14:51	2:50	16:53	3:31	18:41	3:44	20:14	3:30
June	21:57	2:25	22:47	1:15	23:17	-(0:09)	23:27	-(1:40)
July	23:10	-(3:33)	22:34	-(4:48)	21:39	-(5:45)	20:25	-(6:19)
August	18:12	-(6:17)	16:21	-(5:40)	14:17	-(4:35)	12:02	-(3:04)
September	8:33	-(0:15)	5:58	2:03	3:19	4:29	0:36	6:58
October	-(2.54)	10:02	-(5:36)	12:11	-(8:15)	13:59	-(10:48)	15:20
November	-(14:12)	16:20	-(16:22)	16:16	-(18:18)	15:29	-(19:59)	14:02
December	-(21:41)	11:14	-(22:38)	8:26	-(23:14)	5:13	-(23:27)	1:47

Source: 58, p. 286.

Figures 14 and 15 depict these angles. Figure 14 shows incident direct solar radiation (I_N) striking a point, P, on the earth's surface. The solar altitude angle (β) is defined by the solar ray I_N from the sun and the projection of that ray on the horizontal plane defined by point P and its horizon on earth. The solar zenith angle (ψ) is the angle defined by solar ray I_N and the normal to the horizontal plane containing P on earth ($\psi = 90^{\circ} - \beta$). The solar azimuth angle (γ) is the angle in the horizontal plane from North (N) to the projection of solar ray I_N in the plane. Figure 15 reflects these same angles along with l, h, and d in an XYZ coordinate system, where O is again the center of the earth and P a point on the earth's surface. The XY plane is the earth's equatorial plane. Line PN is perpendicular to line OP and lies in the plane defined by OP and OZ.

Two other angles not depicted in Figure 14 or 15 but of importance are the solar angle of incidence for a surface (θ) and the wall-solar azimuth angle for a vertical surface (α). θ is the angle between the solar rays and the normal (i.e., a line perpendicular to a surface) to a tilted surface at the point of incidence on the surface. α is the angle measured in the horizontal plane on the earth's surface between the normal to a vertical surface and the projection of the solar rays on the horizontal plane. For a North-South (N-S) oriented CEVCO house, where a vertical imaginary plane is assumed to exist along the length of each house side, $\alpha = \gamma - 90^{\circ}$.

From an analysis of these angles several identities can be derived including: $\beta = 90^{\circ} - \psi$, $\sin \beta = \cos l \cdot \cos h \cdot \cos d + \sin l \cdot \sin d$, $\cos \gamma = \sec \beta \cdot (\cos l \cdot \sin d - \cos d \cdot \sin l \cdot \cos h)$, and $\cos \alpha = \sec \beta \cdot \cos d \cdot \sin h$ (for N-S oriented CEVCO houses). At solar noon, h = 0 if l > d, $\gamma = 180^{\circ}$ (this is the case for CEVCO), if l < d, $\gamma = 0^{\circ}$, and if l = d, γ is undefined, then $\beta_{noon} = 90^{\circ} - |l - d|$.

Further, in relation to direct solar radiation it can be shown for a:

tilted surface: $\cos \theta = \cos \beta \cdot \cos \alpha \cdot \cos \phi + \sin \beta \cdot \sin \phi$;

vertical surface: $\phi = 0$; $\cos \theta = \cos \beta \cdot \cos \alpha$;

horizontal surface: $\phi = 90^{\circ}$; $\cos \theta = \sin \beta = \cos \psi$: $\theta = \psi$.

Determination of β at CEVCO for:

sunrise: $\sin \beta = \cos 45^{o} \cdot \cos 63^{o} \cdot \cos -23.45^{o} + \sin 45^{o} \cdot \sin -23.45^{o}$

$\beta = .75^{o}$

solar noon: $\beta = 90^{o} - | 45^{o} + 23.45^{o} |$

$\beta = 21.55^{o}$

sunrise: $\sin \beta = \cos 45^{o} \cdot \cos 117^{o} \cdot \cos 23.45^{o} + \sin 45^{o} \cdot \sin 23.45^{o}$

$\beta = -.75^{o}$

solar noon: $\beta = 90^{o} - | 45^{o} - 23.45^{o} |$

$\beta = 68.45^{o}$

The following sections will utilize these angles and relationships to evaluate solar irradiation at CEVCO. Because l, h, and d change with time, any comprehensive evaluation of solar irradiation should be dynamic. For the simple purposes of this study, however, solar irradiation is considered at two extremes (December 22 and June 22) in a static analysis.

House Orientation

The orientation of greenhouses with respect to wall-solar azimuth angle is a subject considered by others. Hydroculture, Inc.9/ has recommended that their houses be oriented with the ridge running north-south (N-S). Generally, a N-S ridge achieves the greatest year-round crop irradiation, but an east-west (E-W) ridge allows maximum solar irradiation for winter and spring crops, especially with N-S rows. North of about 40^{o} latitude indications are that an E-W orientation achieves optimum solar irradiation of a greenhouse crop (45, p. 48). G. F. Sheard of the Glasshouse Crops Research Institute in England stated it more concisely (46, pp. 57-58):

> Before 1950 the majority of glasshouses were built in multispan blocks, oriented N-S. Such glasshouses had a mean overall transmission in midwinter rarely exceeding 40% and in many cases as low as 35%. Many modern glasshouses have a transmission of 70% and it can be inferred as an approximation that a 1% increase in transmission gives a potential increase in yield of 1%. The marked improvement in winter light transmission arises from developments in materials and structural design, from studies of roof geometry and from changing the orientation from N-S to E-W.... The largest improvement in transmission comes from changing the orientation from N-S to E-W.... It is difficult in N-S houses to achieve a transmission in December exceeding 48% but the same house oriented E-W may have a transmission of 70%. Roof shape has a small but significant effect on light transmission. In E-W houses a high south facing side and a Mansard roof improve light transmission.

Further, at least one recent study indicates that wintertime production of tomatoes in colder climates may be further enhanced by conversion of the north wall of a greenhouse into a well-insulated wall with reflective south-facing surface (48, pp. 66, 68; 66, pp. 284-285).

A related question is that of optimum house spacing. Whether greenhouses are oriented N-S or E-W, it is desirable to space them so that optimum PAR reception is available to the plants.10/ Further, the additional radiant energy trapped within the house will help reduce winter heating expenses. Assuming production occurs year round, then consideration of house spacing is straightforward.

The spacing of greenhouses will depend upon latitude, house orientation, crop, and elevation. For CEVCO, the crop is tomatoes, and houses are oriented N-S at equal elevations. The space between houses is currently 4.27 meters (m). Figure 16 presents the relevant dimensions of the houses, while Figure 11, 17, and 18 provide relevant solar times, and altitude and azimuth angles for CEVCO at 45^{o} N latitude.

Observe Figure 19, where: I_D = incident direct solar radiation, Y = height of house at CEVCO less the distance from bottom leaves of plants = 3.35 m, X = distance between the center of the shading house and the outside row of plants in the shaded house; a = length of shadow of I_D in the plane of the house floor between center of shading house to nearest plants of shaded house, γ = solar azimuth angle, β = solar altitude angle, and α = wall-solar azimuth angle = $\gamma \pi/2$ for CEVCO houses, γ and β can be derived from Figure 18 for 45° N latitude for selected dates and times. From this, X is calculated where: $X = \frac{Y \cdot \cos(\alpha - 90^{\circ})}{\tan \beta}$ and is recorded in Table 3. For 42° and 48° N latitude in Table 3, γ and β are derived by the appropriate formulas. At CEVCO on the shortest day of the year (December 22) when the sun rises and sets at 0738 hours LST and 1622 hours LST, respectively (Figure 18), approximately 160 minutes occur during which the houses are shaded to a point above the leaves of the nearest row.11/ If, for example, an additional 3.53 m were added between houses, the shading time would be reduced by 40 minutes.

If this approach is used to consider houses oriented E-W, Z becomes the distance between the center of the shading house and the nearest row of plants in the shaded house.

$Z = \frac{Y \cdot \sin(\gamma - 90^{\circ})}{\tan \beta}$, with values again recorded in Table 3. Note the difference between X and Z for the same dates, times, and latitudes as shown by Figure 20. For example, N-S houses at 45° N latitude at 0800 and 1600 hours LST require an additional 12.6 m between houses over E-W houses to eliminate shading, but the rate of decline in X is more rapid than for Z. At 0850 hours, equal house spacing of about 16 m for N-S and E-W houses eliminates shading. E-W houses at solar noon require 5.9 m spacing to avoid adjacent house shading while N-S houses need no spacing. Further, as can be seen from Figure 20, the E-W house effectively shades more than a N-S house for equal spacing during the period of greatest mean irradiation. Thus, from a shading standpoint it would be advantageous to orient houses on a N-S axis, where a firm has several houses in one confined area.

The shading of the crop by structural members within a CEVCO house is estimated at 6.6% of the covered area. As previously recognized, K_s will change as solar altitude angle β (and wall-solar azimuth angle α also in this case) change, but it is assumed that the proportional effect upon total crop irradiance is relatively constant. Shading differences due to structural members on an E-W versus N-S house can be assumed to be minor.

The shading effects of the opaque house ends upon house orientation is another point to consider. On a N-S house, the plants at one end suffer the full effects of shading due to the house end, while on an E-W house each end shades the crop only half of the solar day. Also, during winter months, when shading is most critical, the total crop area shaded by an opaque house end on a N-S house versus an E-W house at CEVCO cumulated over time is significantly greater based upon total irradiance shaded out. This reflects the fact that a N-S house end, unlike ends on E-W houses, casts its greatest shadow at solar noon, when mean direct solar radiation is maximum. Therefore, reduction of the opaque area of the house ends benefits the plants on the basis of irradiance received, but may also increase heating expenses. In any case, the E-W orientation of CEVCO houses is certainly more desirable in terms of crop shading effects.

Table 3. Desired distances between houses on different dates and times at three latitudes to prevent shading of crop from direct solar radiation.

	Date	LST	Y	γ	β	X	Latitude
North-South Houses	Dec. 22	1200	3.35 m	180.0°	21.5°	0 m	45° N
		1100 & 1300	3.35 m	165.0°	20.0°	2.38 m	
		1000 & 1400	3.35 m	152.0°	16.0°	5.48 m	
		0920 & 1440	3.35 m	143.0°	12.4°	9.17 m	
		0900 & 1500	3.35 m	138.0°	10.0°	12.7 m	
		0800 & 1600	3.35 m	127.0°	3.0°	51.1 m	
	Jan. 1	1200	3.35 m	180.0°	19.0°	0 m	48° N
		1000 & 1400	3.35 m	151.7°	14.07°	6.34 m	
		0900 & 1500	3.35 m	138.9°	8.35°	15.0 m	
	Jan. 1	1200	3.35 m	180.0°	25.0°	0 m	42° N
		1000 & 1400	3.35 m	150.8°	19.3°	4.67 m	
		0900 & 1500	3.35 m	138.1°	12.85°	9.8 m	
		LST	Y	γ	β	Z	Latitude
East-West Houses	Dec. 22	1200	3.35 m	180.0°	21.5°	8.5 m	45° N
		1100 & 1300	3.35 m	165.0°	20.0°	8.89 m	
		1000 & 1400	3.35 m	152.0°	16.0°	10.3 m	
		0920 & 1440	3.35 m	143.0°	12.4°	12.2 m	
		0900 & 1500	3.35 m	138.0°	10.0°	14.1 m	
		0800 & 1600	3.35 m	127.0°	3.0°	38.5 m	
	Jan. 1	1200	3.35 m	180.0°	19.0°	9.7 m	48° N
		1000 & 1400	3.35 m	151.7°	14.07°	11.8 m	
		0900 & 1500	3.35 m	138.9°	8.35°	17.2 m	
	Jan. 1	1200	3.35 m	180.0°	25.0°	7.18 m	42° N
		1000 & 1400	3.35 m	150.8°	19.3°	8.35 m	
		0900 & 1500	3.35 m	138.1°	12.85°	10.9 m	

Reflected Solar Radiation Striking CEVCO Houses

Reflected solar radiation from gravel and snow. The total irradiation of a surface is represented by $I = I_D + I_d + I_R$, where: I = total solar radiance energy incident upon a surface at any moment, I_D = incidence of direct solar radiation, I_d = incidence of diffuse sky radiation, and I_R = incidence of solar radiation reflected upon the surface from surrounding surfaces.

The pyranometer readings taken at the University of Minnesota and used in this paper and in reference 8 record the direct plus diffuse radiation striking a horizontal surface per unit area. To estimate the I_R reflected upon a CEVCO house from surrounding surfaces requires the calculation of the individual reflected radiant intensities for these surfaces. The value of I_R will be estimated at its extreme values on December 22 and June 22 in this paper.12/

The local solar times (LST) can be determined for when the gravel area adjacent to the east side of a CEVCO house is first irradiated the length of the house and for when it is fully irradiated. Based upon the geometric relationships shown in Figure 19 and the relationships of solar angles, a unique time can be found for when the house and adjacent gravel areas are fully irradiated. Assume that Y = 3.22 m, the height of a shading CEVCO house less the distance from the bottom leaves of tomato plants to the bed surface. Assume X = 8.23 m, the distance between the center of the shading house and the east edge of the shaded house. The ray I_D in Figure 19, in order to just strike the

bottom leaves of the east row of plants in the shaded house along the full length of the house, must satisfy two systems of equations. The first system is determined by the fixed positions and dimensions of the CEVCO houses and includes (from Figure 19): $a = \frac{Y}{\tan \beta}$ (equation 1) and $\cos \alpha = \frac{X}{a}$ (equation 2). The second system of equations is determined by the previously discussed solar angle relationships and includes: $\sin \beta = \cos \ell \cdot \cos h \cdot \cos d + \sin \ell \cdot \sin d$ (equation 3) and $\cos \alpha = \sec \beta \cdot \cos d \cdot \sin h$ (equation 4). For any given day ℓ and d can be assumed constant, while X and Y are determined by the house positions and dimensions. Combining equations 2 and 4 gives: $\frac{\cos d \cdot \sin h}{\cos \beta} = \frac{X}{Y} \cdot \tan \beta$. But given: $\tan \beta = \frac{\sin \beta}{\cos \beta}$, then, $\frac{\cos d \cdot \sin h}{\cos \beta} = \frac{X}{Y} \cdot \frac{\sin \beta}{\cos \beta}$. And by cancelling $\cos \beta$ and rearranging: $\sin \beta = \frac{Y \cdot \cos d \cdot \sin h}{X}$ (equation 5). Combining equations 3 and 5 gives: $\cos \ell \cdot \cos d \cdot \cos h + \sin \ell \cdot \sin d = \frac{Y \cdot \cos d \cdot \sin h}{X}$. Rearranging yields, $\sin h - \left(\frac{X \cdot \cos \ell}{Y}\right) \cdot \cos h = \frac{X \cdot \sin \ell \cdot \tan d}{Y}$ (equation 6), where the only unknown on a given day and for a given X and Y is h, the solar hour angle. Lacking a trigonometric identity for simplifying this equation, the easiest method of solving for h is by iteration, where: $0^\circ \leq |h| \leq 180^\circ$ and ℓ, d, X, and Y are given. Thus, as h increases, the left side of equation 6 increases. Using this procedure for December 22 and June 22 where:

<u>December 22:</u>			<u>Gives:</u>
$\ell = 45^\circ$	$d = -23.45^\circ$	$Y = 3.22$ m	LST = 0925 hours
$X = 8.23$ m		$h = 38.7^\circ$	
and			
$X = 3.96$ m		$h = 24.5^\circ$	LST = 1022 hours
<u>June 22:</u>			
$\ell = 45^\circ$	$d = 23.45$	$Y = 3.22$ m	
$X = 8.23$ m		$h = 83.4^\circ$	LST = 0626 hours
and			
$X = 3.96$ m		$h = 57.55^\circ$	LST = 0810 hours

For X = 8.23 m, the respective local solar time (LST) above is the time when the full length of the east side of a shaded CEVCO N-S oriented house is directly irradiated by I_D. For X = 3.96 m, the respective LST above is the time when the entire area (except for a minor section near the shading house) between the N-S CEVCO houses is irradiated by I_D. Thus, on December 22 the time required after sunrise before the east bed is fully irradiated by direct solar radiation is 20% less than on June 22 and similarly less for full direct irradiation of the area between houses. However, the time during which a CEVCO house is receiving any reflected direct solar radiant energy from the ground area between the houses is 57% less on December 22 than on June 22. Figure 20 graphically indicates how the distance between CEVCO houses needed to avoid any house shading will vary on December 22, depending upon the time of day and orientation of the houses.

These calculated solar hour angles will now be used to estimate the value of reflected incident solar radiation (I_R) upon a CEVCO house from areas between houses and from adjacent house covers. Estimates of I_R are based upon mean values of solar irradiation, average periods of reflection, average areas of reflection, and wall shape factors. Because solar angles are symmetric around solar noon for a given point on earth, it is only necessary to evaluate reflected radiation for half the day and then double it.

Figure 21 provides surface reflectivity coefficients (ρ), a dimensionless unit,13/ for several types of surfaces. The plane areas surrounding CEVCO's houses are a grayish-brown crushed rock surface covered by highly reflective snow during winter months. Given a maximum solar zenith angle (ψ) of about 30° for November through February 9 (Figure 18) indicates that the specular reflection angle θ'' will normally exceed 60° during the same period. If the snow reflectivity coefficient (ρ) is assumed to be .7, then specular reflectivity should predominate during winter months. On the other hand, during the summer months of peak solar irradiation θ'' is normally significantly less than 60° and the surface reflectivity coefficients for gravel and fiberglass paneling have a typical value of about .18. This situation generates almost completely diffused reflection radiation.

Figures 22 and 23 depict the general situation of reflection occurring at CEVCO. dA_1 represents a segment of a gravel area either between the houses or on the side of a house. dA_2 represents a segment of the absorbing surface of an adjacent house. Radiation on the lower portion of a house-cover is of primary significance with the angle of incidence being excessive for significant reflected irradiation to occur near the ridge of the house-cover. The calculation of reflected incident solar radiation upon A_2 from gravel or snow surface A_1 is done at the following times: December 22 at 1022 hours, December 22 at solar noon, June 22 at 0810 hours, and June 22 at solar noon. Calculation of reflected diffuse radiation from the adjacent house-cover surface A_1 upon A_2 on December 22 at 0925 hours LST and on June 22 at 0626 hours LST is also done. The angles are derived from those previously ascertained and I_R is considered the sum of radiation reflected from the adjacent house plus the gravel or snow surface between houses. The results are assumed to be symmetric around solar noon.

Determination of I_R on the east side of a CEVCO house on June 22 from the adjacent gravel surface between houses follows (see 58, pp. 329-332). The reflectivity of surface A_1 (gravel) in Figures 22 and 23 is $\rho_1 \simeq .18$. From $q = \rho_1 \cdot I_1 \cdot A_1$ or $dq = \rho_1 \cdot I_1 \cdot dA_1$, where dq is the diffusely reflected radiation from dA_1 upon a hemisphere of radius r, and I_1 is the mean daily total solar radiation (in gram-calories$\cdot cm^{-2} \cdot day^{-1}$) incident upon A_1, on a monthly basis, can be derived $dq = \pi \cdot r^2 \cdot I_{R,N}$ where $I_{R,N}$ = intensity of reflected radiation along the normal to dA_1 at r distance r. If dI_R = intensity incident upon dA_2 due to radiation diffusely reflected by dA_1, then $dI_R = I_{R,N} \cdot \cos \theta_1 \cdot \cos \theta_2$ (see Figure 22 for θ_1 and θ_2). By substitution, $dI_R = \dfrac{\rho_1 \cdot I_1 \cdot dA_1 \cdot \cos \theta_1 \cdot \cos \theta_2}{\pi \cdot r^2}$. From Figure 22:

$dA_1 = dx \cdot dy \qquad \cos \theta_1 = \dfrac{a}{r}$

$\cos \theta_2 = \dfrac{x}{r} \cdot \cos \phi - \dfrac{a}{r} \cdot \sin \phi$

and where $r = \sqrt{x^2 + y^2 + a^2}$

(ϕ is defined by Figure 22). Integration of dI_R over area A_1 gives:

$I_R = \dfrac{\rho_1 \cdot I_1}{\pi} \cdot \left[a \cdot \int_{-c}^{c} \int_{b_1}^{b} \dfrac{(x \cdot \cos \phi - a \cdot \sin \phi)}{(x^2 + y^2 + a^2)^2} \, d\,x\,dy \right]$. Substituting F for the above quantity in brackets gives: $I_R = \dfrac{\rho_1 \cdot I_1 \cdot F}{\pi}$.

The general solution for F is (58, p. 331):

$$F = \cos\phi \cdot \left[\frac{a}{\sqrt{a^2 + b_1^2}} \cdot \arctan \frac{c}{\sqrt{a^2 + b_1^2}} - \frac{a}{\sqrt{a^2 + b^2}} \cdot \arctan \frac{c}{\sqrt{a^2 + b^2}} \right] +$$

$$\sin\phi \cdot \left[\frac{b_1}{\sqrt{a^2 + b_1^2}} \cdot \arctan \frac{c}{\sqrt{a^2 + b_1^2}} - \frac{b}{\sqrt{a^2 + b^2}} \cdot \arctan \frac{c}{\sqrt{a^2 + b^2}} \right] + \frac{\sqrt{a^2 + c^2}}{c \sin\phi} \cdot$$

$$\left[\arctan \frac{b_1}{\sqrt{a^2 + c^2}} - \arctan \frac{b}{\sqrt{a^2 + c^2}} \right].$$

For the situation at CEVCO, depicted by Figure 23: a = 1 m, the height from the gravel surface between the houses to a small surface on the CEVCO house adjacent to the middle of the crop canopy edge inside the house; b = 4.4 m, the distance between the houses, plus b_1 (the distance from the house edge to the perpendicular up to dA_2); c = 20 m, the length between houses of surface A_1, which causes significant diffuse reflection to strike surface A_2; and $\phi = 15^o$, the angle at which surface dA_2, the fiberglass house-cover, tilts from a normal to dA_1. The amount of diffusely reflected solar radiant energy striking dA_2 is independent of the sun's position except as it affects I_1. Therefore, the calculated value of F will not change unless a, b, c, or ϕ changes. dA_2 is assumed to be a representative position on a CEVCO house cover between ground level and about 2 m above ground level. Obviously, the level of I_R upon any one area of the house cover will depend upon ϕ, decreasing in level as ϕ increases.

Solving F for this case, where $\frac{-b}{a} < \tan\phi \leq \frac{b}{a}$ and $b_1 = .268\ m = a \cdot \tan\phi$, is:

$$F = \tan^{-1}\frac{20\cdot\cos 15}{1} - \frac{(1\cdot\cos 15 + 4.4\cdot\sin 15)}{\sqrt{1^2 + 4.4^2}} \cdot \tan^{-1}\frac{20}{\sqrt{1^2 + 4.4^2}} + \frac{20\cdot\sin 15}{\sqrt{1^2 + 20^2}} \cdot$$

$$\tan^{-1}\frac{1\cdot\tan 15}{\sqrt{1^2 + 20^2}} - \tan^{-1}\frac{4.4}{\sqrt{1^2 + 20^2}} = \tan^{-1}19.32 - .4665\cdot\tan^{-1}4.432 + .2585\cdot(\tan^{-1} .0134 -$$

$\tan^{-1} .2197) = 1.519 - .6293 + .2585\cdot(.0134 - .2163) = .837$ (the angles are solved in radians).

For $I_H = 500\ \text{langleys}\cdot\text{day}^{-1} = 500\ \text{g-cal}\cdot\text{cm}^{-2}\cdot\text{day}^{-1}$, $I_R = \frac{\rho_1\cdot I_H\cdot F}{\pi} = \frac{(.18)\cdot(500)\cdot(.837)}{\pi} =$ 24 $\text{lys}\cdot\text{day}^{-1}$. That is, an expected additional irradiation of 24 $\text{lys}\cdot\text{day}^{-1}$ can be expected upon either side of a CEVCO house at 1 m above the ground in June. Calculating values of F at 10-degree arc intervals on the house cover yields the curve of F values versus angle ϕ shown in Figure 24. Beyond $\phi = 60^o$, or for the house cover over the center 3.8 m of a house, F = 0 and no I_R (due to diffuse reflection from the adjacent gravel surfaces) is received from the overhead house cover.

A mean F value, identical for both sides of the house, is about .6 for over approximately two-thirds of the house cover. Calculating I_R upon the house-cover at F = .6 gives:

$I_R = \frac{\rho_1\cdot I_H\cdot F}{\pi} = \frac{(.18)\cdot(500)\cdot(.6)}{\pi} = 17.2\ \text{lys}\cdot\text{day}^{-1}$ reflected upon two-thirds of the house-cover per day.14/ This indicates a significant increase occurs in irradiation levels during non-snow months due to diffuse reflection from surrounding surfaces.

Reflected radiation from adjacent houses. Reflected radiation from the sides of adjacent houses is considered here to be totally diffuse, with a coefficient of reflectivity of .18 for CEVCO's fiberglass panels (filon). Reflected radiation from the crop within adjacent houses is not considered, but if it were, it would be significantly lower in the primary spectral bands of photosynthetically active radiation (PAR). The analysis of diffuse reflection is similar to that for the reflection off the gravel between the houses and follows Figures 22 and 25. The significant reflective surface is the 3.05-m section at the upper end of b in Figure 25, which runs the length of the house, and has an F value equal to the difference in F_b and F_{b_2} where: $F_b - F_{b_2} = .3$ (where F is calculated with the previously stated formula).

$I_{R_{Filon}} \simeq \rho \cdot I_H \cdot \cos 70^o \cdot (F_b - F_{b_2}) \cdot \pi^{-1} \simeq 2.9$ lys·day^{-1} where: $I_H = 500$ lys·day^{-1}, cos 70^o = adjusts I_H to the actual reflected irradiation from the house cover, at a 70^o angle to the horizontal plane, and $\rho = .18$.

I_R = reflected solar radiation and is considered to be fully diffused. Angle ϕ will vary with the position of dA_2 on the receiving house cover and dA_1 on the reflecting house cover. Thus, while it is assumed here that dA_1 and dA_2 are at constant angles of 20^o off the normals to the house floors, this is not true for the entire house cover areas. However, as dA_1 varies from 20^o, two things occur. If dA_1 moves toward a vertical position with respect to the house floor (i.e., the 20^o angle approaches 0^o), the amount of reflected radiation declines relative to I_H, but the percentage of I_R striking dA_2 increases. If dA_1 moves toward a horizontal position with respect to the house floor (i.e., 20^o angle approaches 90^o), these two factors move in opposite directions. Therefore, these two factors counteract each other, thereby diminishing the range of variation in I_R from the house cover due to changes in angles of dA_1 or dA_2.

I_R from the reflecting house cover is of primary significance over a section of house cover about 39 m long and 3 m wide on each side of the house, or about half of the total house cover surface. The effective receiving house cover surface area is about the same size.

From this it can be seen that the adjacent house covers contribute a relatively minor amount to the total irradiance upon a house-cover at CEVCO (about a 1.2% in I, where I = 500 lys·day^{-1}).

Reflected solar radiation and east-west versus north-south houses. Unlike the diffusely reflected radiation from gravel and filon, available specularly reflected radiation from snow is highly dependent upon the angles of incidence and solar position and the amount of direct radiation. The evaluation of specularly reflected radiation from snow onto a CEVCO house uses the methods outlined in reference 58, pp. 331-334.

Figure 26 illustrates the basic angular relationships for direct radiation (I_D) striking the snow-covered area A_1, between CEVCO houses and then being reflected onto dA_2, a small section of a house cover. While Figure 26 indicates the houses to be oriented N-S, similar angular relationships exist for an E-W oriented house. In Figure 26, θ_1 is the angle of incidence for a direct ray I_D striking surface A_1 (N indicates a normal to the surface), while angle θ_R is the angle of incidence for reflected ray I_D to the surface dA_2. Angle α_2 is the wall-solar azimuth angle when $\phi = 0^o$, where ϕ is the angle of inclination of dA_2 from a vertical position. Like before, angle ϕ for the house cover equals 0^o at ground level and increases to 90^o at the ridge of the house. Of course, θ_R will vary as ϕ varies; thus the actual amount of intercepted radiation I_R will depend upon the point of incidence on the house cover. Distance a is the distance between A_1 and the center of dA_1.

Dimensions b and c are the dimensions of A_1, with b being constrained by the position of the adjacent house and the length of shadow that it casts.

Calculation of I_R from the snow surface A_1 is: $I_R = \rho \cdot I_{D,1} \cdot \cos \theta_R$ where, ρ = .70 for clean, smooth snow; $I_{D,1}$ = average day direct solar radiation; θ_R = angle of incidence upon dA_2 for direct radiation reflected from dA_1; and it has been shown that, $\cos \theta_R = \cos \beta \cdot \cos \alpha_2 \cdot \cos \phi - \cos \theta_1 \cdot \sin \phi$. Further, for $0^o \leq \phi \leq 90^o$, three conditions must be satisfied for I_R to occur:

(1) $\tan \phi \leq \frac{\cos \beta \cdot \cos \alpha_2}{\cos \theta_1}$, (2) $\tan \phi \leq \frac{b}{a}$, and (3) $\frac{\sin \beta}{\cos \theta_1} \leq \frac{c}{a}$.

Before proceeding to calculate I_R on December 22, it is important to examine the effects of adjacent houses upon the value of b (see Figure 26). The length of the shadow cast in the b direction (i.e., b_s) can be shown to be: $b_s = h_h \cdot \cos \beta \cdot \cos \alpha_2$, where h_h = house height = 3.83 m at CEVCO, and α_2 is the wall-solar azimuth angle for the shading house, assuming the house to be represented by a vertical surface. On December 22, at hourly intervals, N-S and E-W houses will cast shadows of the lengths shown in Table 4. Figure 20 provides a continuous graph of the needed space between CEVCO houses necessary to avoid shading on December 22 at CEVCO.15/ For CEVCO houses, the radius of each house cover equals 3.83 m and there are 4.3 m between houses. If CEVCO were to reorient its houses onto an E-W axis and use the same spacing, then the area between houses would never receive any direct solar radiation (I_D) on December 22 and, therefore, no I_{DR} from the snow between houses would occur for A_2. Table 5 gives values of $\cos \theta_R$ and langleys·hour^{-1} on December 22 at CEVCO for several times and values of ϕ. Remember, like the previous analyses of I_R, the distribution of solar radiation is assumed to be symmetrical around solar noon. The calculation of values in Table 5 assumes dimension b of surface A_1 in Figure 26 to be infinite. In fact, this is not true for current house spacings at CEVCO and no values for I_R would occur in the column $\phi = 60^o$ under CEVCO's existing house spacing.

Table 4. Lengths of shadows cast in a direction perpendicular to the house length on December 22 at CEVCO.

Local Solar Time	House Orientation	Shadow Length (b_s)
0800	N-S	70.8 m
	E-W	54.0 m
0900	N-S	14.0 m
	E-W	16.0 m
1000	N-S	6.3 m
	E-W	11.5 m
1100	N-S	2.6 m
	E-W	10.1 m
1200	N-S	0.0 m
	E-W	9.7 m

For reflected radiation I_R from the snow in front of an E-W oriented CEVCO house to occur at 0900 hours on December 22 at $\phi \leq 60^o$ at least 16 m between houses must exist, instead of the current 4.3 m. However, with this additional spacing an E-W oriented house should receive more than three times the average I_R from snow that a comparably spaced N-S house receives. Further, an average of 65% of the reflected radiation I_R can be expected to be transmitted by an E-W house cover versus 43% for a N-S house cover. Even with only 3 m additional spacing, an E-W house is expected to receive more I_R from the snow on December 22 than a N-S house because during the period of greatest solar irradiation

(around solar noon) a N-S house receives virtually no I_R while an E-W house receives as much as 9 $lys \cdot hr^{-1}$ along its lower sides, or about 60% of the measured I_{DH} at that time. Thus, from Table 5 it is apparent that an E-W oriented house has a significant advantage in the amount of reflected radiation I_R received from surrounding snow surfaces and the amount of I_R transmitted through the house cover.

Table 5. Computed values of I_R from snow on December 22 for CEVCO houses at various ϕ angles and times for both N-S and E-W orientations values of cos θ_R.***

Local Solar Time	House Orientation	ϕ 10°	ϕ 20°	ϕ 30°	ϕ 40°	ϕ 50°	ϕ 60°	$I_{D,1}$** $lys \cdot hr^{-1}$
0800	N-S	.775	.732	.667	.581	.478	.360	1.97
	E-W	.589	.555	.503	.436	.357	.266	
0900	N-S	.608	.549	.473	.383	.281	.171	7.06
	E-W	.698	.635	.552	.453	.340	.217	
1000	N-S	.403	.335	.257	X	.080	X	11.3
	E-W	.782	.697	.590	.466	.327	.179	
1100	N-S	.174	.105	.033	X	X	X	14.0
	E-W	.834	.735	.614	.474	.319	.155	
1200	N-S	X*	X	X	X	X	X	15.0
	E-W	.852	.748	.622	.476	.317	.147	

I_R (in $lys \cdot hr^{-1}$)

Local Solar Time	House Orientation	ϕ 10°	ϕ 20°	ϕ 30°	ϕ 40°	ϕ 50°	ϕ 60°	$lys \cdot hr^{-1}$
0800	N-S	1.07	1.01	.919	.801	.659	.497	.826
	E-W	.812	.765	.694	.602	.492	.366	.622
0900	N-S	3.00	2.71	2.34	1.89	1.39	.844	2.03
	E-W	3.45	3.14	2.73	2.24	1.68	1.07	2.39
1000	N-S	3.18	2.64	2.03	1.35	.632	X	1.64
	E-W	6.16	5.48	4.65	3.67	2.58	1.41	3.99
1100	N-S	1.71	1.03	.324	X	X	X	.511
	E-W	8.19	7.22	6.02	4.65	3.13	1.52	5.12
1200	N-S	X	X	X	X	X	X	0
	E-W	8.95	7.86	6.53	5.00	3.32	1.54	5.53

Column Sums - 5.01
17.7

* The X's indicate no I_R occurs. It is assumed here that no adjacent houses exist.

** Calculated from $I_T \simeq I_{tm} \cdot \sin(\pi \cdot t \cdot N^{-1})$, where: I_t = total solar radiation at t hours after sunrise, I_{tm} = maximum irradiation at solar noon = .25 $lys \cdot min^{-1}$ of direct radiation, N = daylength in hours = 8.77 hours, and t = hours after sunrise. Total solar irradiation per day is assumed to be 125 lys (41, pp. 31-32; 3, p. 16).

*** Comparisons of the effects of incidence angle θ_R upon the amount of I_R transmitted through the house cover may be done using Table 7 for CEVCO. With a layer of corrugated fiberglass covered with polyethylene, an expected 3% more I_R should enter an E-W versus N-S house due to improved angles of incidence for a larger proportion of I_R.

In summary, Table 6 compares the values derived in this section for various sources of reflected radiation, I_R, upon CEVCO houses oriented either N-S or E-W. The estimated value of I_R on December 22

for an E-W house versus a N-S house is about three times greater and in itself constitutes about 23.8% of the average daily irradiation on a horizontal plane (I_H). However, this increase in I_R requires an approximately four-fold increase in house spacing. But even with only a 3-m increase in house spacing, I_R is estimated to be significantly greater for an E-W versus N-S house of CEVCO design. In the summer, values of reflected radiation I_R are estimated to be approximately equal for E-W versus N-S oriented CEVCO houses. Of course, with a different house design this may not be true.

Table 6. Estimated values of mean daily reflected solar irradiance upon a CEVCO house.

Reflecting Surfaces (A_1)	December 22*	June 22**
Area between N-S houses	10.0 lys·day^{-1} over 2/3 of house cover area****	14.6 lys·day^{-1} over 2/3 of house cover area
	8%	2.9%
Fiberglass panels of adjacent houses***	< 1 lys·day^{-1} over 2/3 of house cover area	2.9 lys·day^{-1} over 2/3 of house cover area
	<1%	<1%
Area in front of E-W house	29.8 lys·day^{-1} over 2/3 of house cover area****	14.6 lys·day^{-1} over 2/3 of house cover area with same distance between houses as N-S
	23.8%	2.9%

* Mean daily solar irradiance assumed to be 125 lys.
** Mean daily solar irradiance assumed to be 500 lys.
*** Houses assumed to be 4.3 m apart.
**** Area between houses assumed to be 17.4 m wide, or approximately 4 times the existing spacing.

Percentage figures indicate what percentage of I_H (i.e., 125 lys·day^{-1} or 500 lys·day^{-1}) each estimated I_R level constitutes. No adjustment is made for possible variations in actually available PAR to the crop due to house shape factors or house cover transmissivities.

Shape Factors and CEVCO Houses

Shape factors are ratios expressing the proportion of radiant energy intercepted by an object's surface relative to the irradiance of a horizontal surface. For example, a surface normal to direct solar radiation will intercept considerably more radiant energy per unit area than a corresponding unit area on a plane parallel to the earth's surface, such as the pyranometer at the University of Minnesota. Shape factors may be used to adjust irradiation measured on a horizontal plane to that intercepted by some nonhorizontal structure. A shape factor is computed as the ratio of the shadow cast by an object on the earth's plane (A_h) to its own irradiated surface area (A). Basic shapes are used here, and the analysis is a basic geometric analysis of such forms as discussed by Monteith (41, pp. 39-58).

The shape factor (K_s) of a N-S oriented CEVCO house varies with season and hour, being one at solar noon if the house ends are ignored and the crop canopy area is assumed to be A; being symmetric around solar noon and increasing as the sun approaches the horizon. Thus, the most significant shape factor for a N-S house will occur at times of low solar altitudes. However, the actual significance of the K_s values of a N-S house is diminished for several reasons. First, except for a small portion of the house cover, most of the shadow cast by the house falls within the crop area. Second, when a significant K_s does occur the angle of incidence is fairly large ($> 45^o$), so the proportion of irradiation transmitted through the house cover is significantly less (Table 7). Third, because shape factors are only relevant to direct radiation, only that portion of irradiation which is diffused by the house cover into the crop canopy, plus that portion of direct radiation which is reflected into the crop canopy as it attempts to exit the house on the opposite side is available to the crop. Fourth, the most significant shape factors for a N-S house occur during the periods of lowest solar irradiation, thereby reducing the significance of K_s.

Examination of CEVCO house shape factors (K_s) for June 22 and December 22 is straightforward. Figure 27 indicates that angles used to define K_s where, $K_s = \frac{\sin \varepsilon \cdot \cot \beta \cdot \cos \alpha + \cos \varepsilon}{1.414}$. In this analysis, the shape of a CEVCO house is represented by an inclined plane at an angle $\varepsilon = 45^o$ with respect to the floor of the house. $K_s = (A_h) \cdot (A)^{-1}$, where in this case A is defined as the area of the crop canopy surface. Consequently, the formula for K_s is divided by 1.414 to adjust for the size of A.

The calculated values of K_s at hourly intervals for both N-S and E-W oriented CEVCO houses on these two dates are given in Table 8. Where $K_s = 1$, no shadow is cast by the house, ignoring the house ends. On June 22, the sun rises at 0412 hours LST, but the effect of the shape factor before 0600 hours on a N-S house is not included as it is balanced by the shading effects of adjacent houses amounting to about 8 lys·day^{-1} on the crop canopy. The weighted factor in Table 8 adjusts the K_s values to the hourly variation in solar irradiation, which is maximum, on the average, at solar noon. Table 8 indicates that on December 22 an E-W oriented house exceeds a N-S oriented house in received solar irradiation due to K_s. On the other hand, on June 22 the N-S house exceeds the E-W house in received solar irradiation due to K_s. Again, as the previous section on reflected radiation (I_R) received by a CEVCO house emphasized, an E-W house orientation is best at CEVCO because during winter months greater solar irradiation is obtained due to K_s, while during the summer months, when cooling and excess solar irradiation are problems, less solar irradiation is recevied than with a similar house oriented N-S.

The estimation of actual levels of irradiation upon the crop canopy caused by the house shape factor K_s cannot be derived directly from Table 8. However, the following four equations calculate this irradiance due to K_s for both a N-S and an E-W oriented house on December 22 and June 22 at CEVCO:

June 22:

lys·day^{-1} for N-S house = (2)·(.45)·(1.74)[(4.8)·(1.13) + (7.2)·(.49) + (8.4)·(.16)] = 16.1 lys·day^{-1} on the crop canopy.

lys·day^{-1} for E-W house = 0 lys·day^{-1} because K_s never exceeds 1.

December 22:

lys·day^{-1} for N-S house = (2)·(.45)·(1.74)[(.6)·(.874)·(.75) + (4.2)·(1.33) + (7.2)·(.32)] = 18.5 lys·day^{-1}.

lys·day^{-1} for E-W house = (2)·(.45)·(1.74)[(.6)·(6.55)·(.75) + (4.2)·(1.59) + (7.2)·(1.0) + (9.6)·(.82)] + (10.2)·(.77)·(.45)·(1.74) = 44.9 lys·day^{-1},

where:

(2): Doubles the values to account for the symmetry of solar irradiation around solar noon.

(.45): That portion of direct solar irradiation trapped by the house cover due to K_s and diffused onto the crop canopy.

(1.74): Derived from Table 7, is the relative increase in diffuse solar radiation caused by the passage of direct solar radiation through corrugated fiberglass at an angle of incidence equal to 67^{o}.

[ ]: The values within brackets are the hourly products of K_s times the estimated hourly values of average diffuse solar radiation at CEVCO (from reference 3, pp. 10, 16). For December 22, the 0800 hours shape factor K_s is reduced by 25% to reflect the rapid change which occurs in shadows (i.e., K_s) for small changes in solar altitude angle β when it is small.

Comparison of these computed mean irradiation values indicates that due to K_s: (1) On December 22 at CEVCO, an E-W house should exceed a N-S house in received solar irradiation by 26.4 lys·day^{-1} on the average, with an estimated yield effect of about 23 kilograms (kg) of tomatoes per house-month (reference 8). (2) On June 22, an average reduction of about 16 lys per day on the crop canopy can be expected with an E-W versus N-S house. This constitutes about 2.9 Mcal less energy needed to be removed from a house each day in the summer.

Recently, considerable interest has been given to the idea of closing the north wall on an E-W house with a reflective surface in an attempt to not only reduce heat loss, but also to increase the net solar irradiation of the crop (reference 66). It is apparent from this brief discussion of shape factors that house shape and orientation have considerable influence upon crop solar irradiation. However, in areas where solar irradiation is highly diffused by clouds, dust, or other factors, the expected gains from house shape, which is dependent upon collecting direct solar radiation, will diminish (this is also true for reflected radiation).

Table 7. Energy transmission of nine house cover materials for various angles of incidence and with a top layer of polyethylene.

Reference Number	Material*
1	Polyethylene, 4-mil
2	Flat fiberglass, regular, 25-mil
3	Flat fiberglass, premium, 40-mil
4	Polyester, weatherable, 5-mil
5	Corrugated fiberglass, 40-mil
6	Corrugated fiberglass, 40-mil
7	Glass, double strength window, .3175 cm
8	Polycarbonate, .1588 cm
9	Polyvinylfluoride, 3-mil

* Sample No. 4, polyester, was Mylar (registered by E. I. DuPont de Nemours and Co.) with a weatherable surface treatment by Martin Processing Co., Martinsville, Virginia. Samples No. 5 and 6, corrugated fiberglass, were both polyvinylfluoride coated, but from different manufacturers. Sample No. 8, polycarbonate, was Lexan (registered by General Electric Co.). Sample No. 9, polyvinylfluoride, was Tedlar (registered by E. I. DuPont de Nemours and Co.).

Table 7 (continued). Single glazing materials.

Material Reference Number	Longwave[a] Transmission %	Type[b]	Solar energy transmission,[c] [d]% angle of incidence, degrees 0	14	30	45	60	67
1	80	Tot.	92	91	88	86	82	67
		Dir.	84	84	82	80	71	60
		Dif.	20	12	16	24	78	45
		PAR	83	82	82	83	74	58
2	12	Tot.	87	84	82	80	73	57
		Dir.	65	66	62	60	51	34
		Dif.	82	59	78	99	176	262
		PAR	83	82	83	79	69	57
3	6	Tot.	77	78	75	65	46	33
		Dir.	11	10	9	8	7	6
		Dif.	200	220	227	257	254	191
		PAR	75	74	76	65	44	30
4	32	Tot.	88	88	88	86	81	72
		Dir.	87	87	86	84	79	72
		Dif.	-7	-8	-5	-5	3	-23
		PAR	85	85	84	81	77	70
5	8	Tot.	83	83	82	80	62	43
		Dir.	38	37	32	24	21	12
		Dif.	132	139	171	252	273	318
		PAR	79	84	82	71	62	51
6	7	Tot.	81	80	78	75	64	43
		Dir.	52	55	51	45	33	21
		Dif.	66	64	76	118	182	174
		PAR	70	72	73	63	54	43
7	3	Tot.	89	89	88	85	82	74
		Dir.	88	88	87	85	81	70
		Dif.	-10	-9	-11	-9	-14	-6
		PAR	88	90	89	86	81	73
8	6	Tot.	86	85	84	83	80	72
		Dir.	84	84	83	82	76	68
		Dif.	-6	-7	-10	-10	17	28
		PAR	84	85	84	81	76	70
9	43	Tot.	93	92	91	90	83	65
		Dir.	85	85	85	78	66	48
		Dif.	22	17	16	52	122	136
		PAR	89	90	89	86	80	69

Table 7 (continued). Combination glazing materials (polyethylene as top cover).

Bottom Cover Material	Longwave[a] Transmission %	Type[b]	Solar energy transmission,[c] % angle of incidence, degrees[d] 0	14	30	45	60	67
Polyethylene	63	Tot.	83	82	81	75	59	37
		Dir.	58	56	53	45	30	17
		Dif.	151	152	193	262	527	844
		PAR	76	78	76	70	57	40
Flat fiberglass	5	Tot.	77	78	75	72	59	35
		Dir.	55	58	54	45	34	16
		Dif.	82	94	119	212	315	272
		PAR	73	76	73	69	54	44
Flat fiberglass	3	Tot.	67	67	64	53	33	22
		Dir.	7	7	8	6	5	3
		Dif.	327	336	420	520	590	551
		PAR	63	63	61	55	35	21
Polyester	21	Tot.	81	81	78	77	67	52
		Dir.	70	71	67	63	59	41
		Dif.	132	98	195	506	360	1362
		PAR	73	75	73	68	58	49
Corrugated fiberglass	4	Tot.	72	72	71	61	49	23
		Dir.	26	27	24	20	18	6
		Dif.	146	150	185	192	378	166
		PAR	65	66	65	59	48	37
Corrugated fiberglass	4	Tot.	70	71	68	61	47	22
		Dir.	45	45	45	33	24	8
		Dif.	71	85	83	165	185	59
		PAR	65	65	63	60	42	31
Glass	1	Tot.	81	80	79	76	66	54
		Dir.	73	68	67	64	57	45
		Dif.	48	83	116	144	231	524
		PAR	78	79	78	74	65	47
Polycarbonate	2	Tot.	78	75	72	70	57	36
		Dir.	65	65	60	56	39	23
		Dif.	88	69	96	138	171	280
		PAR	76	75	74	72	62	48
Polyvinylfluoride	31	Tot.	86	84	82	78	66	45
		Dir.	70	68	66	59	44	28
		Dif.	155	160	181	335	724	1677
		PAR	79	79	78	75	61	46

[a] Longwave > 2.8 m.

[b] Type of solar energy flux transmission measurement:
Tot. - Total solar energy - direct plus diffuse (0.28 to 2.8 μm).
Dir. - Direct beam component of the total solar energy.
Dif. - Percent of change in diffuse radiation due to cover materials.
PAR - Photosynthetic active radiation (0.4 μm to 0.7 μm).

[c] Shortwave < 2.8 μm.

[d] Angle of incidence between collector and sun, degrees.

Source: 6, ERRATA - Tables 1, 2, 4.

Table 8. Shape factors for a CEVCO house on December 22 and June 22 for E-W and N-S orientations.

Local Solar Time	December 22				June 22			
	N-S house		E-W house		N-S house		E-W house	
	Shape Factor (K_s)	Wtd. Factor	Shape Factor (K_s)	Wtd. Factor	Shape Factor (K_s)	Wtd. Factor	Shape Factor (K_s)	Wtd. Factor
0600 hours	none	none	none	none	2.13	15.3	1	7.2
0700 hours	none	none	none	none	1.49	23.2	1	15.6
0800 hours	9.74	29.1	7.55	22.5	1.16	29.2	1	25.2
0900 hours	2.33	25.0	2.59	27.8	1	39.0	1	39.0
1000 hours	1.32	22.6	2.00	34.2	1	48.0	1	48.0
1100 hours	1	21.3	1.82	38.8	1	53.4	1	53.4
1200 hours	1	22.8	1.77	40.4	1	54.0	1	54.0
Mean Wtd. Factor		24.2		32.7		37.4		34.6

The shapes used are simplified where: A = crop canopy area; the west or south wall, depending upon house orientation, is represented by a flat plane at an angle $\varepsilon = 45^{o}$. Therefore, the shape factor $K_s = 1$ when no shadow is cast by the house (i.e., $\{\sin \varepsilon \cdot \cot \beta \cdot \cos \alpha + \cos \varepsilon\} = 1.414$ for $K_s = 1$). The Wtd. Factor is simply the shape factor times the average daily diffuse plus direct radiation for that hour, in $lys \cdot hr^{-1}$.

House Covers

Comparing house covers. The effects of greenhouse covering materials upon the cost effectiveness of a greenhouse are multiple. The covering material will alter the net mean irradiance of the crop, thereby affecting yields. It will also affect rates of heat loss via infiltration, long-wave transmission, and conductivity. Further, cover materials can differ in capital investment expenses, installation and maintenance costs, durability, insurance costs, effectiveness of CO_2 retention, fire resistance, ease of replacement if damaged, effects on cooling methods and costs, use of shading compounds, PAR reduction due to water condensation, and building code qualifications. No comprehensive analysis of the economic tradeoffs among these factors has been found.

Figures 28 and 29 show that a significant deterioration occurs in transmitted spectral energy distribution (SED) levels through polyester fiberglass panels as they weather. It is apparent at CEVCO that a similar reduction in transmittance has occurred with the aging of the house covers, but unfortunately no precise figures are available. Further, no significant yield variations over time are identifiable during the period of observation. However, it is probable that such a factor is confounded with annual variations in other significant independent variables.

Table 7 provides some basic comparisons of house cover materials. It gives measurements of transmittance of PAR for several materials at increasing angles of incidence (θ) to solar irradiance. Notice that a significant decline in transmittance of PAR above a 30^{o} angle of incidence occurs for corrugated fiberglass panels similar to CEVCO's (material reference number 6 in Table 7). A marked reduction in PAR transmittance is also shown to occur with the use of an overlayer of polyethylene, as done at CEVCO during the winter months.16/

Table 7 also shows that fiberglass panels are relatively good at limiting longwave radiation heat loss, but unlike sheeting, such as polyethylene, infiltration losses on poorly sealed fiberglass

panels (e.g., CEVCO houses) can cause a 10-15% increase in heat losses (62, p. 55). The use of two layers of polyethylene or polyethylene over fiberglass or glass panels is becoming an accepted means of cutting heat costs, but at the expense of PAR transmittance as Table 7 shows.17/

In Table 9, T. E. Bond, et al. (reference 6) have compiled an index for categorizing house cover materials on the basis of longwave transmission, shortwave transmission, and initial cost of the material. By this index CEVCO's house covers, without polyethylene rank in the bottom 15%, but with polyethylene rank in the upper 40% of all house covers indexed. However, this scaling places primary emphasis upon longwave radiation transmission and, as the authors emphasize, can cause very misleading conclusions. A comprehensive index must be weighted to reflect yield variations, heating variations, and all cost variations due to the factors previously listed if it is to be viable.

CEVCO house cover transmissivity. The estimation of a net mean PAR transmission factor for CEVCO houses during the months of high solar irradiation for the purpose of estimating artificial light requirements needed to achieve yields equivalent to those achieved under solar radiation is not an accurate procedure. Nevertheless, it is the most practical approach, given the available data at CEVCO. Further, it helps emphasize the factors which significantly affect greenhouse crop solar irradiation.

Aldrich and White (1, pp. 994-996) recorded comparative solar energy levels inside and outside a miniature fiberglass, N-S oriented, quonset-style greenhouse over two winter seasons on 9 selected days. The mean daily in-house irradiation at the center of their house at crop height for these 9 days as a percent of the outdoor horizontal pyranometer readings is 67%. However, in order to utilize such a figure at CEVCO, four factors must be accounted for: (1) differences in the SED curves measured, (2) variations in the physical integrity of the fiberglass panels, (3) variations in shading, and (4) variations in the angle of incidence when shifting away from the path of solar rays followed to the center of the house.

First, comparing the full spectrum recordings measured by Aldrich and White versus the PAR recordings shown in Table 7, indicates that a mean difference of 4% exists between the transmittance of total irraidation versus PAR across the six angles of incidence measured for corrugated fiberglass. Adjustment for this variation reduces the 67% to 63%. Second, the physical integrity of CEVCO's fiberglass panels has deteriorated significantly over the period of observation. For this reason the transmittance values for the lower quality corrugated fiberglass (reference number 6 in Table 7) evaluated by Bond et al. are used, where a mean difference in overall PAR (i.e., photosynthetically active radiation) measurements between house covers 5 and 6 of 9% exists. Third, more shading occurs in CEVCO houses due to overhead polytubes, heavy condensation in winter months, dirt accumulation, and opaque house ends than for the Aldrich-White house. Reductions in estimated radiant energy levels due to this shading will be made later. Finally, solar rays striking at the center of a hemispherical house cover generally experience more optimal angles of incidence at the point of incidence on the house cover, for a given solar altitude angle (β), than other solar rays striking the house cover. Variations in the angle of incidence will occur due to variations in angles β, α and ϕ (Figure 30). Consideration of the general pattern of such changes for June 22, the longest day of the year, indicates that some adjustment of the 63% mean transmittance estimate is necessary.

Figure 136 shows the relationship between height Y versus horizontal distance X from the west side of the house at crop canopy height (1.52 m). This ratio is used to determine the point of incidence on the house cover for a direct solar ray striking the west bed crop canopy in a N-S oriented CEVCO house before solar noon.

Table 9. Comparison of house covers.

1976 estimates

	Reference Number	Longwave Transmission, %	Daily Average Shortwave Transmission, %	Initial Cost ¢ .0929 m^{-2}
		Single glazing		
Polyethylene, 4-mil	1	80	88.8	2
Flat fiberglass, 25-mil	2	12	83.1	28
Flat fiberglass, 40-mil	3	6	72.9	42
Polyester, weatherable, 5-mil	4	32	86.5	18
Corrugated fiberglass, 40-mil	5	8	79.2	55
Corrugated fibergalss, 40-mil	6	7	78.1	49
Glass, double strength, 3.175 mm	7	3	87.8	50
Polycarbonate, 1.59 mm	8	6	84.4	250
Polyvinylfluoride, 3-mil	9	43	91.0	17

Source: 6, ERRATA, Table 13.

1972 estimates

Material	Initial Cost ¢ 929 cm^{-2}	Installation Labor Cost ¢·929 cm^{-2}	Years Expected Life	Maintenance Cost, Avg. per Year 929 cm^{-2}	Cost per year per 929 cm^2
Poly (4,6 mil)	1 to 1½¢	1½ to 2¢	1	-	2½-3½¢
Poly UV (4,6 mil)	2 to 2½¢	1½ to 2¢	2	-[b]	2-2½¢
Vinyl (8,12 mil)	6 to 9¢	1½ to 2¢	4	½¢[b]	2-3¢
Fiberglass, 15% acrylic modified					
(4 oz)	20 to 25¢	1½ to 2¢	8-10	1½¢[c]	3-3½¢
(5,6 oz)	30 to 35¢	1½ to 2¢	12-15	1½¢[c]	2¼-2½¢
Tedlar coated,					
(5,6 oz)	40 to 55¢	1½ to 2¢	15-20	½¢[b]	2½-3¢
Glass	50¢	2 to 3¢	30+	1-1½¢[d]	2 to 3¢

[a] Estimated; actual costs depend on quantity price of materials, quality of product, local wages, type of house, and skill of the installation crew.

[b] Washing every year or two to remove dust, pollution, etc. Estimated one man to wash and clean (maybe scrub) entire surface of 9.1 m x 18.3 m house in 8 hours @ $2 per hour.

[c] Washing every year or two as above, then smoothing with steel wool and applying resealing resin every 4 to 5 years. Labor estimated as above for washing (½¢) doubled for resealing process (1¢) with resin sealer cost added (3¢) and pro-rated over 4- to 5-year interval (1¢ + 3¢ ÷ 4 to 5 years = 4/5 to 1¢ per year).

[d] Glass maintenance depends mainly on cleaning, replacement of broken panes, and reglazing of loose panes. Maintenance costs estimated as 1/2 man-day (4 hours) per month for a 929 m^2 house, $2 per hour, $50 per year for materials.

Source: 10, p. 7.

Table 9 (continued).

Value indices of single and two-layer combinations of greenhouse and solar collector glazing materials based on percent longwave energy transmission, percent shortwave energy transmission, and material cost. The lower the index number, supposedly, the better the house cover material.

	BOTTOM COVER									
TOP COVER	Single Cover	1	2	3	4	5	6	7	8	9
1	311	331	142	162	331	153	153	133	147	321
2	222	242	153	173	142	154	164	144	147	132
3	142	162	173	174	163	174	174	164	167	163
4	311	331	142	163	232	153	153	133	147	322
5	233	143	154	174	143	165	165	145	157	144
6	232	153	154	174	153	165	164	154	157	143
7	112	133	144	164	133	155	154	134	147	123
8	127	147	147	167	147	157	157	137	147	137
9	311	321	132	163	222	143	153	123	137	322

Cover material reference numbers are defined on preceding portion of table.

LEGEND FOR NUMEERS

1st Number of Index	Longwave Transmission %	2nd Number of Index	Shortwave Transmission %	3rd Number of Index	Cost ¢·929 cm^{-2}
1	6 or less	1	>85	1	25 or less
2	7-20	2	80-85	2	26-50
3	>20	3	75-80	3	51-75
		4	70-75	4	76-100
		5	65-70	5	101-150
		6	60-65	6	151-200
		7	<60	7	>200

Source: 6, ERRATA, Table 13.

Given the solar altitude (β) and azimuth (γ) angles, it is possible to determine the angle of incidence (θ) with respect to the house cover. For example, at 1000 hours on June 22 $\beta = 57.5^{o}$ and $\gamma = 121.4^{o}$ (Table 10). Therefore, in Figure 30, $\alpha = 31.4^{o}$ and $X = \frac{Y \cdot \cos \alpha}{\tan \beta}$ or, $X = .544\ Y$ (Table 10). Thus, direct solar rays, which strike the west bed at 1.52 m above ground level, will intersect the fiberglass house cover along a N-S line with an X/Y ratio of .544 derived as shown in Figure 30 (ignoring diffraction). This X/Y ratio, when plotted against the ratio of X to Y determined by the physical house dimensions, determines one unique combination of X and Y. Figure 31 shows the ratio of X/Y for all combinations of X and Y fixed by the house dimensions. From this, angle ϕ is calculated (Figure 30) where, $\phi = \arcsin \frac{Y + 1.52}{3.96} = 32^{o}$ at 1000 hours. Also: $\theta = \arccos \{\cos \beta \cdot \cos \alpha \cdot \cos \phi + \sin \beta \cdot \sin \phi\}$ where θ = angle of incidence and angle α is the difference between γ and the projection in the plane of the floor of the normal to the plane tangent to the house cover at the line of incidence (Figure 27).

Table 10. Weighted house cover transmittance coefficients for: June 22, 45° N latitude, west bed, CEVCO house.

Solar Hour	h	β	γ	lys[4]	lys weight[5]	Angle α[1]	Angle φ[2]	X/Y	Y[7]	Angle θ[3]	τ[8]	(lys·Wt)·τ[9]
0600	90°	16.34°	72.90°	.12	.217	17.10°	62°	3.26	1.98	47°	.61	.13
0700	75°	26.70°	82.75°	.26	.471	7.25°	77°	1.97	2.34	50°	.43	.20
0800	60°	37.28°	93.14°	.42	.760	176.86°	82°	1.31	2.40	61°	.52	.40
0900	45°	47.74°	105.29°	.65	1.18	164.71°	61°	.876	1.96	71°	.40	.51
1000	30°	57.48°	121.43°	.80	1.45	148.57°	32°	.544	.56	87°	.28	.41
1100	15°	65.23°	145.48°	.89	1.61	124.52°	25°	.261	.17	80°	.33	.53
1200	0°	68.45°	180.00°	.90	1.63	90.00°	23°	0.00	0.00	69°	.42	.68
1300	15°	65.23°	145.48°	.89	1.61	55.48°	23°	0.00	0.00	55°	.57	.92
1400	30°	57.48°	121.43°	.80	1.45	31.43°	23°	0.00	0.00	41°	.66	.96
1500	45°	47.74°	105.29°	.65	1.18	15.29°	23°	0.00	0.00	28°	.73	.86
1600	60°	37.28°	93.14°	.42	.760	3.14°	23°	0.00	0.00	15°	.72	.55
1700	75°	26.70°	82.75°	.26	.471	7.25°	23°	0.00	0.00	7.5°	.71	.33
1800	90°	16.34°	72.90°	.12	.217	17.10°	23°	0.00	0.00	17°	.72	.16
											Σ13.0	Mean = .51

1 Angle $\alpha = | \gamma - 90^\circ |$ where the wall of reference changes at solar noon.

2 Angle $\phi = \arcsin \frac{Y + 1.52\ m}{3.96\ m}$; where the closest value of Y is used from Figure 30 to satisfy

$$X = \frac{Y \cdot \cos \alpha}{\tan \beta}.$$

3 Angle $\theta = \arccos \{\cos \beta \cdot \cos \alpha \cdot \cos \phi + \sin \beta \cdot \sin \phi\}$ from Figure 27.

4 lys = values derived from reference 3, page 10 for June 21-27 and are approximately distirbuted as $S_t = S_{tm} \cdot \sin (\pi \cdot t \cdot N^{-1})$; where: S_t = total solar radiation at t hours, S_{tm} = maximum solar irradiance at solar noon ≃ .9, t = # hours after sunrise, and N = daylength in hours.

5 Weight = (lys for 1 hour)·(mean total daily langleys for all hours ≃ .55 lys)$^{-1}$.

6 X/Y is the ratio of run to rise as determined according to Figure 30.

7 Y is the height from the top of the crop canopy to the house cover, which satisfies the ratio X/Y which is dependent upon α and β. Y is required to solve for φ.

8 τ is the transmissivity of PAR for polyvinylfluoride-coated, corrugated, fiberglass panels at the angle of incidence θ. The values of τ are interpolated from Table 7.

9 (lys weight)·(τ) is the weighted τ values based upon the sinusoidal distribution of irradiance during the day. The mean of these daily values is the expected mean value of solar transmittance to the west bed of a CEVCO house during June 22.

With the determination of angle θ for each hour on June 22, it is possible to estimate the transmissivity of the house cover for PAR (see Table 10) from Table 7.

At solar noon the direct solar rays strike the house ridge at an angle of incidence equal to 90° - β (i.e., 21.5° on June 22), but the angle of incidence increases as the rays strike the house cover further from the ridge, reaching 90° (i.e., parallel to the house cover at the point where the

hemispherical house cover joins the floor) at ground level. In the afternoon the irradiance of the west bed improves considerably, approaching 0^{o} angle of incidence upon the west bed at 1700 hours. However, at that time the west side of the house is also starting to be shaded by the adjacent house.

The east bed in each house follows the same cycle except in reverse order because the solar angles are symmetrical around solar noon. The cropping area between the outside beds falls between the extremes of the outside beds and the center bed. Thus, for half of each day each house side receives irradiation varying from the value at the center of the house to that occurring at an angle of incidence reaching nearly 90^{o}. For the other half day, the angle of incidence improves until it is near zero.

It is to be expected that the mean irradiance levels at the crop canopy surface of the outside beds will vary from that occurring at the house center by a weighted average of the cycle just outlined. The weights used here adjust the significance of the angles of incidence to the mean direct irradiance level occurring at that time of day. Table 10 lists these estimated weights and the product of the hourly weights times transmissivities for June 22, with a mean daily value of .54 for each outside bed. Although maximum solar irradiation at the crop canopy surface occurs at the center house bed, the maximum yields per bed normally occur in the outside beds, particularly the east bed, probably because solar penetration into the crop canopy is greatest at these locations. Other related factors such as temperature and air velocity may also be more advantageous in the outside bed regions.

The mean transmissivity for the entire house on June 22 is then calculated as the mean of the extremes (i.e., (.69 + .51)/2), yielding a transmissivity coefficient of .60. This value is used to adjust the mean monthly recorded langleys of direct plus diffuse irradiation. Even though diffuse solar radiation does not have a single angle of incidence, usually it is emitted from the same area in the sky as direct solar radiation and is assumed to be attenuated in similar proportion as that of direct radiant energy (41, p. 30 for further explanation).

In conclusion, the estimated mean house transmissivity, .6, is considerably less than the .67 actually measured by Aldrich and White (1). However, if this same method is utilized to calculate a mean daily transmissivity of PAR on June 22 striking the crop at the house center only, a value of .69 is derived. Given that Aldrich and White measured the full solar spectrum while only PAR transmissivities are used here (previous discussion), and given that these estimates are for June 22, while the Aldrich-White observations cover the period October-March at 40.8^{o} latitude (a period of reduced β (0^{o} - 47^{o}), and γ (101^{o} - 180^{o} angles), this estimated mean house cover transmissivity value appears reasonable.

Following a similar method of comparison for a N-S versus E-W CEVCO house on December 22, indicates the E-W orientation to be significantly better in mean house cover transmissivity coefficients. Table 11 lists the minimum and maximum angles of incidence which occur for direct solar radiation striking the crop canopy surface at 1.52 m height (Figure 30). Diffraction of the solar rays is assumed to be insignificant. The effects of the corrugations of the house cover are also considered insignificant based upon a discussion with T. E. Bond, one of the researchers who measured the data given in Table 7. In their research, they found that orientation of the corrugated fiberglass panels caused no significant difference in transmittance for a given angle of incidence.

Table 11 also lists the interpolated transmissivities for each angle of incidence as derived from Table 7. The estimated distribution of mean direct solar radiation for December 22 ($\bar{I}_{D}$) at each

Table 19. Spectral radiant energy from different lamps.

Light source	Light intensity (ft-c)	Energy from 400-720 mμ (cal/(cm^2 x min))	Energy (cal/(cm^2 x min x mμ x 10^5))				
			Blue 440 mμ	Green 533 mμ	Red 640 mμ	Far-red 740 mμ	Ratio red/far-red
Full light							
GL + I		0.09	34.8	19.3	53.1	10.2	5.2
CW + I		0.11	41.4	32.7	35.2	10.8	3.3
GL		0.07	26.5	13.6	45.6	1.6	29.5
CW		0.10	43.8	31.1	28.9	2.2	13.3
Twilight							
GL/2 + I		0.05	16.0	10.1	27.6	9.1	3.1
CW/2 + I		0.06	20.0	16.9	20.9	9.6	2.2
GL/2		0.03	12.2	5.9	20.4	0.8	25.6
CW/2		0.04	18.6	13.3	12.8	1.1	11.6

Abbreviations: GL = 26 gro-lux fluorescent tubes F96T12/VHO, 200 w each.
CW = 26 cool-white fluorescent tubes F96T12/VHO, 200 w each.
I = 44 frosted incandescent bulbs, 40 w each.
Source: 22, p. 463.

Table 20. Tomato seedling dry weight with fluorescent and incandescent lamps.

Lamps	Mgm dry wt. formed	Conversion factor μW per cm^2/fc	Mgm per microwatt/ cm^2
Cool white	370	3.28	.0823
Warm white	510	2.90	.1207
Daylight	360	3.66	.0901
Blue	440	7.66	.0901
Green	320	2.55	.0470
Gold	380	3.49	.0687
Pink	430	7.89	.0519
Red	170	12.30	.0886
Cool white & Incand.*	600	3.65	.1173
Warm white & Incand.*	720	3.27	.1620
Blue & Incand.*	560	8.03	.0747
Gold & Incand.*	560	3.86	.0188
Red & Incand.*	290	11.93	.0779
Red HA	620	12.30	.1373
Red HA & Incand.*	860	11.93	.1291

*Note: 5% of incandescent light added.
The data were recorded in footcandles and then converted to microwatts·cm^{-2}.

Source: 11, p. 304.

wintertime irradiation plus daylength extension from 0300-0800 hours for two weeks after transplanting, and normal wintertime irradiation plus daylength extension from 0300-0800 hours for 7 weeks after transplanting. Except for the details noted in Figure 32, cultural practices were uniform for all treatments and were in accordance with standard practice.

Table 21 shows the results of this experiment. The first section shows the effects of the seedling treatments upon tomato yields and size per plant. The growth chamber plants, under artificial lighting, were bigger, darker green, and had a more advanced first flower cluster. This difference in plant development persisted for nearly 6 weeks after transplanting. Furthermore, the chamber-grown transplants had greater yields and larger fruit size during the first 4 picking weeks.

Table 21. Tomato cultivar W-R25 responses to pre- and post-transplant artificial lighting.

Harvest Period (Weeks)	kg Fruit·Plant^{-1}		Fruit Size	
	Chamber	Greenhouse	Chamber	Greenhouse
1-4	.844 kg	.52 kg	173 g	125 g
5-8	1.64	3.89	157	159
9-12	2.64	5.88	170	173
13-16	1.11	2.53	135	140
Total	6.23	12.82 Ave.	158	149

Light Treatment	Number of Fruit Per Cluster						
	Cluster - 1	2	3	4	5	6	Total
Normal Light	2.88	3.31	2.79	3.79	4.48	4.79	22.04
Added-Transp. + 2 weeks	2.98	3.38	3.31	4.23	4.39	4.81	23.19
Added-Transp. to Feb. 28	2.88	3.60	3.02	4.15	4.83	4.91	23.39

Harvest Period (Weeks)	No. Fruit·Plant^{-1}			kg Fruit·Plant^{-1}		
	Light-normal	+2 Wks.	Thru Feb.	Normal	+2 Wks.	Thru Feb.
1-4	2.83	3.36	3.24	.499	.562	.562
5-8	10.45	10.64	10.82	1.66	1.74	1.70
9-12	15.16	15.46	15.75	2.64	2.66	2.66
13-16	7.88	7.79	8.90	1.09	1.08	1.22
Total	36.32	37.25	38.71	5.89	6.04	6.15

Source: 33, pp. 11, 13.

The effects of post-transplanting lighting variations are also reflected in Table 21. No significant differences in plants, fruit set of the first six clusters, or yields occurred between the three treatments. Any of several possible factors may have caused the lack of differences between treatments, including incorrect spectral energy distribution of artificially supplied irradiation, inadequate control of other environmental factors, insufficient plants per treatment to isolate statistically significant differences, and inappropriate application of artificial lighting. Even though these several factors exist, it may not be unreasonable to conclude that, in fact, the limiting environmental factor is not daily duration of PAR available, but rather the intensity of such irradiation. Tomato plants grown in growth chambers at the OARDC under levels of irradiation four to five times the levels used in this experiment averaged 4.28 fruits on the first cluster versus 3.3 in this experiment under daylength extension.

A study was also conducted at the GCRI to evaluate the effect of long days on early tomato yields (28, pp. 45-46). Two groups of tomato seedlings were grown under equal quantities of PAR (13.7 lys·day^{-1} in the 400-700 nm waveband), but with different distributions of the radiant energy.

Group one received 8 hours of 18 W·m^{-2} PAR followed by 8 hours of 2 W·m^{-2} PAR per day. Group two received 8 hours of 20 W·m^{-2} PAR per day. Group one had a 10% higher net assimilation rate than group two. The extended daylengths also delayed flowering by two nodes. It was thought that when low supplementary radiant energy was used to extend the daylength it may have acted to suppress nighttime respiration losses (26, p. 69).

A follow-up experiment extended the wintertime daylength to 16 hours, using various levels of radiant energy from artificial lights (28, pp. 45-46). The plants with extended days were taller, darker green, and had early yields 17-41% greater than the control plot, depending upon the level of supplementary irradiation. The control plants received normal solar irradiation only. However, the plants with extended daylength were unable to maintain the early increase in yields over the life of the crops so that the financial returns of the crops were equal. It may be that the control plot received higher levels of irradiation due to no shading by lights so that this accounted for the lack of significant difference in yields. Whatever the cause, this experiment substantiates the previously described experiment conducted at the OARDC and indicates that extending wintertime daylength with low levels of irradiation improves early yields, but not necessarily total yields or net financial returns.

Other studies with mature tomato plants include V. A. Helson's comparison of four combinations of incandescent lamps with Gro-lux and cool-white fluorescent lamps upon tomato fruit yields with the results shown in Table 22. The combination of Gro-lux plus incandescent produced the greatest number and weight of fruit, with the cool-white plus incandescent combination second. No comparison was made with solar radiation. However, Wittwer did compare the Gro-lux spectrum and cool-white lamps with solar radiation. Tomato plants were grown with supplemental CO_2 at 1000 ppm and daylength extension for 6 hours at 215 $W \cdot m^{-2}$ and harvested from October 15 to January 10. The results of the experiment are shown in Table 23. The Gro-lux wide-spectrum lamp with solar radiation was most effective, with an average yield increase of 39% over normal solar radiation for the three tomato varieties tested. The cool white plus normal solar irradiation caused an average yield increase of 31%. This experiment was similar to the one done at the OARDC and outlined in Figure 32 except that here CO_2 levels were raised by about 700 ppm. It would seem logical that this raised level of CO_2 must account for at least part of the difference in results. R. A. Norton of Washington State in the early 1970s briefly studied the effects of using artificial lighting with producing tomato plants but concluded that it was not economical (42).

Table 22. Mature tomato plant flowering and fruit yields under four different sources of radiant energy.

Characters	Light Sources: Gro-lux + incand.	Cool-white + incand.	Cool-white	Gro-lux	S.E.
Days to first flower open	40.1[1]	40.7	45.4	43.2	±0.46
Node no. of first truss	10.3	9.3	8.7	8.9	±0.20
No. of flowers at day 63	16.7[2]	15.8 ± 1.26[3]			
No. of flowers at day 70	21.2	15.7 ± 1.94			
Total no. of ripe fruit	15.3	12.8 ± 0.87			
Weight of ripe fruit (g)	963.1	731.7 ± 50.50			

[1] Mean of 14 plants in experiments 1 and 2.

[2] Mean of 6 plants in experiment 3.

[3] S.E.

Note: All means with a horizontal line in common are not significantly different at the 5% level of significance.

Source: 22, p. 464.

Table 23. Mature tomato plant fruit yields for three tomato varieties under three different sources of radiant energy*.

Light Sources	Fruit yield of varieties					
	R-25		R-29		WR-7	
	Fruit/ Plant (kg)	Avg. Fruit wt. (g)	Fruit/ Plant (kg)	Avg. Fruit wt. (g)	Fruit/ Plant (kg)	Avg. Fruit wt. (g)
Solar irradiation	2.07	188	2.56	210	1.98	213
Solar & cool-white	3.22	208	2.96	260	3.45	244
Solar & Gro-Lux/WS	3.33	242	3.34	271	4.12	294

* Harvest period October 15 to January 10 at Michigan.
Note: CO_2 level at 1000 ppm.
Source: 71.

The most extensive work using artificial lighting has been done outside the United States, particularly in Europe. A. E. Canham, described several attempts at using artificial lighting with mature tomato plants (9, pp. 139-144). For example, one study used mercury lamps on mature tomato plants at 200 $W \cdot m^{-2}$ for 16 hours daily. The time from sowing to plant maturity was reduced by five to six weeks, but the crop yield was not significantly improved (9, p. 142).

Studies have also been done in the Scandinavian nations, the U.S.S.R., and other nations with varying results, using irradiance levels of 100-600 $W \cdot m^{-2}$. The best results to date have usually been with fluorescent lamps, but this may be because many of the better, high-intensity, discharge lamps have only recently become available.

In summary, these experiments point toward several general conclusions: the use of artificial lighting as a total source of irradiance for commercial tomato production has not been economically successful to date; the use of artificial lights to supplement solar radiation reduces the time to maturity of tomato seedlings; the use of artificial lights to supplement solar radiation via daylength extension using low levels of irradiation does improve early yields, but does not significantly improve total crop yields; the use of artificial lights for tomato plant physiological effects has not been fully examined6/; and the use of artificial lights in growth chambers for pre-transplant tomato seedling development appears to be currently economically and technically feasible--at least during those months of low solar irradiation.

Fluorescent Lamps and Luminaires

Comparing the alternative artificial lights currently available is a necessary part of evaluating the economic feasibility of artificial lighting. Physical construction, type of ballast and luminaire lamp, operating characteristics, SED curve, spectral flexibility, and the cost of installation and operation of the system are all economically and/or physiologically important. Tables 27-30 and 33-37 provide such data for seven lamps frequently used as sources of photosynthetically active radiation (PAR). Each of these lamps' spectral energy distribution (SED) curves is examined and compared to that of a typical solar SED curve in an effort to determine their respective costs per effective PAR output watt (i.e., effective watts out). The lamps considered are FR96T12/CW/VHO/235/1 (fluorescent); F96T12/GRO/VHO (fluorescent, designed for plant growth); FR96T12/GRO/VHO/235/WS/1 (fluorescent, designed for plant growth); LU400 (high-pressure sodium);

LU1000 (high-pressure sodium); H36GW-1000/C (mercury); and MV1000/C/BUH (multi-vapor). These lamps can be divided into two groups, fluorescent lamps and high-intensity discharge lamps.

Physical characteristics. Fluorescent lamps are electronic gaseous discharge devices normally shaped like a long cylindrical tube. Depending upon the lamp's sidewall temperature it may be located above, beside, or within the crop canopy. It is the ability to place fluorescent lamps within the plant canopy, in direct contact with plant leaves, which is one of this lamp's most desirable features. Another distinctive advantage of the fluorescent lamp is its wide range of spectral flexibility.

Several different ballast designs exist for fluorescent lamps and several features are worth noting about ballasts when designing a plant lighting system. First, the better the voltage is regulated, the longer the average lamp life. Second, high power factor ballasts are typically more efficient to operate. Third, built-in overheating protection reduces the risk of ballast loss due to overloading. Further, ballasts should be moisture resistant. Fourth, an increase in the line current frequency allows reductions in ballast size, weight, and internal losses. Fifth, on the average, fluorescent lamp ballasts are expected to last 50,000 to 60,000 operating hours depending upon the quality and design of the components and their operating environment. Sixth, if lamp voltage and current levels are not at their rated levels, shifts in the SED curve will occur (31, pp. 4-14). Finally, if light chopping is desired, special ballasts and particular lamp types must be used. Cold cathode, rapid start, and preheat start hot cathode fluorescent lamps can be flashed with good performance although some reduction in lamp life is to be expected (31, pp. 8-32).

Fluorescent lamp luminaires come in a multiplicity of designs. The primary factors to consider are cost, radiant energy distribution curves, and ease of maintenance. Lamps without a luminaire or internal reflector coating may be used within the plant canopy.7/ Fluorescent lamps are made with reflective coatings covering 235° or 300° of the inside surface of the lamp. One advantage of using such lamps is reduced cleaning maintenance and shading because of no external reflectors. However, their efficiency is also lower. Whatever type luminaire is used, the even distribution of radiant energy upon the crop canopy is desired.

Operating characteristics. Fluorescent lamps also possess several important operating characteristics that need to be considered when designing an artificial lighting system for plants. First, Table 24 depicts the rated average lamp life for low, high, and very high output fluorescent lamps having different burning cycles (rated average life is the time in hours at which 50% of a large group of lamps burn out). From Table 24, it is apparent that continuous burning significantly increases the operating lamp life, thereby allowing fixed costs to be spread over more "effective watts out." The implications of this are that movable luminaires within a greenhouse are desirable for at least two reasons: it reduces total fixed costs and it increases total effective watts out per lamp. Of course, the plants and house must be amenable to such a system. Second, the effective radiant energy emitted by all lamps, including fluorescent, declines with lamp age. Figure 33 depicts typical fluorescent lamp lumen maintenance curves.8/ Figure 33 also shows that lumen maintenance declines more rapidly with increasing watts out. However, physical space prohibits the use of lightly loaded fluorescent lamps (e.g., 40 W lamps) when levels of irradiation of 500 langleys$\cdot$day^{-1} are desired. Third, the luminous efficacy (total luminous flux/total watts input) of fluorescent lamps is affected by lamp diameter (Figure 34). The optimum fluorescent lamp diameter for maximum luminous efficacy is 3.81 cm. Fourth, the luminous efficacy of fluorescent lamps increases as the lamp's length

increases (Figure 35). Thus, longer lamps have a higher luminous efficacy. Fifth, rapid start fluorescent lamps normally have a greater luminous efficacy than other forms of fluorescent lamps (Table 25). Sixth, the lamp wall temperature significantly affects PAR output and the spectral energy distribution. Figure 36 indicated the effects of lamp temperature and wind upon lamp radiant energy output.9/ As lamp temperature rises the spectrum usually shifts towards the blue-green spectrum (31, pp. 8-26). In a greenhouse, wind velocity is normally below 3.2 $km \cdot hr^{-1}$; therefore, a spectral shift and reduced luminous efficacy may occur due to excessive lamp wall temperatures. Seventh, relative humidity levels above 65% may hinder lamp starting and, therefore, lamps should be silicone coated (5, p. 36). All of these factors should be considered in selecting a fluorescent lamp and designing a radiant energy system for greenhouses.

Table 24. Average life in hours of fluorescent lamps at various burning cycles.

	Hours Per Start					
Lamp Type	3	6	10	12	18	Continuous
40W Preheat	15,000	17,500	21,250	22,500	25,000	28,125
40W Rapid Start	20,000+	24,420	27,750	28,860	31,600	37,700
High Output (HO)	12,000	14,000	17,000	18,000	20,000	22,500
Very High Output (VHO)	10,000	12,500	14,990	15,980	17,980	24,980
Slimline (96T12)	12,000	14,000	17,000	18,000	20,000	22,500

Source: Sylvania, GTE Corp., Effect of Burning Periods on Fluorescent Lamp Life, Sylvania Engineering Bulletin 0-335, Danvers, Mass., December 1974.

Evaluation of fluorescent lamp spectral characteristics reveals that a great deal of spectral flexibility exists relative to most other lamps. The one area of weakness of fluorescent lamps is in the 700-800 nm range. Cool white fluorescent lamps must be supplemented with another source that can supply an adequate level of 700-800 nm irradiance. Frequently, inefficient incandescent lamps are used.

Figure 38-40 are SED curves for several fluorescent lamps that are currently available. The SED curves for the three fluorescent lamps evaluated have been divided into four spectral bands having wavelengths of 350-530 nm, 530-580 nm, 580-690 nm, and 690-780 nm. The areas under the curves for each band have been determined using a planimeter. A. E. Canham made similar measurements which have been recorded in Table 26. Canham's table does not include any of the seven lamps considered here. Table 27 presents the spectral energy data for the three fluorescent lamps considered in this study. The column headed "Effective Watts Output" is the sum of the watts output of the four bands except for the 530-580 nm (i.e., 530-580 nanometer wavelengths) band, which is summed at half its value to reflect its relatively lower significance as a source of photosynthetically active radiation (PAR). The next-to-last column, "Input Watts/Effective Watts Output", indicates on a per-luminaire basis the total amount of electrical energy that must be supplied per effective watt of PAR out. Thus, of the three lamps listed in Table 27, the FR96T12/GRO/VHO/235/WS/1 is the most efficient at converting input energy into effective watts out. Of course, the effectiveness of this conversion is dependent upon the lamp, ballast, and lighting system factors previously described.

Table 25. Relationship of arc length and lumens per watt for typical cool-white fluorescent lamps.

Approximate Arc Length (inches)	Hot Cathode				Low Pressure T-8 Cold Cathode
	Approximate Efficacy (lumens per watt)	Approximate Lamp and Auxiliary Efficacy (lumens per watt)			Approximate Efficacy (lumens per watt)
		Preheat Start	Instant Start	Rapid Start	
5	33.0	22			
10	45.0	34			
15	53.0	42			
20	59.0	48			
25	63.0	53			
30	66.0	57			
35	68.0	59			
40	69.0	61	52	60	38
45	70.0	62			
50	71.0	63	54	63	41
55	72.0				
60	72.5		56	65	44
65	73.0				
70	74.0		59	67	47
75	75.0				
80	76.0		61	69	50
85	76.5				
90	77.0		63	71	52

Source: 31, pp. 8-23.

Table 26. Energy output in three bands of the spectral energy distribution curves for several lamps.

(a) Incandescent and discharge lamps:

Lamp type	Radiant flux in watts for wavelengths given (in nm)			
	400-510	510-610	610-700	400-700
500W incandescent	3.8	11.2	17.0	32.0
400W mercury	14.5	21.7	0.1	36.3
400W mercury-fluorescent	13.8	28.3	15.5	57.6
500W mercury-tungsten	11.6	21.2	5.9	38.7
400W neon	--	2.5	21.5	24.0
200W sodium	--	43.8	0.2	44.0
1000W xenon	37.8	29.0	26.0	92.8

(b) Fluorescent tubes (80W):

Lamp type	Radiant flux in watts for wavelengths given (in nm)			
	400-510	510-610	610-700	400-700
White	3.3	7.7	4.0	15.0
Warm white	2.0	7.5	4.5	14.0
Daylight	4.3	7.6	3.5	15.4
Natural	4.0	5.7	4.6	14.3
Deluxe warm white	1.7	6.8	4.9	13.4
Color matching	5.5	5.1	3.9	14.5
Magnesium arsenate	0.4	0.7	13.1	14.2

Source: 9, p. 55.

Table 27. Energy output in four bands of the spectral energy distribution curves for three fluorescent lamps.

ANSI Lamp	350-530 nm Watts Output	530-580 nm Watts Output	580-690 nm Watts Output	690-780 nm Watts Output	Effective Watts Output[1]	Input Watts/ Effective Watts Output	Lamp/Solar Radiation Effectiveness Weight[4]
FR96T12/GRO/VHO/235/WS/1 (Gro-lux wide-spectrum very high output fluorescent lamp with 235° internal reflector)	15.9 W[3]	7.5 W[3]	19.4 W[3]	5.5 W[3]	44.6 W	5.04	8.9
	32.9 %	15.5 %	40.2 %	11.4 %			12.5
FR96T12/CW/VHO/235/1 (cool-white very high output fluorescent lamp with 235° internal reflector)	12.1 W	8.0 W	9.9 W	.99 W	27.0	8.33	13.1
	39.0 %	25.8 %	31.9 %	3.2 %			13.5
F96T12/GRO/VHO (Gro-lux very high output fluorescent lamp)	15.7 W[2]	3.1 W[2]	16.8 W[2]	.20 W[2]	34.3 W	6.56	15.7
	43.9 %	8.7 %	46.9 %	.6 %			24.5
	% of PAR Band						
Direct solar radiation E (d = 400; m = 1; w = 30)	39.12 %	14.0 %	29.1 %	17.1 %			
Direct solar radiation (d = 400; m = 5; w = 30)	21.6 %	15.4 %	40.4 %	22.8 %			
Total cloud radiation	50.0 %	22.8 %	18.8 %	9.1 %			
Solar weighting (mean)	36.9 %	17.4 %	29.4 %	16.3 %			

[1] Effective watts output = (350-530 nm watts) + (.5)(530-580 nm watts) + (580-780 nm watts)

[2] Source: 43, Appendix II, p. 3.

[3] Source: 50, p. 1. (integration of SED curve)

[4] The upper lamp/solar radiation effectiveness weight is the sum of the percentage point differences between the solar weights and the lamp SED percentages for bands 350-530, 580-690, and 690-780 nm, where the percentage value for the lamp SED band is exceeded by the solar weight for that band. The lower weight for each lamp in the same column, is the square root of the sum of the squares of the differences in percentages between the lamp and solar weight for bands 350-530, 580-690, 690-780 nm.

Table 27 also shows in percentage terms the breakdown of solar radiation occurring within the PAR band of 350-780 nm that is also within one of the four bands previously described. Comparing these percentage figures gives a rough indication of how each of the three lamps compares with a typical solar distribution of PAR. The last column, entitled "Lamp/Solar Radiation Effectiveness Weight", provides two weights by which to compare the PAR output of these lamps with solar radiation. The top weight is the sum of the percentage point differences between the solar weights and the lamp SED percentages for bands 350-530 nm, 580-690 nm, and 690-780 nm, where the percentage value for the lamp SED band is less than the solar weight for that band. The lower weight in the same column for each lamp is the square root of the sum of the squares of the differences in percentages, between the lamp and solar radiation weights for bands 350-530 nm, 580-690 nm, and 690-780 nm. Both weights are simply two different methods used to make the same comparison. For both weights, the lower the value, the better the fit of the lamp's PAR output to the estimated solar PAR distribution. Of the three

fluorescent lamps compared in Table 27, the FR96T12/GRO/VHO/235/WS/1 resembles the solar distribution of PAR most closely, while the FR96T12/CW/VHO/235/1 is second best. But all three lamps are notably weaker than solar radiation in the 690-780 nm range. Of these three fluorescent lamps, overall, the Gro-lux wide-spectrum, very high output, fluorescent lamp has the best PAR energy distribution and the best ratio of input watts to effective watts out (5.04 versus 6.56 and 8.33). It is probably this improved PAR energy distribution that causes the Gro-lux wide-spectrum lamp to excel over the others in tomato plant dry weight and fruit yields, as shown in Tables 18, 19, and 23. It must be emphasized that any imbalances in lamp spectral radiant energy distributions compared to the solar SED curve may cause significant changes in plant responses, such as internode elongation, fruit disorders, yield variations, etc. While such effects are not specifically considered here, they should be in any application of artificial lighting to plants.

Table 28 indicates for each of these three fluorescent lamps the total input watts per lamp and associated luminaire (based upon two lamp luminaires), and the different means by which this energy is expended. Use of energy expended by conductive-convective means, or by the ballast, may be controlled and/or stored in some mass storage system (such as gravel or water as is used with solar collector systems) for heating. Energy expended as infrared radiation is more difficult to control and/or collect and requires its effective entrapment within the house--preferably not at the house surface, where it can be readily lost to the outside environment. If an artificial lighting system expends more heat than is necessary to maintain house temperatures, and no system for storage is available, then it will be necessary to vent the house. Proper mixing of incoming cool external air before it reaches the crop is necessary, but caution must also be taken to prevent changes in the lamp wall temperatures, which cause adverse SED curve shifts.

Table 28 also indicates the waste energy expended as ballast, conductive-convective, and infrared energy per effective watt out for each of these three fluorescent lamps. Generally, large artificial lighting systems produce excessive heat. If this is the case, then the FR96T12/GRO/VHO/235/WS/1 is most advantageous in that it expends the least waste heat per effective watt of PAR put out by each luminaire.

While a particular lamp(s) and associated luminaire may be more efficient in producing effective watts of PAR out per input watt, several other factors determine which lighting system is most effective in delivering this PAR to the crop. The actual irradiation striking the crop canopy is dependent upon lamp and luminaire orientation to the crop; lamp spacing; luminaire efficiency; luminaire dirt depreciation (LDD) factor; lamp luminous efficacy; and input power. A discussion of those factors not already considered will come after the following discussion of high-intensity discharge lamps, which is similar in format to this discussion of fluorescent lamps.

High Intensity Discharge Lamps and Luminaires

Physical characteristics. HID lamps utilize an arc tube operating at pressures and currents sufficient to radiate PAR from the arc itself, without the utilization of phosphor coatings on the glass envelopes. HID lamps include mercury, metal-halide, and high-pressure sodium lamps among others, and constitute an alternative source of PAR to that of fluorescent lamps. Mercury HID lamps were the first of the HID lamp group to be developed commercially, while high-pressure sodium HID lamps are the most recent addition to this group of lamps (1960s). Because of the recent entrance of the latter lamps into the marketplace, most studies evaluating artificial lighting for plant growth, to date, do not include the sodium HID lamp. However, this lamp is rapidly becoming accepted as a

viable source of radiant energy for plant growth. Figure 41 portrays the relative efficiencies of several lamp groups as light sources. High-pressure sodium lamps (e.g., Lucalox) are most efficient in terms of converting input watts into effective watts out.

Table 28. Input energy and its distribution among output forms for three fluorescent lamps.

ANSI lamp	Total Input Watts	Ultraviolet Watts Output	Infrared Watts Output	Conductive-Convective Watts Output	Ballast Watts Output	Effective Watts Output[A]
FR96T12/GRO/VHO/235/WS/1 (Gro-lux wide spectrum very high output fluorescent lamp with 235° internal reflector)	225[B]	1.5	65	84	27	44.6
FR96T12/CW/VHO/235/1 (cool-white very high output fluorescent lamp with 235° internal reflector)	225[B]	1.1[C]	73[C]	93[C]	27[C]	27.0
F96T12/GRO/VHO (Gro-lux very high output lamp)	225[B]	.55	71.7	89.7	27	34.3

[A] Effective watts output = (350-530 nm watts) + (.5)·(530-590 nm watts) + (580-780 nm watts).

[B] Source: 18, p. 13 (integration of SED curve) calculated as half of the input watts to a ballast designed for two lamps.

[C] Source: 31, pp. 16-3.

The following are some of the important characteristics of HID lamps and luminaires. First, HID lamps cannot be placed within the crop canopy due to their high envelope temperatures. Second, all ballasts used inside greenhouses should be moisture resistant. Third, HID lamp ballasts generally are not interchangeable because each lamp requires particular ballast characteristics (complete ballast descriptions may be found in references 18 and 29).10/ This reduces the flexibility of these lamps as compared with fluorescent lamps, which may be operated on any equivalent wattage ballasts.

The functions of a HID lamp ballast are to (18, p. 5) limit the lamp's current flow, provide the correct lamp starting voltage, provide the correct lamp arc operating voltage, isolate the line voltage and current from lamp voltage and current fluctuations, and compensate for the low power factor of HID lamps. Generally speaking, as the line voltage regulation improves, less expensive ballasts may be employed. Therefore, higher and/or very stable line voltages (e.g., 240 vac or 480 vac versus 120 vac) may allow the utilization of lower cost ballasts. Another factor to consider is that ballasts with low power factors draw higher line currents and, therefore, require larger feeder wires, swtiches, circuit breakers, and distribution transformers (18, p. 18), and are more expensive to operate (5, p. 23). For lighting installations operating over extended periods of time, a high power factor ($\geq$ .9) is essential for economic operation, but the capital investment for ballasts will most likely also be greater. The efficiency of the ballast (i.e., watts radiated/watts used by the

ballast) is also of economic importance. However, the adequate current and/or voltage regulation required to meet the nominal demands of the lamp is the most crucial factor in ballast selection because if the lamp voltage and/or current is allowed to vary significantly, lamp life and/or spectral radiant energy distribution will also vary. Figure 42 for mercury HID lamp ballasts, and Figure 43 for sodium HID lamp ballasts indicate the significantly greater variation that will occur in "effective watts out" for variations in line voltage, when using cheaper reactor ballasts. The ballasts, therefore, plays a significant role in the economic efficiency of a luminaire and lamp.

For the four HID lamps evaluated in this study, it is assumed that regulated ballasts are used and that lamp current and voltages are maintained at their rated values. The ballasts are assumed to have a life expectancy of 150,000 operating hours using 55° C rated luminaires operating in maximum greenhouse temperatures of 45° C. Figure 44 indicates the variations in expected ballast life which can be expected for variations in ambient house temperatures, with life expectancies declining nearly 10% for every 3° C rise in ambient house temperatures.

The reflector for HID lamps may be directly attached to the ballast or separated from it. A luminaire should have a high coefficient of utilization, a uniform radiant intensity appropriate for the desired level of irradiance, be easily cleaned, and be properly ventilated (see references 15, 30, 52). Because of the high temperatures generated by HID lamps, adequate clearance must be provided for the lamps inside the greenhouse.11/ Solar shading caused by luminaires is dependent upon their size and the irradiance levels desired. However, for equivalent levels of irradiance, HID lamps cause less shading than overhead VHO (1500 ma) internally reflectorized fluorescent lamps (15, p. 2). This would not be true, however, for fluorescent lamps used within the crop canopy.

Operating characteristics. Figure 45 shows mortality curves for several HID lamps, which indicate that their lives are significantly longer than the lives of fluorescent lamps (compare with Figure 33). Furthermore, little change occurs in the length of the lamp's life with increasing numbers of starts for ten hours or more per start. Thus, HID lamps are somewhat more flexible than fluorescent lamps in terms of economically efficient burning period (18, p. 14).

Figure 46 provides lamp lumen maintenance curves for several HID lamps (lumens are used here as a surrogate for PAR). High-pressure sodium lamps, over their average life expectancy, exhibit the lowest drop in lumen maintenance of any of these HID lamps. The luminous efficacy of most HID lamps is high (Figure 41), and improves with higher wattages for both metal halide and high-pressure sodium lamps. Furthermore, HID lamps compared to fluorescent lamps, are relatively insensitive to ambient air temperature changes and external air movements because of their protective outer bulb. They normally have a slightly higher efficacy when operating in the vertical versus horizontal orientation, and are not significantly affected by the typical humidity levels occurring in controlled environments. Finally, unlike fluorescent lamps with hot cathodes, HID lamps are not readily adaptable to chopping of the input current at millisecond intervals (i.e., light chopping via chopping the input energy) because of the mechanical problems in chopping high currents, and because of the problems of spectral shifts occurring in the lamp's emittance.

Figures 47-49 are SED curves for several common HID lamps. Mercury HID lamps emit radiant energy at specific wavelengths with phosphor coatings frequently added to expand the spectral distribution. Metal halide lamps have good spectral flexibility with the use of different metal halides, while high-pressure sodium lamps currently lack such flexibility. Further, high-pressure sodium lamps are weak in the shorter wavelengths of PAR and must usually be supplemented with radiation from other lamps,

such as clear mercury HID lamps. On the other hand, the SED curves of metal halide lamps are very sensitive to wattage changes. Other common factors causing shifts in HID lamp SED curves include lamp burning position, line voltage fluctuations, ballast design, luminaire reflector contour causing redirection of radiant energy through the lamp, color of surrounding surfaces, and ambient temperatures exceeding operating design temperatures of the ballast and/or lamp.

Table 29 presents the four spectral energy bands for the four HID lamps evaluated in this study. This table is identical to Table 27 for the fluorescent lamps. The 1,000-watt high-pressure sodium lamp (LU1000) has the lowest ratio of input watts to effective watts output, but like all of the HID and fluorescent lamps it has significantly less output (on a percentage basis) in the 690-780 nm band than solar radiation (7.1% versus 16.3%). Furthermore, the LU1000 lamp is low in the blue spectrum (350-530 nm), producing only 12.2% of its effective watts output in this range, versus 36.9% for solar radiation. Therefore, it is expected that LU1000 lamps must be supplemented in the 350-530 nm spectrum with radiation from another source, perhaps the multi-vapor lamp MV1000/C/BUH. The last column, titled "Lamp/Solar Radiation Effectiveness Weight", provides two weights by which to compare the PAR output of these lamps with solar radiation. The top weight is the sum of the percentage point differences between the solar weights and the lamp SED percentages for bands 350-530 nm, 580-690 nm, and 690-780 nm, where the percentage value for the lamp SED band is less than the solar weight for that band. The lower weight for each lamp, in the same column, is the square root of the sum of the squares of the differences in percentages between the lamp and solar radiation weights for bands 350-530 nm, 580-690 nm, and 690-780 nm. Both weights are simply two different methods used to make the same comparison. For both weights, the lower the value, the better the fit of the lamp's PAR output to the estimated solar PAR distribution. Of the four HID lamps compared in Table 29, the metal halide lamp MV1000/C/BUH has the lowest combined lamp/solar effectiveness weights, while the high-pressure sodium lamps have the highest weights. However, the high-pressure sodium lamps, as already indicated, have the highest conversion of input energy into effective watts out (LU1000 input/output watts = 3.33; MV1000/C/BUH input/output watts = 4.28). On the other hand, the MV1000/C/BUH lamp is more efficient than the best fluorescent lamp (4.28 versus 5.08), but has a higher lamp-solar radiation effectiveness weight (11.4 and .316 versus 8.9 and 12.5). Thus, while the LU1000 is more efficient to operate, the MV1000/C/BUH has a significantly better PAR distribution which may result in significantly better growth than with LU1000 lamps.

Table 29 indicates that the 400 watt and 1000 watt high-pressure sodium lamps have the same spectral energy distribution (SED) curves. This is also true for the other lamps. However, as is shown, the lower wattage LU400 lamp is somewhat less efficient in converting input energy into effective output watts (i.e., 3.95 versus 3.33).

Table 30 indicates for these four HID lamps the total input watts per lamp and associated luminaire and the different means by which this energy is expended (Table 30 is identical to Table 28, which is for the three fluorescent lamps already considered). Considerable amounts of heat are generated for each effective watt produced and in any large lighting system can be expected to substantially fulfill all heating needs, with the use of a heat storage system and house insulation. Excess amounts of heat will allow some relative humidity control via venting.

Table 29. Energy output in four bands of the spectral energy distribution curves for four HID lamps.

ANSI Lamp	350-530 nm watts output	530-580 nm watts output	580-690 nm watts output	690-780 nm watts output	Effective watts output[A/]	Input watts/ effective watts output	Lamp/solar radiation effectiveness weight[B/]
MV1000/C/BUH (phosphor-coated standard metal halide lamp)	116.8 W	50.5 W	95.2 W	13.5 W	251 W	4.28	
	42.3 %	18.3 %	34.5 %	4.9 %			11.4
							13.6
H36GW-1000/DX (1,000-watt mercury deluxe white HID lamp)	50.8 W[C/]	61.6 W[C/]	38.7 W[C/]	8.0 W[C/]	128 W	8.40	
							21.4
	31.9 %	38.7 %	24.3 %	5.0 %			13.4
LU400 (400-watt high-pressure sodium HID lamp)	15.8 W[D/]	32.2 W[D/]	72.5 W[D/]	9.3 W[D/]	114 W	3.95	
							33.9
	12.2 %	24.8 %	55.9 %	7.2 %			37.4
LU1000 (1,000-watt high-pressure sodium HID lamp)	44.8 W[D/]	91.2 W[D/]	205 W[D/]	26 W[D/]	321 W	3.33	
							33.9
	12.2 %	24.9 %	55.9 %	7.1 %			37.4
	% of PAR Band						
Direct solar radiation[E/] (d = 400; m = 1; w = 30)	39.1 %	14.0 %	29.1 %	17.1 %			
Direct solar radiation[E/] (d = 400; m = 5; w = 30)	21.6 %	15.4 %	40.4 %	22.8 %			
Total cloud radiation	50.0 %	22.8 %	18.8 %	9.1 %			
Solar weighting (mean)	36.9 %	17.4 %	29.4 %	16.3 %			

[A/] Effective watts output = (350-530 nm watts) + (.5)(530-580 nm watts) + (580-780 nm watts).

[B/] The upper lamp/solar radiation effectiveness weight is the sum of the percentage point differences between the solar weights and the lamp SED percentages for bands 350-530, 580-690, and 690-780 nm, where the percentage value for the lamp SED band is exceeded by the solar weight for that band.

[C/] Source: 18, p. 13 (integration of SED curve).

[D/] Source: 18, p. 31 (integration of SED curve).

[E/] Source: 9, p. 50 (integration of SED curve).

Other Lamps

Another lamp which is not currently used as a radiator of PAR, but which may be in the future, is the xenon short-arc lamp, which has an SED curve very similar to the sun's at solar noon, at a large solar altitude angle (β). Further, it is capable of radiating extremely high radiant intensities. Flashtube lamps may also become practical in the future as the chopping effects of irradiation upon plant growth become more fully understood. Supplementing the solar irradiation of crops during winter months with radiation from a flashtube, xenon lamp, or sequence of flashtubes may be economical if the radiant energy can be effectively utilized by plants. These lamps warrant further study.

Table 30. Input energy and its distribution among output forms for four HID lamps.

ANSI Lamp	Total input watts	Ultraviolet watts output	Infrared watts output	Conductive-convective watts output	Ballast watts output	Effective watts output[A/]
MV1000/C/BUH (phosphor-coated standard metal halide HID lamp)	1075	19	360	256	164	251
H36GW-1000/DX (1,000-watt mercury deluxe white HID lamp)	1075	18[B/]	499[B/]	289[B/]	110[B/]	128
LU400 (400-watt high-pressure sodium HID lamp)	450	.9[B/]	158[B/]	94[B/]	67[B/]	114
LU1000 (1,000-watt high-pressure sodium HID lamp)	1068	2.1[B/]	338[B/]	202[B/]	159[B/]	321

[A/] Effective watts output = (350-530 nm watts) + (.5)(530-580 nm watts) + (580-780 nm watts) (see reference 5, p. 134).

[B/] Source: 31, p. 16-3 .

General Factors to Consider in Establishing and Evaluating Artificial Lighting Systems for Plant Growth

Calculation of the available photosynthetically active radiation at the crop canopy surface requires knowing how much PAR a lamp produces and also how much of it reaches the crop canopy surface. The Illuminating Engineering Society Lighting Handbook (31, pp. 9-1 to 9-32) provides a systematic method of evaluating the many factors which affect the net available PAR at the crop canopy surface. The basic relationship for determining the irradiation on the crop canopy is:

$$\text{Crop Canopy Irradiation} = \frac{(\text{Lamp effective watts output}) \cdot (CU) \cdot (PARLF)}{\text{Area Irradiated}}$$

where:

CU is the coefficient of utilization, the ratio of PAR intercepted by the crop canopy to the total quantity of PAR emitted by a lamp. It is a measure of the optical efficiency of the luminaire and surrounding surfaces and ideally would equal 1,

PARLF is the photosynthetically active radiation loss factor. It is the product of all contributing factors which reduce the available PAR at the crop canopy surface, where factors not included are assumed to be equal to one (i.e., cause no loss in PAR available to the crop canopy). The factors included in PARLF include luminaire ambient temperature, voltage to luminaire ballast factor, luminaire surface depreciation, room surface dirt depreciation, burnouts, lamp radiant energy output depreciation, and luminaire dirt depreciation, and

Area Irradiated is the area of the crop canopy surface in square meters which each luminaire of the lighting system irradiates. It is assumed here that the lamps are distributed such that the entire crop canopy surface receives a relatively constant level of irradiation.

The following describes in greater detail the calculation of the CU and PARLF values for the seven lamps and luminaires evaluated.

The coefficient of utilization adjusts the effective watts output for a lamp (Tables 27 and 29, footnote A), to reflect the optical efficiency of the associated luminaire and surrounding surfaces in effectively distributing the emitted energy upon the crop canopy. It adjusts for radiant energy lost through the house cover by calculating the effective reflectances of such surfaces in conjunction with the reflective parameters of the luminaire's reflector.

The Zonal-Cavity Method (31, p. 9-8) accounts for the effects of room proportions, luminaire suspension length, and crop canopy height upon the coefficient of utilization. Figure 50 shows the cavities of a greenhouse. The room cavity ratio (RCR) is $$RCR = \frac{(5\ h_{RC}) \cdot (\text{Room length} + \text{Room width})}{(\text{Room length}) \cdot (\text{Room width})}$$

where for a CEVCO house h_{RC} = 1.2 m, Room length = 34 m, and Room width = 7.9 m. Therefore, RCR = .94, or nearly 1.

The effective ceiling cavity reflectance (ρ_{cc}) is: $$\rho_{cc} = \frac{\rho \cdot A_o}{A_s - \rho \cdot A_s + \rho \cdot A_o}$$ where: A_o = area of surface of luminaires, A_s = area of house cover above the surface of luminaires, and ρ = reflectance of house cover. Thus, ρ affects the ceiling cavity reflectance (ρ_{cc}) and ultimately, the coefficient of utilization (CU). If ρ = .18 for fiberglass panels, and A_o = 241 m^2 and A_s = 220 m^2, then ρ_{cc} = .19 (ignoring reflectance off the top of the luminaires). The effective wall reflectance (ρ_w) is, therefore, assumed to be equal to the ceiling cavity reflectance (ρ_{cc}). However, if some form of highly reflective cover were placed over or inside the house cover such that ρ = .7, then ρ_{cc} = .72 (given the same values of A_o and A_s).

Table 31 provides coefficient of utilization (CU) values for several luminaire designs. Luminaire number 6 (porcelain-enameled reflector with 35° CW shielding) is used as a surrogate for internal reflector lamps. From Table 31 the CU value can be determined, given the type of luminaire, RCR, ρ_{cc}, ρ_w, and ρ_{FC}. Table 31 assumes a constant floor cavity reflectance ρ_{FC} = 20%, but Table 32 provides correction factors to adjust the CU values such that ρ_{FC} = 0% or 10%. In all cases, this causes the reduction in estimated CU values.

As an example, to determine the coefficient of utilization for a narrow distribution, ventilated reflector with a clear HID lamp, such as a high-pressure sodium lamp, the following factors are assumed: ρ_{cc} = 70, ρ_{FC} = 0, ρ_w = 70, and RCR = 1.

Luminaire type #1 in Table 31 is used. The CU multiplying factor from Table 32 is .933 for a 10% floor reflectance. Table 31 does not provide a CU value where ρ_w = .7, but it can be extrapolated to be about .88. Adjusting by .933 gives: CU ≈ .82. If $\rho_{cc} = \rho_w$ = .19, however, then CU ≈ .74, by the same method.

Table 33 provides estimated coefficients of utilization (CU) for three different luminaires, which are representative of the lamps considered in this study. The floor cavity reflectance (ρ_{FC}) is assumed to be 10%, while the wall and ceiling cavity reflectances are assumed to be either 19% or 70%. Note that when no radiation is reflected from the floor (i.e., ρ_{FC} = .0), the coefficient of reflectivity of the house cover causes little variation in the estimated CU values, except with the

Table 31. Coefficients of utilization for several different luminaires.

Luminaire Type	Typical Distribution and Percent Lamp Lumens		$\rho cc \rightarrow$ [a]	80			70			50			30			10			0
			$\rho w \rightarrow$ [b]	50	30	10	50	30	10	50	30	10	50	30	10	50	30	10	0
	Maint. Cat.	Maximum S/MH Guide[d]	RCR [c] ↓	Coefficients of Utilization for 20 Percent Effective Floor Cavity Reflectance (ρ_{rc} = 20)															
1 Narrow distribution ventilated reflector with clear HID lamp	III	0.7	0	.92	.92	.92	.90	.90	.90	.86	.86	.86	.82	.82	.82	.78	.78	.78	.76
			1	.87	.85	.83	.85	.83	.82	.81	.80	.70	.78	.77	.76	.75	.75	.74	.72
			2	.81	.79	.76	.80	.77	.75	.77	.75	.73	.75	.73	.72	.72	.71	.70	.69
			3	.77	.73	.71	.76	.72	.70	.73	.71	.69	.71	.69	.67	.70	.68	.66	.65
			4	.73	.69	.66	.72	.68	.65	.70	.67	.64	.68	.66	.64	.67	.65	.63	.62
			5	.69	.65	.62	.68	.64	.61	.66	.63	.61	.65	.62	.60	.64	.61	.59	.58
			6	.65	.61	.58	.64	.61	.58	.63	.60	.57	.62	.59	.57	.61	.58	.56	.55
			7	.62	.57	.54	.61	.57	.54	.60	.56	.54	.59	.56	.53	.58	.55	.53	.52
			8	.58	.54	.51	.58	.54	.51	.57	.53	.51	.56	.53	.51	.55	.52	.50	.49
			9	.55	.51	.48	.55	.51	.48	.54	.50	.48	.53	.50	.48	.53	.50	.48	.47
			10	.53	.49	.46	.52	.48	.46	.52	.48	.46	.51	.48	.45	.50	.47	.45	.44
2 Intermediate distribution ventilated reflector with clear HID lamp	III	1.0	0	.91	.91	.91	.89	.89	.89	.84	.84	.84	.81	.81	.81	.77	.77	.77	.73
			1	.84	.81	.79	.82	.80	.78	.79	.77	.76	.76	.74	.73	.73	.72	.71	.69
			2	.77	.73	.70	.76	.72	.70	.73	.70	.68	.70	.68	.66	.68	.66	.65	.63
			3	.71	.66	.63	.69	.65	.62	.67	.64	.61	.65	.62	.60	.63	.61	.59	.57
			4	.65	.60	.56	.64	.59	.56	.62	.58	.55	.60	.57	.54	.59	.56	.54	.52
			5	.59	.54	.50	.59	.54	.50	.57	.53	.50	.56	.52	.49	.54	.51	.48	.47
			6	.54	.49	.45	.54	.49	.45	.52	.48	.45	.51	.47	.44	.50	.47	.44	.42
			7	.50	.44	.40	.49	.44	.40	.48	.43	.40	.47	.43	.39	.46	.42	.39	.38
			8	.45	.40	.36	.45	.40	.36	.44	.39	.36	.43	.39	.35	.42	.38	.35	.34
			9	.41	.36	.32	.41	.36	.32	.40	.35	.32	.39	.35	.32	.38	.35	.32	.30
			10	.38	.33	.29	.37	.32	.29	.37	.32	.29	.36	.32	.29	.35	.31	.28	.27
3 Wide distribution ventilated reflector with clear HID lamp	III	1.5	0	.92	.92	.92	.90	.90	.90	.86	.86	.86	.82	.82	.82	.79	.79	.79	.77
			1	.85	.82	.80	.83	.81	.79	.79	.78	.76	.76	.75	.74	.74	.72	.71	.70
			2	.77	.73	.70	.75	.72	.69	.73	.70	.67	.70	.68	.66	.68	.66	.64	.63
			3	.70	.65	.61	.68	.64	.60	.66	.62	.59	.64	.61	.58	.62	.59	.57	.56
			4	.63	.58	.53	.62	.57	.53	.60	.56	.52	.58	.55	.52	.57	.54	.51	.49
			5	.57	.51	.47	.56	.51	.47	.55	.50	.46	.53	.49	.46	.52	.48	.45	.44
			6	.51	.45	.41	.51	.45	.41	.49	.44	.40	.48	.43	.40	.47	.43	.40	.38
			7	.46	.40	.35	.45	.39	.35	.44	.39	.35	.43	.38	.35	.42	.38	.34	.33
			8	.41	.35	.31	.41	.35	.31	.40	.34	.31	.39	.34	.30	.38	.33	.30	.29
			9	.37	.31	.27	.37	.31	.27	.36	.30	.27	.35	.30	.27	.34	.30	.26	.25
			10	.33	.27	.24	.33	.27	.23	.32	.27	.23	.31	.27	.23	.31	.26	.23	.22

Table 31. Coefficients of utilization for several different luminaires (continued).

Luminaire Type	Typical Distribution and Percent Lamp Lumens		$\rho cc \xrightarrow{a/}$	80			70			50			30			10			0
			$\rho w \xrightarrow{b/}$	50	30	10	50	30	10	50	30	10	50	30	10	50	30	10	0
	Maint. Cat.	Maximum S/MH_d Guide	RCR $\xrightarrow{c/}$	Coefficients of Utilization for 20 Percent Effective Floor Cavity Reflectance (ρ_{rc} = 20)															
4 Intermediate distribution ventilated reflector with phosphor coated HID lamp	III	1.0	0	.96	.96	.96	.93	.93	.93	.87	.87	.87	.82	.82	.82	.77	.77	.77	.75
			1	.89	.87	.84	.86	.84	.83	.82	.80	.79	.78	.76	.75	.74	.73	.72	.70
			2	.82	.79	.76	.80	.77	.74	.76	.74	.72	.73	.71	.69	.70	.68	.67	.65
			3	.76	.72	.68	.74	.70	.67	.71	.68	.65	.68	.66	.63	.66	.63	.61	.60
			4	.70	.66	.62	.69	.65	.61	.66	.63	.60	.64	.61	.58	.62	.59	.57	.55
			5	.65	.60	.56	.64	.59	.56	.62	.58	.54	.60	.56	.53	.58	.55	.52	.51
			6	.60	.55	.51	.59	.55	.51	.57	.53	.50	.56	.52	.49	.54	.51	.48	.47
			7	.56	.51	.47	.55	.50	.46	.53	.49	.46	.52	.48	.45	.50	.47	.44	.43
			8	.52	.47	.43	.51	.46	.43	.50	.45	.42	.48	.44	.41	.47	.43	.41	.40
			9	.48	.43	.39	.47	.42	.39	.46	.42	.39	.45	.41	.38	.44	.40	.38	.36
			10	.45	.40	.36	.44	.39	.36	.43	.39	.36	.42	.38	.35	.41	.37	.35	.34
5 Wide distribution ventilated reflector with phosphor coated HID lamp	III	1.5	0	.93	.93	.93	.89	.89	.89	.83	.83	.83	.77	.77	.77	.71	.71	.71	.68
			1	.85	.83	.81	.82	.80	.78	.77	.75	.74	.72	.71	.69	.67	.66	.65	.63
			2	.78	.74	.71	.76	.72	.69	.71	.68	.66	.67	.65	.63	.63	.61	.60	.58
			3	.71	.67	.63	.69	.65	.62	.65	.62	.59	.62	.59	.57	.58	.56	.54	.53
			4	.65	.60	.56	.64	.59	.55	.60	.56	.53	.57	.54	.51	.54	.52	.50	.48
			5	.60	.54	.50	.58	.53	.49	.55	.51	.48	.53	.49	.46	.50	.47	.45	.43
			6	.54	.49	.45	.53	.48	.44	.51	.46	.43	.48	.45	.42	.46	.43	.40	.39
			7	.49	.44	.40	.48	.43	.39	.46	.41	.38	.44	.40	.37	.42	.39	.36	.34
			8	.45	.39	.35	.44	.38	.35	.42	.37	.34	.40	.36	.33	.38	.35	.32	.31
			9	.41	.35	.31	.40	.34	.31	.38	.33	.30	.36	.32	.29	.35	.31	.28	.27
			10	.37	.31	.27	.36	.31	.27	.34	.30	.26	.33	.29	.26	.32	.28	.25	.24
6 Porcelain-enameled reflector with 35° CW shielding	II	1.3	0	.99	.99	.99	.94	.94	.94	.84	.84	.84	.76	.76	.76	.68	.68	.68	.65
			1	.88	.85	.82	.84	.81	.78	.76	.74	.72	.69	.67	.66	.62	.61	.60	.57
			2	.78	.73	.68	.74	.70	.66	.68	.64	.61	.62	.59	.56	.56	.54	.52	.49
			3	.69	.63	.58	.66	.61	.56	.61	.56	.53	.56	.52	.49	.51	.48	.46	.43
			4	.62	.55	.50	.60	.53	.49	.55	.50	.46	.50	.46	.43	.46	.43	.40	.37
			5	.55	.48	.43	.53	.47	.42	.49	.44	.39	.45	.41	.37	.41	.38	.35	.32
			6	.50	.43	.38	.48	.41	.37	.44	.39	.35	.41	.36	.33	.37	.34	.31	.29
			7	.45	.38	.33	.43	.37	.32	.40	.34	.30	.37	.32	.29	.34	.30	.27	.25
			8	.40	.34	.29	.39	.32	.28	.36	.30	.27	.33	.28	.25	.31	.27	.24	.22
			9	.36	.30	.25	.35	.29	.24	.32	.27	.23	.30	.25	.22	.28	.24	.21	.19
			10	.33	.27	.22	.32	.26	.22	.29	.24	.20	.27	.23	.19	.25	.21	.18	.17

Table 31. Coefficients of utilization for several different luminaires (continued).

Luminaire Type	Typical Distribution and Percent Lamp Lumens		ρcc[a] →	80			70			50			30			10			0
			ρw[b] →	50	30	10	50	30	10	50	30	10	50	30	10	50	30	10	0
	Maint. Cat.	Maximum S/MH$_d$ Guide	RCR[c] ↓	Coefficients of Utilization for 20 Percent Effective Floor Cavity Reflectance (ρ_{rc} = 20)															
7	I	1.3	0	1.02	1.02	1.02	.98	.98	.98	.92	.92	.92	.86	.86	.86	.80	.80	.80	.78
			1	.86	.82	.78	.83	.79	.75	.78	.74	.71	.73	.70	.67	.68	.66	.64	.61
Two-lamp, surface mounted, bare lamp unit - Photometry w/18" panel above luminaire (lamps on 6' centers)			2	.74	.67	.61	.71	.65	.60	.67	.61	.57	.62	.58	.54	.58	.55	.52	.49
			3	.64	.56	.50	.62	.55	.49	.58	.52	.47	.54	.49	.45	.51	.47	.43	.41
			4	.56	.48	.42	.55	.47	.41	.51	.45	.39	.48	.42	.38	.45	.40	.36	.34
			5	.49	.41	.35	.48	.40	.34	.45	.38	.33	.42	.36	.32	.39	.34	.30	.28
			6	.44	.36	.30	.43	.35	.29	.40	.33	.28	.38	.32	.27	.35	.30	.26	.24
			7	.39	.31	.25	.38	.30	.25	.36	.29	.24	.34	.28	.23	.32	.27	.23	.21
			8	.35	.27	.22	.34	.27	.22	.32	.26	.21	.30	.24	.20	.29	.23	.19	.18
			9	.32	.24	.19	.31	.23	.18	.29	.22	.18	.27	.21	.17	.26	.20	.17	.15
			10	.29	.21	.17	.28	.21	.16	.26	.20	.16	.25	.19	.15	.23	.18	.15	.13

[a] ρcc = percent effective ceiling cavity reflectance.

[b] ρw = percent wall reflectance.

[c] RCR = Room Cavity Ratio.

[d] Maximum S/MH guide = ratio of maximum luminaire spacing to mounting or ceiling height above work plane.

Source: 31, pp. 9-16, 9-18, 9-20, 9-22.

internally reflectorized fluorescent lamps, where a considerable portion of the emitted effective watts out is radiated upwards toward the house cover. However, a 10% floor reflectance (based upon the expected approximate PAR reflectance from the crop canopy and aisles), versus 0%, causes a significant increase in the CU value, especially with the fluorescent lamps. Thus, the effective entrapment of the effective watts output from the luminiares to within the greenhouse structure is expected to significantly reduce the total input energy needed from artificial lights to match equivalent solar PAR energy levels measured at the crop canopy surface.

Table 33. Coefficients of utilization for six lamps.

Luminaire type from Table 31 / Similar lamps	Coefficients of utilization[1/] $\rho_{cc} - \rho_W = .19$		$\rho_{cc} = \rho_W = .72$	
	$\rho_{FC} = .0$	$\rho_{FC} = .10$	$\rho_{FC} = .0$	$\rho_{FC} = .10$
Luminaire #2 LU400 LU1000	.71	.72	.72	.78
Luminaire #4 MV1000/C/BUH H36GW-1000/DX	.72	.73	.76	.83
Luminaire #6 FR96T12/CW/VHO/235/1 FR96T12/GRO/VHO/235/WS/1	.62	.62	.74	.81

[1/] For all CU values, RCR = 1.

Calculation of coefficients of utilization (CU) for bare lamps used within the crop canopy would be mere speculation. Some basic research is needed in this area. For the purposes of this study, it is assumed that the CU values match the best CU values of either of the fluorescent lamps used in an overhead configuration. However, it may well be that lamps used within the crop canopy will be less efficient, because the nearest leaves will be saturated while others receive very little PAR. Further, the lamp operating efficiency may be severely reduced due to excessive lamp wall temperatures and/or the reflection of output radiation back into the lamp by adjacent plant leaves, which cover the lamp.

The photosynthetically active radiation loss factor (PARLF) accounts for losses due to luminaire ambient temperature, line voltage to luminaire, ballast factor, luminaire surface depreciation, room surface dirt depreciation, luminiaire dirt depreciation, burnouts, and lamp PAR output depreciation. The luminaire ambient temperature, surface depreciation, and line voltage factors are assumed to be equal to one. That is, they are assumed to be optimized; causing no decrease in the effective watts output over the luminaire's life expectancy. The ballast factor is already accounted for in the determiniation of the effective watts output. Therefore, is not accounted for here.

The room surface dirt depreciation is considered minor in a greenhouse atmosphere, where heavy condensation on house cover surfaces washes it off frequently. The estimated reduction in effective output watts due to room surface dirt depreciation is set at 1% for all luminaires considered, based upon procedures outlined in reference 31, p. 9-4. The room surface dirt depreciation increases in significance as the amount of emitted radiation directed towards them increases (see 31, p. 9-4,

Table 32. CU multiplying factors for adjusting ρ_{FC} = 20% to ρ_{FC} = 0% or 10%.

% Effective Ceiling Cavity Reflectance, ρcc	80				70				50			30			10		
% Wall Reflectance, ρw	70	50	30	10	70	50	30	10	50	30	10	50	30	10	50	30	10
For 10 percent effective floor cavity reflectance (20 percent = 1.00)																	
Room Cavity Ratio																	
1	.923	.929	.935	.940	.933	.939	.943	.948	.956	.960	.963	.973	.976	.979	.989	.991	.993
2	.931	.942	.950	.958	.940	.949	.957	.963	.962	.968	.974	.976	.980	.985	.988	.991	.995
3	.939	.951	.961	.969	.945	.057	.966	.973	.967	.975	.981	.978	.983	.988	.988	.992	.996
4	.944	.958	.969	.978	.950	.963	.973	.980	.972	.980	.986	.980	.986	.991	.987	.992	.996
5	.949	.964	.976	.983	.954	.968	.978	.985	.975	.983	.989	.981	.988	.993	.987	.992	.997
6	.953	.969	.980	.986	.958	.972	.982	.989	.977	.985	.992	.982	.989	.995	.987	.993	.997
7	.957	.973	.983	.991	.961	.975	.985	.991	.979	.987	.994	.983	.990	.996	.987	.993	.998
8	.960	.976	.986	.993	.963	.977	.987	.993	.981	.988	.995	.984	.991	.997	.987	.994	.998
9	.963	.978	.987	.994	.965	.979	.989	.994	.983	.990	.996	.985	.992	.998	.988	.994	.999
10	.965	.980	.989	.995	.967	.981	.990	.995	.984	.991	.997	.986	.993	.998	.988	.994	.999
For 0 percent effective floor cavity reflectance (20 percent = 1.00)																	
Room Cavity Ratio																	
1	.859	.870	.879	.886	.873	.884	.893	.901	.916	.923	.929	.948	.954	.960	.979	.983	.987
2	.871	.887	.903	.919	.886	.902	.916	.928	.926	.938	.949	.954	.963	.971	.978	.983	.991
3	.882	.904	.915	.942	.898	.918	.934	.947	.936	.950	.964	.958	.969	.979	.976	.984	.993
4	.893	.919	.941	.958	.908	.930	.948	.961	.945	.961	.974	.961	.974	.984	.975	.985	.994
5	.903	.931	.953	.969	.914	.939	.958	.970	.951	.967	.980	.964	.977	.988	.975	.985	.995
6	.911	.940	.961	.976	.920	.945	.965	.977	.955	.972	.985	.966	.979	.991	.975	.986	.996
7	.917	.947	.967	.981	.924	.950	.970	.982	.959	.975	.988	.968	.981	.993	.975	.987	.997
8	.922	.953	.971	.985	.929	.955	.975	.986	.963	.978	.991	.970	.983	.995	.976	.988	.998
9	.928	.958	.975	.988	.933	.959	.980	.989	.966	.980	.993	.971	.985	.996	.976	.988	.998
10	.933	.962	.979	.991	.937	.963	.983	.992	.969	.982	.995	.973	.987	.997	.977	.989	.999

Source: 31, p. 9-32.

Figure 9-5). Thus, in this analysis, the overhead fluorescent lamps can be expected to suffer most from increases in room surface dirt.

The accumulation of dirt upon the luminaires will also cause a reduction in the effective watts output. Table 31 indicates a maintenance category for each type of luminaire, and when used in conjunction with estimates of the atmospheric dirt conditions and the frequency of cleaning, provides an estimate of the luminaire dirt depreciation factor (see reference 31, Figure 9-7). The greenhouse atmosphere is considered very clean and luminaire cleaning is assumed to occur at least once a month. Under such circumstances, the luminaire dirt depreciation factor is .98 for the HID lamps and .99 for the overhead internal reflector fluorescent lamps. Within-crop fluorescent lamps are also a given factor of .99, but this is only a guess.

Lamp burnouts for all lighting systems are assumed to be replaced immediately. Under such a system, 70% of the average rated lamp life is the minimum system lamp age reached (31, p. 9-5). Table 34 lists the lamp life expectancies in burn hours for the seven lamps in this analysis, with the metal halide lamp (MV1000/C/BUH) having the shortest life and the mercury vapor lamp (H36GW-1000/DX) having the longest.

Finally, the lamp PAR output depreciation factor reflects the expected decline in effective watts output with increasing lamp age, and is the mean output for the expected system lamp age. Table 34 lists these lamp radiant flux depreciation factors for the seven lamps considered. The expected number of burn hours per start is 10 for all lamps. The 1,000-watt high-pressure sodium lamp (LU1000) has the highest factor (.94); that is, the least depreciation in effective watts output over its life expectancy of any of the seven lamps.

Combining these several factors into one PAR loss factor (PARLF) allows for the adjustment of the lamp effective watts output in order to account for these several factors. In this study, all artificial lighting costs are based upon a comparative unit entitled an "effective watthour" (effective whr). An effective watthour equals (effective watts output)·(CU)·(PARLF)·(lamp life expectancy), except where the life expectancy of the component differs. For example, for the ballast the effective watthour is multiplied by the expected ballast life in operating hours as shown in Table 34, instead of the lamp life. For the wiring, switches, and movable system, the life expectancy of the equipment is estimated to be 172,800 hours for all lamp systems. For those lamps with external reflectors, the reflectors have the same life expectancy as the ballast. Thus, the costs of the equipment (lamp, ballast, reflector, wiring, movable system) and the variable cost of electricity are put on the common basis of an effective watthour.

Costs of Artificial Lighting for Plants

Table 35 gives the categorized costs per effective watthour for each of the seven lamps and then combines them to give the total cost per effective watthour. Under this cost analysis, all costs are assumed to occur only when the system is in operation. Further, all artificial lighting systems are assumed to include a sufficient number of lamps so the costs per additional effective watthour form a smooth continuous total cost curve per unit of output. Thus, while the fixed costs are included on a per-unit-of-output-energy basis, it is assumed that the system output energy is of large quantity and is used in a sufficiently continuous manner during that portion of the year when artificial lighting is necessary, such that this method of distributing fixed costs does not distort the "costing out" of the system. That is, it is assumed that the equipment depreciates only when in use (i.e., productive-output method of depreciation).

Table 34. Ballast and lamp life expectancies and radiant flux depreciation.

Lamp	Ballast & lamp life expectancies[A]	Lamp radiant flux depreciation[B]
	(in operating hours)	
FR96T12/GRO/VHO/235/WS/1 (Gro-lux wide-spectrum, very high output fluorescent lamp with 235° internal reflector)	60,000 hrs/ballast 10,500[C] hrs/lamp	.78[D]
FR96T12/CW/VHO/235/1 (cool-white very high output fluorescent lamp with 235° internal reflector)	60,000 hrs/ballast 10,500 hrs/lamp	.78[D]
F96T12/GRO/VHO (Gro-lux very high output fluorescent lamp)	60,000 hrs/ballast 10,500[C] hrs/lamp	.78[D]
MV1000/C/BUH (phosphor-coated standard metal halide HID lamp)	150,000[E] hrs/ballast 7,000[F] hrs/lamp	.82
H36GW-1000/DX (1,000-watt deluxe white mercury HID lamp)	150,000[E] hrs/ballast 16,800[F] hrs/lamp	.72[G]
LU400 (400-watt high-pressure sodium HID lamp)	150,000[E] hrs/ballast 14,000[F] hrs/lamp	.93[G]
LU1000 (1,000-watt high-pressure sodium HID lamp)	150,000[E] hrs/ballast 10,500 hrs/lamp	.94[G]

[A] These are 70% of the rated average lamp life expectancies and is the assumed minimum lamp age reached where burnouts are replaced immediately (31, p. 9-5).

[B] PARLF = photosynthetically active radiation loss factor, the product of several factors which diminish the level of PAR delivered to the crop. The primary factor of significance included in the PARLF is the lamp radiant flux depreciation factor.

[C] Sources: 53, pp. 40, 44-45; 17, pp. 63, 65; 5, p. 35.

[D] Sources: 31, pp. 8-95, 8-98; 5, p. 36.

[E] Sources: Holophane sales engineer.

[F] Sources: 18, pp. 36-37; 53, pp. 33, 35.

[G] Source: 18, pp. 36-37.

Table 35 includes the costs per effective watthour for lamp; ballast; wiring, switches, and movable luminaire system; cleaning, maintenance, and insurance; and electricity. The cost of each lamp is depreciated over its expected total delivered effective watts, which are based upon its mean life expectancy and mean radiant flux delivered to the crop canopy (the house cover coefficient of reflectivity is assumed to be .7). The ballasts and luminaires are depreciated over the expected total delivered effective watts during their operating lives. Lamp bases and holder (fluorescent lamps only) are depreciated with the wiring, entrance panels, switches, and other hardware necessary for the lighting system. The estimated cost of a movable lighting system ($6,000 per CEVCO hours) is included with the cost of wiring, etc. and is depreciated over 172,800 operating hours, or more precisely, over

Table 35. Costs per effective watthour for seven lamps.

Lamps	Effective Watts Output[A]	Coefficient of Utilization (CU)[B]	PARLF[C]	Ballast Lamp Life Expectancies[D]	Cost of Lamp per Effective Whr[E]	Cost of Ballast per Effective Whr[F]	Cost of Wiring per Effective Whr[G]	Cost of Cleaning, Maintenance, & Insurance per Effective Whr[H]	Cost of Electricity per Effective Whr[I]	Total Cost per Effective Whr[J]
FR96T12/GRO/VHO/235/WS/1 (Gro-lux, wide-spectrum, very high output fluorescent lamp)	44.6	.81	76	60,000 10,500	$2.43 x 10^{-5}	$7.28 x 10^{-6}	$4.00 x 10^{-6}	$8.43 x 10^{-6}	$2.46x10^{-4}$ $3.28x10^{-4}$ $4.09x10^{-4}$	$2.90x10^{-4}$ $3.72x10^{-4}$ $4.53x10^{-4}$
FR96T12/CW/VHO/234/1 (cool-white, very high output fluorescent lamp)	27.0	.81	.76	60,000 10,500	$4.75 x 10^{-5}	$1.20 x 10^{-5}	$6.06 x 10^{-6}	$1.39 x 10^{-5}	$4.06x10^{-4}$ $5.41x10^{-4}$ $6.76x10^{-4}$	$4.85x10^{-4}$ $6.20x10^{-4}$ $7.55x10^{-4}$
F96T12/GRO/VHO (Gro-lux very high output fluorescent lamp	34.3	.81	.76	60,000 10,500	$4.48 x 10^{-5}	$9.47 x 10^{-6}	$4.95 x 10^{-6}	$1.10 x 10^{-5}	$3.19x10^{-4}$ $4.26x10^{-4}$ $5.32x10^{-4}$	$3.89x10^{-4}$ $4.96x10^{-4}$ $6.02x10^{-4}$
MV1000/C/BUH (phosphor coated-standard metal halide HID lamp)	251	.83	.80	150,000 7,000	$5.01 x 10^{-5}	$9.36 x 10^{-6}	$7.51 x 10^{-6}	$1.39 x 10^{-5}	$1.94x10^{-4}$ $2.58x10^{-4}$ $3.23x10^{-4}$	$2.75x10^{-4}$ $3.39x10^{-4}$ $4.04x10^{-4}$
H36GW-1000/DX (1,000-watt deluxe white mercury HID lamp)	128	.83	.70	150,000 16,800	$2.09 x 10^{-5}	$2.11 x 10^{-5}	$1.60 x 10^{-5}	$3.11 x 10^{-5}	$4.34x10^{-4}$ $5.78x10^{-4}$ $7.23x10^{-4}$	$5.23x10^{-4}$ $6.67x10^{-4}$ $8.12x10^{-4}$
LU400 (400-watt high-pressure sodium HID lamp)	114	.78	.90	150,000 14,000	$3.75 x 10^{-5}	$1.24 x 10^{-5}	$8.15 x 10^{-6}	$1.45 x 10^{-5}	$1.69x10^{-4}$ $2.25x10^{-4}$ $2.81x10^{-4}$	$2.42x10^{-4}$ $2.98x10^{-4}$ $3.54x10^{-4}$
LU1000 (1,000-watt high-pressure sodium HID lamp)	321	.78	.91	150,000 10,500	$3.58 x 10^{-5}	$6.87 x 10^{-6}	$5.84 x 10^{-6}	$1.02 x 10^{-5}	$1.41x10^{-4}$ $1.87x10^{-4}$ $2.34x10^{-4}$	$2.00x10^{-4}$ $2.46x10^{-4}$ $2.93x10^{-4}$

A/ Effective watts output = (350-530 nm watts) + (.5)(530-580 nm watts) + (580-780 nm watts).

B/ Source: 43, Appendix II, p. 3.

C/ PARLF = photosynthetically active radiation loss factor = product of several factors which diminish the level of PAR delivered to the crop. The primary factor of significance included in the PARLF factor is the lamp radiant flux depreciation factor.

D/ These are 70% of the rated average lamp life expectancies and is the assumed minimum lamp age reached where burnouts are replaced immediately (31, p. 9-5).

E/ $$\frac{\text{Cost of Lamp}}{\text{Effective Whr}} = \frac{\text{Lamp Cost}}{(\text{Effective Watts Output})\cdot(\text{Lamp Life Expectancy})\cdot(\text{CU})\cdot(\text{PARLF})}$$

F/ $$\frac{\text{Cost of Ballast}}{\text{Effective Whr}} = \frac{\text{Ballast and Luminaire Cost per Lamp}}{(\text{CU})\cdot(\text{PARLF})\cdot(\text{Effective Watts Output})\cdot(\text{Ballast Life Expectancy})} \cdot$$

G/ $$\frac{\text{Cost of Wiring}}{\text{Effective Whr}} = \frac{\text{Wiring and Movable Luminaire System Cost per Lamp}}{(\text{CU})\cdot(\text{PARLF})\cdot(\text{Effective Watts Output})\cdot(172800\ \text{hrs})} \cdot$$

H/ $$\frac{\text{Cost of Cleaning Maintenance \& Insurance}}{\text{Effective Whr}} = \frac{\text{Cost of Cleaning etc. per Lamp Year}}{(\text{CU})\ (\text{PARLF})\ (\text{Effective Watts Output})\ (4320\ \text{hrs yr})^{-1}} \cdot$$

I/ $$\frac{\text{Cost of Electricity}}{\text{Effective Whr}} = \frac{(\text{Input Watts})\cdot(\text{Cost per Watthour})}{(\text{Effective Watts Output})\cdot(\text{CU})\cdot(\text{PARLF})} \cdot$$

J/ Total Cost per Effective Watthour = Cost of Lamp per Effective Whr + Cost of Ballast per Effective Whr + Cost of Wiring per Effective Whr + Cost of Cleaning, Maintenance and Insurance per Effective Whr + Cost of Electricity per Effective Whr.

the expected delivered watts to the entire crop canopy during that time (this cost is $8.421 x 10^{-7} Whr^{-1}). The insurance expense is estimated at 1% of the total capital investment and is included with the annual cleaning and maintenance cost and spread over an expected 4,320 hours of operation annually. The cleaning and maintenance cost is based upon an estimated monthly labor expense for cleaning the lamps and luminaires, lamp replacement labor, ballast maintenance, and lighting system maintenance. The cost of electricity is included at three alternative prices ($.03, $.04, $.05 per Kwh) and is based upon the amount of input energy necessary for each effective watthour out. This is the single greatest cost component per effective watthour out.

Table 36. Total costs and capital investments required to supply 100 lys per CEVCO house crop surface per month for seven alternative lamp systems.

Lamp	Total cost to supply 100 lys over 266 m^{-2} for 30 days		No. luminaires needed for:	Estimated capital investment to supply 100 lys PAR per day (15%)
FR96T12/GRO/VHO/235/WS/1 (Gro-lux wide-spectrum, very high output fluorescent lamp)	$2,691	$.03 Kwh^{-1}	379	$2,833
	$3,452	$.04 Kwh^{-1}		
	$4,204	$.05 Kwh^{-1}		
FR96T12/CW/VHO/235/1 (cool-white, very high output fluorescent lamp)	$4,501 $5,754 $7,007		625	$4,209
F96T12/GRO/VHO (Gro-lux very high output fluorescent lamp)	$3,610 $4,603 $5,587		492	$3,626
MV1000/C/BUH (phosphor-coated standard metal halide HID lamp)	$2,552 $3,146 $3,749		65	$5,623
H36GW-1000/DX (1,000-watt deluxe white mercury HID lamp)	$4,854 $6,190 $7,536		144	$10,751
LU400 (400-watt high-pressure sodium HID lamp)	$2,246 $2,766 $3,285		126	$6,419
LU1000 (1,000-watt high-pressure sodium HID lamp)	$1,856 $2,283 $2,719		44	$4,316

A/ Total cost to supply 1000 lys of effective watts output over 266 m^2 for 30 days = $\left(\frac{\text{Total Cost}}{\text{Effective Whr}}\right) \cdot \left(\frac{309,358 \text{ Whr}}{\text{House}}\right)$. Three separate costs are listed for each lamp in this column; the first one estimated at $.03 Kwh^{-1}, the second at $.04 Kwh^{-1}, and the last at $.05 Kwh^{-1}.

No tax is assumed upon capital equipment. Any estimated rate of return on capital investment, however, must account for corporate income taxes upon the net revenue generated by that asset. For tax purposes, accounting practice generally depreciates lighting systems over five years (16, p. 2).

Table 36 provides comparative total costs and capital investments required (using a movable lighting system covering one-half of a CEVCO house) to supply 100 langleys of PAR per day to an entire CEVCO house crop canopy surface for 30 days. The 1,000-watt high-pressure sodium lamp system is least expensive, costing 17% less than the LU400 lamp system at $.03 Kwh^{-1}. The 1,000 watt metal

halide lamp (i.e., MV1000/C/BUH) is the third cheapest system, with the wide spectrum Gro-lux fluorescent lamp a close fourth at \$.03 Kwh^{-1}. However, the relative difference in total costs increases for the Gro-lux fluorescent lamp with rising electricity costs.

The last two columns of Table 36 indicate the number of lamps and 15% of the expected capital investment (i.e., 15% return on investment) needed to supply 100 langleys of PAR to the crop using a movable luminaire system. The FR96T12/GRO/VHO/235/WS/1 has the lowest expected capital investment, being \$1,483 (at 15%) below the capital investment required for the LU1000 lamp system. At \$.03 Kwh^{-1} it would require 1.8 months of operation before the LU1000 lamp system could match the costs plus return on investment of 15% of the wide-spectrum Gro-lux fluorescent lamp system. Furthermore, it would require at least six months of operation for the metal halide lamp system to undercut the wide-spectrum Gro-lux fluorescent lamp system at 100 langleys per day. However, the advantage of the fluorescent Gro-lux lamp declines as the radiant energy supplied increases due to economies in wiring and lighting system design. Thus, the LU1000 lamp can be expected to be the cheapest artificial source of PAR at high levels of irradiation over several winter months. But, for minimal amounts of irradiation or for systems using very little, the lower return on capital expense is expected to make the FR96T12/GRO/VHO/235/WS/1 fluorescent lamp cheaper.

Finally, it should be remembered that the movable lighting system is assumed to cost \$6,000, while for the cheapest system in terms of capital investment, the lamps, wiring, etc. costs \$12,887. Thus, if the movable lamp system were to be replaced by fixed artificial lamps over the entire crop canopy surface, the capital investment is expected to increase by \$6,866 (15% of which equals \$1,033). Furthermore, the deleterious effects of fewer burning hours per start, as previously discussed, would reduce the expected lamp life. Thus, the advantages of a movable luminaire system are apparent; with the only major disadvantage being the reduced flexibility in crop irradiation patterns.

It is now possible to estimate the costs and expected returns in yields of tomatoes for artificial lighting. Remembering that the estimated level of available solar radiation at the crop canopy surface was for periods of high irradiation, it follows that the input level of artificial lighting PAR must be equivalently high. It is assumed, therefore, that the mean daily level of solar irradiation is 500 langleys. The effective photosynthetically active irradiation at the crop canopy surface is: $(500 \text{ lys})\cdot(.5)\cdot(.65) = 162.5$ lys. Furthermore, the hours of direct sunshine (i.e., HRSSUN) is: $HRSSUN \approx .017 \text{ lys} + 1.67 \approx (.017)\cdot(500 \text{ lys}) + 1.67 \approx 10.2$ hours. Therefore, LANGHRS1 = (lys)·(HRSSUN).

From reference 8, the best ordinary least squares regression function for estimating tomato yields per month per CEVCO house is: Tomato yield = (31.089)·(mean external temperature) + (.295)·(LANGLEYS)·(HRSSUN) + (19.62)·(hours of pollination per month) - (1,787.58)·(nutrient solution pH)^2 + (23,344.58)·(nutrient solution pH) - (.004)·(CROPAGE)·(LANGLEYS)·(HRSSUN) - (.191)·(dissolved solids in nutrient solution) - $(2.306 \times 10^{-9})\cdot((\text{LANGLEYS})\cdot(\text{HRSSUN}))^3$ - 76,796.5.

In this function, several of the variables are from one month prior to the dependent variable, tomato yields--including LANGLEYS, HRSSUN, and mean external temperature. The hours of pollination, pH of the nutrient solution, and the dissolved solids are from two months prior to the tomato yield. Setting the independent variables near their optimum values yields:12/ mean external temperature = 49.5; LANGHRS = (LANGLEYS)·(HRSSUN) = 5,100; hours of pollination = 18; nutrient solution pH = 6.53; crop age = 3½ months (or 7 half-months); and dissolved solids in nutrient solution = 1,200 ppm. Solving the function for tomato yield gives a value of 2,132 kg. Thus, for an estimated 162.5 lys per

day of PAR upon the crop canopy surface, a monthly yield of 2,132 kg of tomatoes is expected (based upon the best ordinary least squares estimate).

Using the lowest estimated cost to supply 162.5 langleys per day from Table 36 (i.e., using the LU1000 lamp at $.03 Kwh^{-1}) gives a total cost per month of $3,016, not including any return on capital invested. Fifteen percent of the estimated capital investment is $6,451. At 2,132 kg per month, the cost of artificial lighting per kilogram of tomatoes is $1.41. Clearly, the cost of total substitution of solar irradiation with artificial lighting radiation is prohibitively expensive. Even if it is assumed that 150 lys per day is supplied from the sun with the LU1000 lamps supplying 114 lys of PAR, the cost per kilogram is $.99 kg^{-1}. Thus, the cost of artificial lighting is such that it does not appear to be a viable total source of radiant energy for tomatoes--yet.

Examining the expected revenue and costs due to artificial lighting by a different method gives essentially the same conclusion. This approach makes some rather gross assumptions. From reference 8 it was estimated that the $MPP_{LANGHRS1} = .295 - 6.917 \times 10^{-9}$ $LANGHRS1^2$ - .004 CROPAGE, where the marginal physical product (MPP) is the increase in tomato yields caused by the addition of one unit of LANGHRS1. From this function it can be seen that the maximum $MPP_{LANGHRS1}$ is .295 kg, where LANGHRS1 = 0 and declines with every additional unit of LANGHRS1. If tomatoes could be wholesaled at $1.69 per kilogram, the revenue generated by one additional LANGHR1 per house per month would be 50 cents. However, the lowest possible cost to supply this radiant energy artificially using LU1000 lamps at $.03 Kwh^{-1} is about 62 cents. Clearly, artificial lighting of a mature tomato crop as the source of PAR is not yet economically feasible.

These previous estimates of yields and costs derived for the artificial lighting of a tomato crop do not answer the question of whether or not the special use of artificial lighting such as with chopping or for side shoot control is economically feasible. They also do not consider the effects of artificial irradiation upon tomato quality. Nevertheless, these estimates do reflect the existence of a large difference between likely revenues and costs when using the cheapest of the artificial lighting systems considered. In fact, the magnitude of the apparent unprofitability of artificial lighting diminishes the significance of the tenuous estimates used in this analysis.

Considerable improvement is required before the economic feasibility of artificial lighting is likely to be favorable. Several possible areas exist for improving the economics of the situation, including lower electricity costs, improved luminaire efficiency, improved plant efficiency in utilizing radiant energy, improved crop efficiency in utilizing available PAR, and improved methods of applying radiant energy to a crop of tomato plants. As improvements are made in any of these factors, the reevaluation of the costs and revenues (following the outline provided here) will indicate the feasibility of the new lighting system.

In conjunction with the costs and revenues generated by artificial lighting systems, a significant amount of heat is also produced. Tables 28 and 30 reflect the amount of heat (in watts) generated for each of the seven lamps considered. As the efficiency of producing PAR improves, the amount of heat generated per effective watt output declines. Thus, the high-pressure sodium LU1000 lamp generates the least waste heat of the seven lamps considered for a given quantity of PAR generated. Nevertheless, this heat will have a substantial impact upon the demand for heat within a greenhouse during the winter months. For example, using the previous artificial lighting system with LU1000 lamps and providing 162.5 langleys per day of PAR, it can be expected to generate 1031 Mcal of infrared, conductive, convective, and ballast heat or 533 Mcal of conductive, convective, and ballast heat each

day.13/ Depending upon external temperatures, this may constitute anywhere from 19% to 100% of the daily heat demand per CEVCO house. However, a major problem with such energy is that it cannot be turned on and off as desired.14/ The net cost/benefits of this heat will depend upon whether it can be used efficiently and what the costs of a mass storage system and other necessary capital equipment are.

Notes to Chapter 4

1/ Some research indicates that longer periods of low irradiation may help suppress respiration losses and thereby improve net assimilation for a given level of irradiation (28, p. 45).

2/ Decreasing the oxygen concentration from 21 percent to 1 percent also increased net CO_2 uptake at atmospheric CO_2 levels.

3/ It now appears that subjective taste tests of tomatoes were right in evaluating summertime tomatoes as tasting better. Taste has been shown to be related to acid and sugar content within the tomato in addition to freshness. Studies show a strong positive relationship between levels of irradiation and tomato sugar levels (68, pp. 134-142.)

4/ The relative responses are of significance, but specific responses are dependent upon cultivar, temperatures, humidity, CO_2 levels, etc.

5/ Some people have attributed the increases in dry weight gains, which occurred with additional energy in the far-red region, as being due to the increase in plant height, which permitted more radiant energy to reach the lower leaves (5, p. 146).

6/ Some of the more recent discoveries include Tucker's finding that partial suppression of side-shoot growth can be achieved with short periods of far-red (700-750 nm wavelength) irradiation at the end of the day. Also, the effects of sunflects or chopping, upon the efficiency of PAR energy conversion into plant products may permit more efficient usage of energy supplied by artificial lights. Future discoveries may reveal significant effects caused by early morning irradiation of plants with particular spectral energy. Potential benefits may also occur with changes in daily lighting cycles. The future possibility of being able to modify plant functions such that continuous positive net assimilation may be achieved under artificial lighting is another possibility.

7/ For effective starting of rapid start lamps, a grounded conducting plate within 2.54 cm of the lamp and running the length of it is necessary (31, pp. 8-29).

8/ Note that lumens is a term relevant to visual radiant energy and not to the PAR spectrum. However, when it is used here it is assumed to be a surrogate for photosynthetically active radiant energy (PAR) in lieu of more adequate data.

9/ Figure 36 is for high output lamps. Very high output lamps operate at slightly higher temperatures (see Figure 37).

10/ High-pressure sodium lamps will not start on either mercury or metal-halide ballasts of equivalent wattage, although this may change in the near future. Using mercury or metal halide lamps on equivalent wattage high pressure sodium ballasts causes the lamps to operate on an over-wattage condition which results in reduced lamp life and/or lamp shattering.

11/ One study, using 400-watt high-pressure sodium lamps giving an irradiance of 26.9 $W \cdot m^{-2}$ for 400-700 nm, recorded a temperature rise of 1.11° C at 1.52 m above the soil surface with the artificial lights on (43, p. 3).

12/ Assuming the optimum values of the other factors ignores the likely additional costs necessary for their effective control. For example, CO_2 supplementation will be required and will have a cost, but it is not included here.

13/ The ability to capture and/or store the infrared energy is remote but the conductive, convective, and ballast heat is controllable.

14/ This fact leads one to speculate that if large proportions of PAR are supplied by artificial lighting, then other compatible changes in greenhouse design will also occur, including improved house insulation; reflective surfaces for higher coefficients of utilization and/or insulating effect; heat storage systems such as are being developed for solar heating systems; and improved humidity control due to increased potential for ventilating.

Chapter 5

SUMMARY

A significant amount of interaction exists among the several input factors to plants and this affects yields. PAR, for example, affects both photosynthesis and photolysis either directly or indirectly and these two processes have opposite effects upon yields. Consequently, the optimization of PAR levels is not easily determined.

Many of the currently used methods of measuring inputs to plants are inadequate and need to be refined so they identify the significant quantities and qualities distinguished by plants. This is true for the measurement of PAR, where variations in spectral radiant intensities, crop canopies, and leaf angles of incidence, and patterns of radiation application all need to be distinguished.

While large segments of the plant life processes have been precisely defined and modeled, many important functions remain to be explained. This prevents the optimization of inputs because the technical system is unknown.

The complete control of plant processes in the future will require continuous monitoring of the important variables in the plant's processes. This will be necessary for product optimization. Dynamic computer models and feedback systems will be utilized. The continuous monitoring of PAR in discrete wavebands (as exemplified in this publication) is needed today so tomorrow's researchers can isolate the effects of spectral energy distribution fluctuations upon field crops via large amounts of data over extended time spans.

Transmitted radiation through a crop canopy declines exponentially with respect to increases in the crop shape factor (K_s) and total leaf area (L_t) of the crop, and with respect to decreases in leaf transmissivity (τ). Therefore, location of artificial lights within the crop canopy would seem to have a potential advantage over overhead solar radiation or overhead artificial lights. However, the lack of chopping effect, older, less-efficient leaves lower in the crop canopy, and reduced lamp efficiency are possible drawbacks to such lamp location.

Differences in the altitude angle β for the sun versus artificial lights with respect to a greenhouse crop canopy should not cause significant differences in yields. It is expected that any advantage due to differences in altitude angle β will go to the artificial lights. The effectiveness of artificial lighting over equivalent solar radiation should increase as solar altitude angle β declines toward 0^{o}.

The time required after sunrise before the east bed is fully irradiated by direct solar radiation is 20% less than on June 22 and similarly less for full direct irradiation of the area between two CEVCO houses. However, the time during which a CEVCO house is receiving any reflected direct solar radiant energy from the ground area between the houses is 57% less on December 22 than on June 22.

The significance of CEVCO house shape factor K_s for a N-S oriented house is diminished for four reasons:

(1). Most of the shadow cast by the house falls within the crop area.

(2). When significant shape factors do occur, the angles of incidence are also fairly large, resulting in radiant energy through the house cover.

(3). Only the portion of direct radiation (due to the shape factor) diffused or reflected by the house cover into the crop canopy is available to the crop.

(4). The most significant shape factors (K_s) occur during the periods of lowest solar irradiation.

Due to CEVCO house shape factors, on December 22 an E-W house should exceed a N-S house in received solar irradiation by 26.4 lys·day^{-1} on the average, with an estimated yield effect of about 23 kg of tomatoes per house-month. And, on June 22 an average reduction of about 16 lys per day on the crop canopy can be expected with an E-W versus N-S house. This constitutes a reduced cooling load of about 2.9 Mcal per day per cm^2.

The angle of incidence of solar radiation with respect to a house cover can have a very marked effect upon the amount of radiation transmitted through the house cover to the crop canopy. Thus, house shape is very important with respect to solar radiation received by the crop.

House cover transmissivities decline rapidly at angles of incidence exceeding about 30^o.

During the period of maximum mean available solar radiation, around solar noon, an E-W house cover has its best transmissivities while a N-S house cover has its poorest ones (see Table 11).

No comprehensive analysis of the economic tradeoffs among house cover materials or house designs have been found. A comprehensive evaluation of house cover materials must consider capital investment expenses, installation and maintenance costs, durability, insurance costs, effectiveness of CO_2 retention, ethylene release rates, fire resistance, ease of replacement, effects on cooling, use of shading compounds, PAR reduction due to water condensation, building code qualifications, transmissivity of PAR, and heat retention.

An E-W versus N-S house orientation is best at CEVCO because during winter months greater solar irradiation is obtained, while during the summer months, when cooling and excessive solar irradiation are problems, less solar irradiation is received.

A significant increase in CEVCO house irradiation levels occurs due to reflected radiation from surrounding ground surfaces (see Table 6), while adjacent house covers contribute a significantly smaller amount of reflected radiation. The house covers adjacent to a CEVCO house contribute a relatively minor amount to the total irradiance of the house's cover (about a 1.2% increase in I, where I = 500 lys·day^{-1}.

From Table 6, the estimated value of reflected radiation I_R on December 22 for an E-W versus N-S CEVCO house is about three times greater and in itself constitutues about 23.8% of the average daily irradiation measured on a horizontal plane (i.e., I_h measured by a pyranometer). However, this increase in I_R requires an approximately four-fold increase in house spacing. But even with only a 3-meter increase in house spacing, I_R is estiamted to be significantly greater for an E-W versus N-S house of CEVCO design. In the summer, values of reflected radiation I_R are estimated to be approximately equal for E-W and N-S oriented CEVCO houses, thus causing no significant difference in cooling load due to absorbed radiation. If greater spacing between houses is desirable but not economically feasible, elevation of the houses lying to the north may be a practical alternative. From reference 8, the estimated increase in monthly tomato yields due to an expected 20 lys·day^{-1} increase in I_R is slightly less than 18 kg. This does not include any effects due to an expected 22% greater transmissivity for E-W versus N-S house covers due to differences in angles of incidence.

For the period May-July, when solar irradiation at CEVCO is at or near 500 lys·day^{-1}, it is expected that only 64% of the solar radiation measured on a horizontal pyranometer at the University of Minnesota will on an average day reach the tomato crop canopy within a CEVCO house. Therefore, in terms of equivalent energy inputs it is assumed that artificial lights need to supply to the crop canopy only 64% of the measured PAR on a pyranometer (S_t) outside a CEVCO house.

A review of artificial lighting research with tomato plants indicates:

(1). The use of artificial lighting as a total source of irradiance for commercial tomato production has not been economically successful to date.

(2). This use of artificial lights to supplement solar radiation reduces the time to maturity of tomato seedlings.

(3). The use of artificial lights to supplement solar radiation via daylength extension using low levels of irradiation improves early yields, but does not significantly improve total crop yields.

(4). The use of artificial lights for tomato plant physiological effects has not yet been fully examined.

(5). The use of artificial lights in growth chambers for pre-transplant tomato seedling development currently appears to be economically and technically feasible--at least during those months of low solar irradiation.

(6). The extension of wintertime daylength with low levels of irradiation improves early yields but not necessarily total yields or net financial returns.

The advantages of a moveable luminaire system are that it reduces capital investment, reduces maintenance costs, and that it increases lamp life expectancies because operating cycles are longer. The major disadvantage is reduced flexibility in crop irradiation patterns.

Several factors determine the effectiveness of delivering PAR to a crop canopy within a greenhouse including lamp and luminaire orientation to the crop, lamp spacing, luminaire efficiency, luminaire dirt depreciation, input power, and lamp luminous efficacy.

The correct ballast design loading and line conditions are of significant economic importance for the long-term efficient operation of an artificial lighting system.

When no radiation is reflected from the floor, the coefficient of reflectivity of the house cover causes little variation in the estimated CU values, except with internally reflectorized fluorescent lamps, where a considerably greater portion of the emitted effective watts output is radiated upwards toward the housecover. The effective entrapment of the effective watts output from the luminaires to within the greenhouse structure is expected to significantly reduce the total input energy needed from artificial lights to match equivalent solar PAR energy levels measured at the crop canopy surface.

Compared with fluorescent lamps, HID lamps are relatively insensitive to ambient air temperature changes and external air movements.

HID lamps, unlike most fluorescent lamps, cannot be placed within the crop canopy due to their high temperatures. However, the efficiency of fluorescent lamps placed within the crop canopy may be diminished by at least three factors:

(1). The leaves immediately surrounding the lamps may become saturated with PAR, while more distant leaves receive very little PAR.

(2). Excessive lamp wall temperatures and/or excessive moisture may reduce lamp efficiency.

(3). Reflection of emitted radiation back into the lamp by adjacent plant leaves may reduce lamp operating efficiency.

HID lamps are somewhat more flexible than fluorescent lamps in terms of economically efficient burning period. High-pressure sodium lamps have the lowest drop in PAR output of any of the seven lamps studied.

Lower wattage HID lamps are somewhat less efficient in converting input energy into effective PAR out, as exemplified by the LU400 versus the LU1000 lamp in Table 29.

Of the three fluorescent lamps analyzed, the Gro-lux wide-spectrum, very high output, fluorescent lamp (i.e., FR96T12/GRO/VHO/235/WS/1) has the best PAR energy distribution and the best ratio of input watts to effective watts out (i.e., 5.04 versus 6.56 and 8.33 for the other two lamps).

Of the seven lamps considered, the mercury vapor lamp has the longest life expectancy, while the metal halide lamp has the shortest (see Table 34).

The 1000-watt high-pressure sodium lamp has the highest lamp radiant flux depreciation factor of the seven lamps considered (see Table 34). This indicates it has the least depreciation in effective watts output over its lifetime of the seven lamps evaluated.

Of the seven lamps evaluated, the 1000-watt high-pressure sodium lamp system is least expensive to operate, costing 17% less than the LU400 lamp system at \$.03 Kwh^{-1}. The 1000-watt metal halide lamp system is third cheapest and the wide-spectrum Gro-lux fluorescent lamp a close fourth.

Of the seven lamps considered, the 1000-watt high-pressure sodium lamp LU1000 has the lowest ratio of input watts to effective watts output, but like all of the seven lamps analyzed has significantly less output percentage-wise in the 690-780 nm waveband than average solar radiation (7.1% versus 16.3%). The high-pressure sodium lamp is also low in energy output in the blue spectrum relative to the estimated normal solar energy distribution of PAR (12.2% versus 36.9%). Therefore, this lamp will likely need to be supplemented with lamps providing more output energy in the blue spectrum.

Of the seven lamps considered,the FR96T12/GRO/VHO/235/WS/1 has the lowest expected capital investment needed to supply 100 lys per day to a CEVCO house crop.

Of the four HID lamps analyzed, the metal halide lamp (MV1000/C/BUH) has the lowest combined lamp/solar effectiveness weight, while the high-pressure sodium lamps have the highest weights. Thus, while the high-pressure sodium lamp is more efficient to operate, the metal halide lamp has a significantly better PAR distribution which may result in significantly better plant growth (see Table 29) for an equal amount of energy.

Of the seven lamps considered, the LU1000 lamp is expected to be the cheapest source of artificially generated PAR at high levels of irradiation over extended periods of time. The FR96T12/GRO/VHO/235/WS/1 fluorescent lamp is expected to be the cheapest source of artificially generated PAR for minimal amounts of irradiation or for infrequently used systems.

The large amount of excess heat generated by any large greenhouse lighting system implies that if artificial lighting does become economically feasible for controlled environments, then other compatible changes in greenhouse design will also occur, perhaps including improved house insulation, reflective surfaces for higher coefficients of utilization and/or insulating effect, heat storage systems such as are being developed for solar heating systems and improved humidity control due to increased potential for ventilating. This factor implies that reconsideration of the entire greenhouse design may be desirable in cooler regions where artificial lighting is necessary.

For the production of tomato seedlings, artificial lighting is becoming accepted and appears to be currently economically feasible.

Few studies to date have indicated that growing mature tomato plants under artificial lighting is economically successful. With respect to tomato plants, the most successful work to date has been with seedlings.

The cost of artificial lighting is too high to currently allow it to be a viable source of total radiant energy for commercial tomato production. In fact, the magnitude of the apparent unprofitability of artificial lighting diminishes the significance of the tenuous estimates used in this analysis.

Appendix A

GREEK SYMBOLS

α	Wall-solar azimuth angle (in degrees).
β	Solar altitude angle (in degrees).
γ	Solar azimuth angle (in degrees).
ε	Mean angle of house cover to house floor.
θ	Solar angle of incidence for a surface.
θ''	Specular angle of reflection.
λ	Wavelength; normally in nanometers (nm).
μ	Micron; a unit of measure equal to 10^{-6} meters.
ρ	Surface coefficient of reflectivity (dimensionless).
ρ_{cc}	Ceiling cavity reflectance.
ρ_{w}	Wall reflectance.
ρ_{FC}	Floor cavity reflectance.
σ	Angle by which a surface is tilted from horizontal position (in degrees).
τ	Coefficient of transmissivity (dimensionless).
ϕ	Angle by which a surface is tilted from the vertical plane (in degrees).
Φ	Radiant flux; the time rate of flow of radiant energy.
ψ	Solar zenith angle (in degrees).
ω	Solid angle; a ratio of area on sphere's surface to radius squared.

OTHER SYMBOLS

a	Linear dimension (in meters).
A	Irradiated surface area of an object.
A_o	Area of surface of luminaires.
A_s	Area of house cover above the surface of luminaires.
A_h	Area of shadow cast upon a horizontal plane.
b	Linear dimension (in meters).
Btu	British thermal unit.
C	Net thermal convection to or from a plant.
CM	Contribution margin.
CO_2	Carbon dioxide.
CU	Coefficient of utilization.
d	Solar angle of declination.
d	Dust factor.
DS	Dissolved solids (in parts per million).
F	A dimensionless factor defined on page.
FC	Fixed cost.
g	Gram(s).
h	Solar hour angle (in degrees).
hr	Hour(s).
H	Solar hour angle at sunrise or sunset.
HID	High intensity discharge.
I	Incident total solar radiation upon a surface.
I_d	Incident solar diffuse radiation upon a surface.
I_D	Incident direct solar radiation upon a surface.
I_{DH}	Incident direct solar radiation upon a horizontal surface.
I_H	Incident total solar radiation upon a horizontal surface.
I_N	Incident direct solar radiation upon a surface normal to sun's rays.
I_λ	Incident monochromatic solar radiation upon a surface.
I_R	Incident solar radiation upon a surface reflected from surrounding surfaces.
K_S	Shape factor. Expressed by the equation $A_h \cdot A^{-1}$.
KNO_3	Potassium nitrate.
kg	Kilogram(s). One kilogram equals 1,000 grams.

OTHER SYMBOLS (continued)

Kwh Kilowatthour(s). One kilowatthour equals 1,000 watthours.

l Latitude angle (in degrees).

L_t Total leaf area (in meters squared).

LAI Leaf area index.

LAR Leaf area ratio.

LCT Local civil time.

LDD Luminaire dirt depreciation factor.

LST Local solar time.

m Air mass.

m Meter(s).

Mcal Megacalorie(s). One megacalorie equals 1,000,000 calories, where 252.161 calories equals 1 Btu.

mm Millimeter(s).

MPP_{x_i} Marginal physical product of x_i.

mps Meters per second.

n The number of some factor, such as moles.

n_L Number of layers of leaves in a crop canopy.

nm Nanometer(s). One nanometer equals 10^{-9} meter.

N Normal to the surface.

NAR Net assimilation rate.

p Pressure. Expressed in millibars (mbar).

PAR Photosynthetically or physiologically active radiation.

PARLF Photosynthetically active radiation loss factor.

ppm Parts per million.

r Hypotenuse.

R Incident thermal radiant energy.

Ra Incident thermal radiant energy from the atmosphere.

Rg Incident thermal radiant energy from the ground or floor.

RCR Room cavity ratio.

RH Relative humidity.

S Sunfleck area; equal to $1 - K_s$.

S_o Solar irradiation at the top of a crop.

S_t One-half of the measured solar irradiation striking a pyranometer near CEVCO.

SED Spectral energy distribution.

t Elapsed time.

TC Total cost.

TFC Total fixed cost.

TR Total revenue.

TVC Total variable cost.

vac Volts of alternating current.

VC Variable cost.

VHO Very high output.

w Precipitable water depth (in millimeters).

W Watt(s).

Whr Watthour(s).

x Independent variable or a factor of production.

$\bar{x}$ Estimate of the population mean (μ).

x1 The y-axis intercept shift variable activated at TPVARI $\geq$ 50.

x2 A slope shift variable activated at TPVARI $\geq$ 50.

y Linear dimension (in meters).

z Linear dimension (in meters).

DEFINITIONS

Air mass (m): The ratio of the length of path of the sun's rays through the atmosphere to the length of path if the sun is at its zenith. m = 1 at sea level when $\beta = 90^{\circ}$ and m $\approx$ cosec β when $\beta > 10^{\circ}$.

Ballast: A device used with an electric discharge lamp for providing necessary voltage, current, and waveform conditions for correct lamp operation. The absolute efficiency of a ballast is important

DEFINITIONS (continued)

to the economical operation of an electric-discharge lamp.

Beer's Law: It describes the transmission of a parallel beam of monochromatic radiation through a homogeneous medium. It describes the attenuation of radiation as it passes through the medium and is dependent upon an attenuation coefficient and the initial radiant flux density entering the medium.

Blackbody: A temperature radiator of uniform temperature with the maximum radiant exitance over the entire spectrum obtainable from any temperature radiator at the same temperature. All other temperature radiators may be considered non-blackbodies.

Candela (cd): The unit of luminous intensity; it is not properly used in discussing PAR.

Clear sky: A sky that has less than 30% cloud cover.

Cloudy sky: A sky having more than 70% cloud cover.

Coefficient of utilization (CU): The ratio of lumens from a luminaire received on a work-plane to the lumens emitted by the luminaire's lamps alone. It is used here as a surrogate for a measure of the the ratio of PAR from a luminaire received on a work-plane to the PAR emitted by the luminaire's lamps alone. In this case the work-plane is the crop canopy.

Cosine law: The irradiation on any surface varies as the cosine of the angle of incidence. The angle of incidence θ is the angle between the normal to the surface and the direction of the incident radiation. The inverse-square law and cosine law can be combined to give:

$$E = (I \cos \theta)d^{-2}$$

where: E = density of luminous flux incident at a point on a surface, I = intensity of a point source radiator, and d = distance between the point source radiator and the point on the surface. The cosine law is assumed to hold for PAR.

Cropage: A term representing the age of the crop in a house at CEVCO from the time of transplant, where one equals one-half month of age.

Cultivar: A specific variety of plant that is persistent in growth when under cultivation. As used here, it is synonymous with variety.

Cyclic lighting: The application of radiation in patterns at night to plants in short, regular intervals over three to five hours. It may be done to control plant growth at critical stages. It is not the same as quick-flashing light or sunflecks.

Diffuse reflection: The process by which incident flux is re-directed over a range of angles.

Diffuse transmission: The process by which the incident flux passing through a surface or medium is scattered.

Dissolved solids (DS): A mean monthly measure of ions dissolved in water in the nutrient solution at CEVCO based upon daily observations, recorded in parts per million (ppm).

Effective ceiling cavity reflectance (ρ_{cc}): The effective reflectance of all the area above the luminaire plane as seen from the room cavity. For greenhouses this reflectance is normally very low.

Effective floor cavity reflectance (ρ_{FC}): The effective reflectance of all the area below the work-plane as seen from the room cavity. The reflected radiation from within a plant canopy is significantly lower in the PAR range.

Effective watts output: A term defining the number of watts radiated by a lamp within the PAR range (350-780 nm) with the watts within the 530-580 nm range reduced by 50%. It is used as a measure of a lamp's effectiveness as a radiator of PAR.

Einstein's Law: Each molecule is activated by the absorption of one photon to the primary photo-chemical process condition. In actual experimental work, this one-to-one relation does not hold, but this does not disprove the law.

Electric-discharge lamp: A lamp in which PAR is produced by the passage of an electric current through a vapor or gas. These lamps are named by the filling gas, their physical dimensions, operating parameters, or by their application. Examples include fluorescent lamps, mercury vapor lamps, high-pressure sodium lamps, and xenon lamps.

Electromagnetic spectrum: A continuum of electric and magnetic radiation encompassing all wave-lengths. Although the primary plant responses to electromagnetic radiation occur within the range of 290-850 nm, considerable scientific evidence indicates that other wavelengths can significantly affect plant functions. The study of the effects of magnetic fields upon plants is one such area of interest.

Equation of time: The difference between local solar time (LST) and local civil time (LCT) and is due to the irregularities of the earth's rotation, obliquity of the earth's orbit and other factors (see Table 2).

DEFINITIONS (continued)

Fixed cost (FC): A cost which in total is independent of the volume of activity.

Fluorescent lamp: A low-pressure mercury electric-discharge lamp utilizing a fluoresent coating to transform part of the ultraviolet energy generated into PAR.

Gaseous discharge: The emission of light from gas atoms excited by an electric current.

Hand (or cluster): One group of tomatoes growing from the same stem of a tomato plant. Tomato plants normally have several hands at one time, developing in chronological order such that plant age is frequently described in terms of which hand is now in production.

High-intensity discharge (HID) lamps: A general group of lamps including mercury, metal halide, and high-pressure sodium lamps.

High-pressure sodium lamp: A sodium vapor lamp in which the partial pressure of the vapor during operation is on the order of one atmosphere.

Infrared radiation: For practical purposes, any radiant energy within the wavelength range of 780 nm-1 x 10^5 nm. Infrared radiation is generally evaluated as a total quantity of energy with an effective heating capacity.

Intensity: An abbreviation of the term radiant intensity.

Interest: As used here, it reflects an assumed reasonable dollar return on the investment in capital equipment and structures.

Irradiation: The time rate of flow of radiant energy incident on a surface; measured in gram-calories per cm^2 per minute or watts per cm^2.

Lambert's Law: The transmission of a clear transmitting medium (e.g., filon) is an exponential function of the medium's thickness traversed.

$$I = I_o \cdot r^x$$

where: I = radiant intensity of transmitted light, I_o = radiant intensity of light entering the medium after surface reflection, r = transmittance of unit thickness, and x = thickness of sample traversed.

Lamp lumen depreciation (LLD): The multiplier used in illumination calculations to relate the initial rated output of lamps to the anticipated minimum rated output based upon the relamping program to be used. It is used here as a surrogate for identical calculations for PAR from lamps.

Lamp lumen maintenance curve: A graphic representation of the change in output radiant flux over lamp age, in operating hours. Examples of such curves are Figures 33 and 46.

LANGHRS: The mean daily product of hours of sun times langleys on a monthly basis. It is a measure of solar irradiation and direct solar radiation duration at CEVCO.

Langley (ly): A measure of irradiance:

$$1 \text{ ly} = 1 \text{ (gram-calorie)} \cdot (cm^{-2}).$$

$$1 \text{ ly} \cdot min^{-1} = 1 \text{ cal} \cdot cm^{-2} \cdot min^{-1}$$
$$= 697.5 \text{ W} \cdot m^{-2}$$
$$= 6.98 \times 10^5 \text{ erg} \cdot sec^{-1} \cdot cm^{-2}.$$

Leaf area index (LAI): The area of leaves above unit area of ground taking only one side of each leaf into account. It will normally vary between one and eight depending upon the species and environment of the plant.

Leaf area ratio (LAR): The ratio of the leaf area to plant dry weight. (LAR)·(net assimilation rate) = relative growth rate.

Light: For the purposes of the illuminating engineer, it is visually evaluated radiant energy. Light is not synonymous with radiant energy nor is it merely sensation. In a general sense, light is the aspect of radiant energy of which a human observer is aware through the stimulation of the retina of the eye (see Figure 2). Thus, light is not an accurate term for PAR, but is frequently used for it because it is commonly understood and is included within the range of PAR.

Local civil time (LCT): The local standard time adjusted 4 minutes for each degree latitude from the standard meridians (i.e., 75°, 90°, 105°, 120°, etc.).

Local solar time (LST): LST = LCT + equation of time. See Figure 11 for a comparison of LST with local standard time at CEVCO.

Lumen (lm): The unit of luminous flux, it is the flux through a unit solid angle (steradian), from a uniform point source of one candela, or to the flux on a unit surface all points of which are at unit distance from a uniform point source of one candela. This is not a good term for use with PAR.

Luminaire: A complete lighting unit consisting of a lamp or lamps, together with the parts designed to distribute the light, to position and protect the lamps, and to connect the lamps to the power supply.

Luminaire dirt depreciation factor (LDD): The multiplier used to calculate the depreciation in

DEFINITIONS (continued)

initial lumens due to dirt collection on the luminaire. It is used here as a surrogate for PAR depreciation due to dirt collection on the luminaire.

Luminaire efficiency: The ratio of lumens emitted by a luminaire to that emitted by the lamp or lamps used therein. It is used here as a surrogate for the ratio of PAR emitted by a luminaire to that emitted by the lamp or lamps used therein.

Marginal physical product of x_i (MPP_{x_i}): The addition to total physical production attributable to the addition of one unit of the variable input x_i to the production process, other inputs remaining fixed. For a production function $q = f(x|y)$. The MPP_x is: $\frac{\partial q}{\partial x} = \frac{\partial f(x\ y)}{\partial x}$.

Megacalorie (Mcal): 1.0×10^6 calories; it is a unit of energy equivalent to 3965.7 Btu. One calorie is the amount of energy required at a pressure of one atmosphere to raise the temperature of one gram of water one degree centigrade.

Mercury lamp: An electric discharge lamp in which the major portion of the radiation is produced by the excitation of mercury atoms.

Metal halide lamp: An electric discharge lamp in which the radiation is produced by the radiation from a mixture of a metallic vapor and the products of the disassociation of halides (e.g., halides of thallium, indium, or sodium).

Nanometer (nm): Unit of distance or wavelength equal to 10^{-9} meter.

Net assimilation rate (NAR): The net increase in total dry weight per unit leaf area per unit time.

Overcast sky: A sky that has 100% cloud cover; the sun is not visible and all its radiant energy is diffuse.

Partly cloudy sky: A sky that has 30 to 70% cloud cover.

Perfect diffusion: Diffusion in which the flux is scattered in accord with Lambert's cosine law. Diffuse radiation is normally considered preferable to direct radiation for plant growth.

PH (pH): The mean monthly pH reading of the nutrient solution in a CEVCO house on the basis of daily observations.

Photosynthetically active radiation (PAR): Also physiologically active radiation here; it is the radiation at wavelengths which induce physiological and, in particular, photosynthetic responses in plants. 290 nm-850 nm is the range of PAR currently known to be significant, with 350 nm-780 nm of primary importance.

Photosynthetically active radiation loss factor (PARLF): The product of all contributing factors which reduce the available PAR at the crop canopy surface, where factors not included are assumed to be equal to one. PARLF includes such factors as luminaire ambient temperature, voltage to luminaire, ballast factor, luminaire surface depreciation, room surface dirt depreciation, burnouts, lamp radiant energy output depreciation, and luminaire dirt depreciation. It is used to account for declines in PAR output from luminaires over their expected lives and under given operating conditions.

Planck's Law: The energy of a photon is inversely proportional to wavelength in accordance with:

$$\varepsilon = h\ \nu$$

where: ε = energy of a photon (ergs sec^{-1}), h = Planck's constant = 6.62×10^{-27} erg sec^{-1}, and ν = cycles per second. ε constitutes the quantum energy of the photon imparted to an electron of a molecule, atom, or ion which causes photochemical changes in matter.

POLL: The total hours per month per CEVCO house spent mechanically pollinating the tomato plants. The primary method utilized is direct physical vibration of the flower with an electric toothbrush once daily except on Sundays.

Power factor: Power factor = $(\frac{\text{true power}}{\text{apparent power}}) \cdot (100\%)$

where the true power is that which is actually used. Power factors of less than 1.0 occur with ballasts, which cause less economical operation because of increased current load. Thus, a high power factor ballast, while initially more expensive, is economically more efficient over the long run. A difference in true and apparent power arises when a difference in voltage and current phases arises.

Production function: A relationship (e.g., table, schedule, or mathematical function) showing the maximum amount of output that can be produced from any specified set of inputs, given the existing technology or "state of the art." As used here, it is the mathematical relationship of TTPROD dependent upon several independent variables as defined by ordinary least squares regression methods.

Quick-flashing light: A rhythmic light exhibiting very rapid regular alternations of light and darkness. There is no restriction on the ratio of the durations of the light to the dark periods. This term is used by illuminating engineers and is considered here to be synonymous with "sunflecks" or "light-chopping."

DEFINITIONS (continued)

Radiance (L): Radiance in a direction, at a point of the surface of a source, of a receiver, or of any other real or virtual surface, is the quotient of the radiant flux leaving, passing through or arriving at an element of the surface surrounding the point, and in directions defined by an elementary cone containing the given direction, by the product of the solid angle of the cone and the area of the orthogonal project of the element of the surface on a plane perpendicular to the given direction.

$$L = d^2 \cdot \Phi(dw \cdot (dA \cdot \cos\theta))^{-1} = dI(dA \cdot \cos\theta)^{-1}$$

where: L = radiance in watts·steradian^{-1}·cm^{-2}, Φ = radiant flux in ergs·sec^{-1} = watts = d Q/dt, w = radiant density in ergs·cm^{-3}, A = area irradiated in cm^2, and θ = angle between the normal to the element of the source and the direction of observation.

Radiant exitance (M): The density of radiant flux leaving a surface. It is expressed in watts per unit area of the surface.

Radiant energy (Q): Energy traveling in the form of electromagnetic waves. It is measured in units of energy, such as joules, ergs, or kilowatthours.

Radiant flux (ϕ): The time rate of flow of radiant energy. It is expressed preferably in watts, or joules per second. Φ = dQ/dt.

Radiant flux density at an element of a surface: The quotient of radiant flux at that element of surface to the area of that element (e.g., watts·cm^{-2}) = d Φ/dA. The preferred term for radiant flux leaving a surface is radiant exitance (M). When referring to radiant flux incident on a surface, it is called irradiance (E).

Radiant intensity (I_i): The radiant flux proceeding from the source per unit solid angle in the direction considered (e.g., watts·steradian^{-1}). I_i = d Φ/dw.

Radiator: An emitter of radiant energy. Examples include blackbodies, sun, and lamps.

Rated average lamp life: The life expectancy of lamps in operating hours based upon properly designed ballasts, 10 or more burning hours per start, optimum operating temperatures, optimum voltage and current, and proper cleaning and maintenance. The rated life is the average of a large group of lamps.

Regression coefficient (B): An unstandardized regression coefficient representing $B = \frac{\Sigma(X - \overline{X})(Y - \overline{Y})}{\Sigma(X - \overline{X})^2}$. For simple regressions, B is the slope of the regression line. In multiple regressions, the B value of X_i essentially stands for the expected change in Y with a change on one unit in X_i when all other X_i are held constant or are otherwise controlled.

Regular (specular) reflection: That process by which incident flux is redirected at the specular angle (i.e., the angle between the normal to the surface and the reflected ray that is equal to the angle of incidence) and lies in the same plane as the incident ray and the normal, but on the opposite side of the normal to the surface.

Regular transmission: That process by which incident flux passes through a surface or medium without scattering.

Room cavity: The cavity formed by the plane of the luminaires, the work-plane, and the wall surfaces between these two planes.

Room cavity ratio (RCR): A number indicating room cavity proportions calculated from the room length, width, and height.

Shape factor (K_s): The ratio of the horizontally projected area of an object to its plane or total surface area.

Sky light: Visible radiation from the sun redirected by the atmosphere. This term is assumed to cover PAR also.

Solar altitude angle (β): The angle defined by a ray from the sun to a point P on the earth and the projection of the ray in the horizontal plane defined by point P and its horizon on earth. β is depicted in Figures 14 and 15.

Reciprocity law: The production of photochemical products may be proportional to the total radiant energy absorbed by a photoreacting substance. The total radiation is the product of the radiation intensity and the time exposed. This phenomenon is known as the Bunsen-Roscoe reciprocity law, where I·T = K where: I = radiant intensity, T = time, and K = a constant. Studies with certain plants have indicated that the law is valid over a wide range of radiant intensity-time combinations, at least at low values near threshold levels (5, p. 108).

Reflectance of a surface or medium (ρ): The ratio of the reflected flux to the incident flux. $\rho = \Phi_r/\Phi_i$, where: Φ_r = reflected radiant flux, and Φ_i = incident radiant flux. Values of reflectance are dependent upon the angles of incidence and view and upon the spectral (wavelength) distribution of the incident flux. Therefore, such items should be specified with values of ρ.

DEFINITIONS (continued)

Refraction: The process by which the direction of a ray of light changes as it passes obliquely from one medium to another in which its speed changes.

Regions of electromagnetic spectrum: (the transitions between bands are gradual)

	Wavelength
ultraviolet	150-380 nm
violet	420 nm
blue	470 nm
green	530 nm
yellow	580 nm
orange	620 nm
red	700 nm
near infrared	1,000 nm
far infrared	10,000 nm

Solar angle of declination (d): The angular distance of the sun's rays either north or south of the equator (see Figures 12 and 13). It is the angle between a line extending from the center of the sun to the center of the earth and the projection of said line upon the plane defined by the equator.

Solar angle of incidence (θ): The angle between the solar rays and the normal to a surface. It is associated with a definite surface position.

Solar azimuth angle (∂): The angular distance between the vertical plane containing the sun and the plane of the meridian (see Figure 14). At solar noon, $\partial = 180^{\circ}$ if $\ell > d$ and $\partial = o^{\circ}$ if $\ell < d$.

Solar constant: The irradiance (averaging about 1,393 $W \cdot m^{-2}$ = 1.998 lys) from the sun at its mean distance from the earth before modification by the earth's atmosphere.

Solar hour angle (h): The angle measured in the equatorial plane of the earth between the projection of the solar rays onto the equatorial plane and the projection of a line from the center of the sun to the center of the earth (see Figure 12).

Solid angle (ω): A ratio of the area on the surface of a sphere to the square of the radius of the sphere. It is expressed in steradians. It is approximately equal to: $\omega = \frac{Ap}{D^2}$, where:

Ap = projected area of the luminaire, and D = distance between luminaire and the irradiated surface.

Spectral energy distribution (SED) curve: A curve depicting the radiant energy per wavelength for a particular type of radiator. Examples of such curves include Figures 3, 38, 39, 40, 47, 48, and 49.

Spectral radiant energy (Q_λ): Radiant energy (Q) per unit wavelength interval at wavelength (e.g., ergs/nanometer). $Q_\lambda = dQ/d\lambda$.

Spectral radiant flux (Φ_λ): Radiant flux per unit wavelength interval at wavelength λ (e.g., watts·nanometer^{-1}).

Spectral radiant intensity (I_λ): Radiant intensity per unit wavelength interval (e.g., watts·steradian^{-1}·nanometer^{-1}). $I_\lambda = dI/d\lambda$.

Specular angle: The angle between the perpendicular to the surface and the reflected ray that is numerically equal to the angle of incidence and that lies in the same plane as the incident ray and the perpendicular, but on the opposite side of the perpendicular to the surface.

Specular surface: One from which the reflection is predominantly regular.

Steradian (sr): A solid angle subtending an area on the surface of a sphere equal to the square of the sphere's radius.

Sunflecks: Short bursts of direct solar radiation striking a photosynthesizing surface within a crop canopy followed by short bursts of relative darkness. The effect upon net assimilation rates of plants can be very significant.

Total cost (TC): In the short run (i.e., where fixed costs occur), it is the sum of total variable and total fixed costs.

Total fixed costs (TFC): The short-run costs which in total are independent of volume of production (i.e., level of TTPROD). In economics, TFC includes both explicit and implicit costs, which means both actual costs and the costs of profits foregone by not investing one's resources in the best alternative investment available.

Total incident energy of a light ray (I_t): $I_t = R + A + T$, where: I_t = total incident energy, R = reflected energy, A = absorbed energy, and T = transmitted energy.

Total leaf area (Lt): The total surface area of all the leaves of a plant or crop, taking only one side of each leaf into account.

Total physical product (TPP): The total production in terms of physical units. Here, TPP = TTPROD.

DEFINITIONS (continued)

Total revenue (TR): Total revenue is the sum of all the marginal revenues (MR). For CEVCO where the market price is assumed given and unaffected by CEVCO output, TR = (yield in kg)·(price per kg).

Total variable cost (TVC): The sum of the costs for each of the variable inputs such as picking and packing labor hours, boxes, and transportation costs.

TPVAR: The mean monthly temperature based upon the mean of daily maximum-minimum temperature observations recorded by the national weather bureau at the Minneapolis-St. Paul airport. It is in degrees centigrade plus 30 so that no negative values occur.

Transmission: A general term for the process by which incident flux leaves a surface or medium on a side other than the incident side.

Tropic: A widely grown, indeterminate tomato cultivar yielding very large fruit. It is highly susceptible to certain tobacco mosaic virus strains. The fruit tends to have open or distorted blossom ends and less-than-perfect shape and smoothness.

TTPROD: The total monthly production of tomatoes in kilograms per CEVCO house.

Value of the marginal product (VMP): The marginal physical product ($MPPx_i$) multiplied by the market price of the project (i.e., $ per kilogram of tomatoes).

Variable cost (VC): A cost which is constant per unit of output.

Watt (W): A measure of power that is normally used in conjunction with electromagnetic forces. 1 watt = 10^7 ergs·sec^{-1}.

Watthour (Whr): A unit of work, measuring power over time. It is the energy equivalent to one watt over one hour. Frequently, watthours are spoken of in kilowatthours (Kwh), that is, 1,000 Whr. 1 watthour = 860.6 calories.

Wavelength: The distance between two successive points of a periodic wave in the direction of propogation, in which the oscillation has the same phase.

Work-plane: The plane at which work usually is done, and at which the illumination is specified and measured. This term is used here in reference to the irradiance of the crop canopy with PAR.

Zonal-cavity inter-reflectance method: A procedure for calculating coefficients of utilization (CU) taking into consideration the luminaire intensity distribution, room size (cavity ratio concepts), and room reflectances.

Appendix B

REFERENCES

1. Aldrich, R.A., and J.W. White, "The Design and Evaluation of Rigid Plastic Greenhouses," Transactions of the ASAE 16(5):994-996, September-October 1973.

2. Anderson, Margaret C., "Radiation Climate, Crop Architecture and Photosynthesis," Prediction and Measurement of Photosynthetic Productivity, Center for Agricultural Publishing and Documentation, Wageningen, Netherlands: 71-78, 1970.

3. Baker, Donald G., Climate of Minnesota, Part VI, Solar Radiation at St. Paul, University of Minnesota, Agricultural Experiment Station Technical Bulletin 280:1-19, 1971.

4. Baker, Donald G., and John C. Klink, Solar Radiation Reception, Probabilities and Areal Distribution in the North-Central Region, University of Minnesota, Agricultural Experiment Station Technical Bulletin 300:1-54, 1975.

5. Bickford, Elwood D., and Stuart Dunn, Lighting for Plant Growth, Kent, Ohio, Kent State University Press, 1972.

6. Bond, T.E., L.C. Godbey, and H.F. Zornig, "Solar, Long Wavelength, and Photosynthetic Energy Transmission of Greenhouse Cover Materials," Proceedings - A Conference on Solar Energy for Heating Greenhouses and Greenhouse - Residential Combinations, Ohio Agricultural Research and Development Center, Wooster, Ohio: 235-255, March 1977.

7. Bowman, G.E., "Principles and Progress in Environmental Control Systems," Crop Processes in Controlled Environments, Academic Press, New York: 63-77, 1972.

8. Bredvold, C.G., "The Economic Feasibility of Producing Tomatoes in Northern Latitudes Utilizing Controlled Environment Systems." Staff Paper P-78-7.

9. Canham, A.E., Artificial Light in Horticulture, Eindhoven, The Netherlands, Centrex Publishing Company, 1966.

10. Duncan, G.A. and J.N. Walker, Greenhouse Coverings, AEN-10, Department of Agricultural Engineering, University of Kentucky, August 1973.

11. Dunn, S., and F.W. Went, "Influence of Fluorescent Light Quality on Growth and Photosynthesis of Tomato," Lloydia, 22:302-324, 1959.

12. Edling, R.J., B.J. Barfield, C.T. Haan, and M.E. Fogleman, "Prediction of Leaf Temperature Under Unstable Atmospheric Conditions," Transactions of the ASAE 14:1095-1099, November-December 1971.

13. Gates, D.M., "Leaf Temperatures and Transpiration," Agronomy Journal 56:273-277, 1964.

14. Gates, D.M., and C.M. Benedict, "Convection Phenomena From Plants in Still Air," American Journal of Botany, 50(6):563-573, July 1963.

15. General Electric, General Electric Horticultural Lighting, Bulletin No. OLW-9053, Hendersonville, N.C., December 1971.

16. General Electric, General Electric Horticultural Lighting, Bulletin No. OLW-9053A, Hendersonville, N.C., January 1975.

17. General Electric, General Electric Lamp Catalog, Form 9200, Nela Park, Cleveland, Ohio, January 1975.

18. General Electric, High Intensity Discharge Lamps, Pamphlet TP-109R, Nela Park, Cleveland, Ohio, March 1975.

19. General Electric, Fluorescent Lamps, Bulletin TP-111, Nela Park, Cleveland, Ohio, revised January 1973.

20. "Greenhouse Update 1977," American Vegetable Grower, 26(11):11-13, November 1977.

21. Handbook of Geophysics, revised edition, U.S. Air Force, Macmillan, New York, 1960.

22. Helson, V.A., "Comparison of Gro-Lux and Cool-White Fluorescent Lamps With and Without Incandescent as Light Sources Used in Plant Growth Rooms for Growth and Development of Tomato Plants," Canadian Journal of Plant Science, 45(5):461-466, September 1965.

23. Hesketh, J.D., and J.M. McKinion, J.W. Jones, D.N. Baker, H.C. Lane, A.C. Thompson, and R.F. Colwick, "Problems in Building Computer Models for Photosynthesis and Respiration," Environmental and Biological Control of Photosynthesis, edited by R. Marcelle, Dr. W. Junk b.v. publishers, The Hague, The Netherlands: 53-60, 1975.

24. Ho, L.C., "Relation Between Carbon Transport and Photosynthesis in Tomato Leaves," 1975 Annual Report, The Glasshouse Crops Research Institute, Littlehampton, West Sussex, England: 44-45, 1976.

25. Hurd, R.G., "Comparison of Tomato Growth in Artificial and Natural Light," 1968 Annual Report, The Glasshouse Crops Research Institute, Littlehampton, West Sussex, England: 54-55, 1969.

26. Hurd, R.G., "Daylength Effects on Tomato Plants," 1970 Annual Report, The Glasshouse Crops Research Institute, Littlehampton, West Sussex, England: 69, 1971.

27. Hurd, R.G., "Growth of Tomato Plants in High Radiation Integrals," 1972 Annual Report, The Glasshouse Crops Research Institute, Littlehampton, West Sussex, England: 45, 1973.

28. Hutchinson, G.L., R.J. Millington, and D.B. Peters, "Atmospheric Ammonia Absorption by Plant Leaves," Science, 175:771-772, February 18, 1972.

29. Johns-Manville Sales Corp., Holophane Division, Holophane Ballast Handbook, Pamphlet HL-301, Greenwood Plaza, Denver, Colorado, November 1975.

30. Johns-Manville Sales Corp., Holophane Prismpack II Luminaires for Metal Halide and High Pressure Sodium Lamps, Pamphlet No. 27-Y, Montvale, New Jersey, 1972.

31. Kaufman, John E., ed., IES Lighting Handbook, Illuminiating Engineering Society, 1972.

32. Kretchman, Dale W., "A Preliminary Report on Supplemental Lighting for Tomato," Research Summary, Ohio Agricultural Research and Development Center, Wooster, Ohio, 34:1-4, April 1969.

33. Kretchman, Dale W., "Supplemental Lighting for the Greenhouse Tomato," Research Summary, Ohio Agricultural Research and Development Center, Wooster, Ohio, 41:9-13, April 1970.

34. Kretchman, Dale W., and William L. Bauerle, "Supplemental Lighting for the Spring Crop of Greenhouse Tomatoes," Research Summary, Ohio Agricultural Research and Development Center, Wooster, Ohio, 50:19-26, April 1971.

35. Kriedemann, P.E., Edith Torokfalvy, and R.E. Smart, "Natural Occurrence and Photosynthetic Utilization of Sunflecks by Grapevine Leaves," Photosynthetica, 7(1):18-27, 1973.

36. List, R.J., ed., Smithsonian Meteorological Tables, Smithsonian Misc. Coll., Publication 4014, Vol. 114, Smithsonian Institute, Washington, D.C., 1958.

37. Ludwig, L.J., "Effects of Light Flux Density, CO_2 Enrichment and Temperature on Leaf Photosynthesis," 1973 Annual Report, The Glasshouse Crops Research Institute, Littlehampton, West Sussex, England: 47-49, 1974.

38. Ludwig, L.J., "Photosynthesis and Respiration in Tomato Leaves," 1972 Annual Report, The Glasshouse Crops Research Institute, Littlehampton, West Sussex, England: 46-47, 1973.

39. Marr, C., and I.G. Hillyer, "Effect of Light Intensity on Pollination and Fertilization of Field and Greenhouse Tomatoes," Proc. Amer. Soc. Hort. Sci., 92:526-530, 1968.

40. McCree, K.J., and R.S. Loomis, "Photosynthesis In Fluctuating Light," Ecology, 50(3):422-428, 1969.

41. Monteith, John L., Principles of Environmental Physics, Edward Arnold Limited, London, 1973.

42. Norton, R.A., Northwestern Washington Research and Extension Unit, Washington State University, personal letter received May 5, 1976.

43. Pinchbeck, William, F.K. Johnson, D.N. Stiles, and S.J. Noesen, Increased Production of Forever Yours Roses With Supplemental Lighting, General Electric Technical Information Series No. 71-OL-001:1-7, Appendices I and II, July 1971.

44. "Report of Workgroup Discussions," Tennessee Valley Greenhouse Vegetable Workshop, Muscle Shoals, Ala., National Fertilizer Development Center, T.V.A., Bulletin Y-94:124-144, June 1975.

45. Roberts, W.J., "Greenhouse Structures," Tennessee Valley Greenhouse Vegetable Workshop, Muscle Shoals, Ala., National Fertilizer Development Center, T.V.A., Bulletin Y-94:48-50, June 1975.

46. Sheard, G.F., "Future Trends in Structures for Protected Cropping," Crop Processes In Controlled Environments, Academic Press, London: 57-61, 1972.

47. Smith, M. Ray, "A Process Model for Computer Control of Crop Growth," Transactions of the ASAE, 14:475-79, May-June 1971.

48. "Solving The Wasteful Wall Problem," American Vegetable Grower, 24(11):66, 68, November 1976.

49. Stevenson, Enola L., and S. Dunn, "Plant Growth Effects of Light Quality in Sequences and in Mixtures of Light," Advanc. Frontiers Plant Sci., 10:177-190, 1965.

50. Sylvania GTE Corp., Gro-Lux, Wide Spectrum Fluorescent Lamp, Sylvania's New Energy Source for Economic Crops, Sylvania Engineering Bulletin 0-285, Danvers, Massachusetts, December 1972.

51. Sylvania GTE Corp., Radiant Energy Sources for Plant Growth, Sylvania Engineering Bulletin 0-278, Danvers, Massachusetts, February 1972.

52. Sylvania GTE Corp., Rose Lighting With Lumalux High Pressure Sodium Lamps, Sylvania Engineering Bulletin 0-351, Danvers, Massachusetts, October 1974.

53. Sylvania GTE Corp., Sylvania Lamp Ordering Guide 75-1, Danvers, Massachusetts, September 2, 1975.

54. Takakura, T., K.A. Jordan, and L.L. Boyd, "Dynamic Simulation of Plant Growth and Environment in the Greenhouse," Transactions of the ASAE, 14:964-971, September-October 1971.

55. Takakura, T., T. Kozai, K. Tachibana, and K.A. Jordon, "Direct Digital Control of Plant Growth - I. Design and Operation of the System," Transactions of the ASAE, 17:1150-1154, November-Decmeber 1974.

56. Thomas, A.S., Jr., and S. Dunn, "Plant Growth With New Fluorescent Lamps, Fresh and Dry Weights of Tomato Seedlings," Planta, 72:198-207, 1967.

57. Threlkeld, J.L., "Solar Irradiation of Surfaces on Clear Days," ASHRAE Trans., 69:24-36, 1963.

58. Threlkeld, J.L., Thermal Environmental Engineering, 2nd ed., New Jersey, Prentice-Hall, Inc., 1970.

59. Threlkeld, J.L., and R.C. Jordan, "Direct Solar Radiation Available on Clear Days," ASHAE Trans., 64:45-68, 1958.

60. Tucker, D.J., "Far-Red Light As A Suppressor Of Side Shoot Growth In The Tomato," Plant Science Letters, 5:127-130, 1975.

61. VanderVeen, R., and G. Meijer, Light and Plant Growth, Centrex Publishing Company, Eindhoven, Holland, 1959.

62. Walker, J.N., and G.A. Duncan, "Environmental Equipment and Traditional Energy Considerations for Heating Systems," Tennessee Valley Greenhouse Vegetable Workshop, Muscle Shoals, Ala., National Fertilizer Development Center, T.V.A., Bulletin Y-94:53-63, June 1975.

63. Walker, J.N., and G.A. Duncan, Greenhouse Heating Systems, AEN-31, Department of Agricultural Engineering, University of Kentucky, July 1974.

64. Walker, J.N., and W.E. Splinter, "Introduction: Mathematical Modeling of Plants," Trans. of ASAE, 14:945-49, 959, September-October 1971.

65. Went, Frits W., The Experimental Control of Plant Growth, Waltham, Massachusetts, Chronica Botanica Company, 1957.

66. Wilson, G.E., D.R. Price, L.D. Albright, N.R. Scott, R.W. Langhans, Pitam Chandra, "Experimental Results of a Greenhouse Solar Collection and Modular Gravel Storage System," Proceedings - A Conference on Solar Energy for Heating Greenhouses and Greenhouse-Residential Combinations, Ohio Agricultural Research and Development Center, Wooster, Ohio: 256-286, March 1977.

67. Wilson, J. Warren, "Control of Crop Processes," Crop Processes In Controlled Environments, Academic Press, New York: 7-30, 1972.

68. Winsor, G.W., and P. Adams, "Changes in the Composition and Quality of Tomato Fruit Throughout the Season," 1975 Annual Report, The Glasshouse Crops Research Institute, Littlehampton, West Sussex, England: 134-142, 1976.

69. Withrow, R.B., "A Kinetic Analysis of Photoperiodism," Photoperiodism and Related Phenomena in Plants and Animals, edited by R.B. Withrow, publication number 55 of the American Association for the Advancement of Science: 439-471, 1959.

70. Wittwer, S.H., "Carbon Dioxide and Its Role in Plant Growth," XVII Int. Hort. Congress Proc., Vol. III: 311-321, April 1967.

71. Wittwer, S.H., "Fruit Yield of Three Tomato Varieties With Supplemental CO_2 and Light from Two Sources," (unpublished report), Michigan Agricultural Experiment Station, 1966.

72. Wittwer, S.H., "Photoperiod and Flowering in the Tomato (Lycopersicon esculentum Mill.)," Proc. Amer. Soc. Hort. Sci., 83:688-694, 1963.

Appendix C

SOLAR WEIGHTS

For Tables 27 and 29, a solar weight is provided for each of four spectral bands: 350-530 nm; 530-580 nm; 580-690 nm; and 690-780 nm. These solar weights are the means of the percentage distributions of the following three solar PAR distributions:

Table C1. Solar weights for four PAR bands.

	Percent of PAR band			
	350-530 nm	530-580 nm	580-690 nm	690-780 nm
Direct solar radiation d=400, m=1, w=30	39.1%	14.0%	29.1%	17.1%
Direct solar radiation d=400, m=5, w=30	21.6%	15.4%	40.4%	22.8%
Total cloud radiation	50.0%	22.8%	18.8%	9.1%
Solar weights = $\overline{X}$ =	36.9%	17.4%	29.4%	16.3%

Source: integration of SED curves from references 9, p. 50.

Direct solar radiation at sea level with an air mass m (ratio of the length of the path of solar rays through the atmosphere to the length of path if the sun were at its zenith) equal to one (i.e., solar altitude angle $\beta = 90^{o}$), a dust factor d = 400 (moderately dusty atmosphere) and precipitable water depth (w) = 30 mm, normally provides the highest solar irradiation, with significantly more radiation occurring at the shorter wavelengths. However, as the air mass m increases to 5 (i.e., solar altitude angle $\beta = 11.5^{o}$), where the sun is close to the horizon, the solar SED curve shifts toward the longer wavelengths. Under a totally cloudy day, the longer wavelengths are drastically reduced due to scattering, while clear skylight radiation (not direct solar radiation) is fairly evenly distributed across the spectrum of PAR. The significance of these percentage breakdowns becomes important if it is assumed that plants have evolved to where they maximize their utilization of the "average" solar SED curve. Even if this is not strictly true, nevertheless, because this study compares artificial lighting with solar irradiation to estimate production yields of tomato plants, it is necessary to compare the distribution of radiant energy among the four spectral bands for artificial lights and solar radiation. It is immediately apparent that all the lamps analyzed, on a percentage basis, fall short of solar radiation within the 690-780 nm spectral band; particularly the Gro-lux fluorescent lamp. It is because of this that these lamps must be supplemented with a source of 690-780 nm radiant energy--normally incandescent lamps. Further, in studies comparing Gro-lux and Gro-lux wide-spectrum lamps, with and without incandescent lamps, the wide-spectrum lamp did significantly better in growth and yields, presumably because of its higher output in the 690-780 nm spectral band.

Figure 1. Action spectra of the five principal plant photochemical reactions.

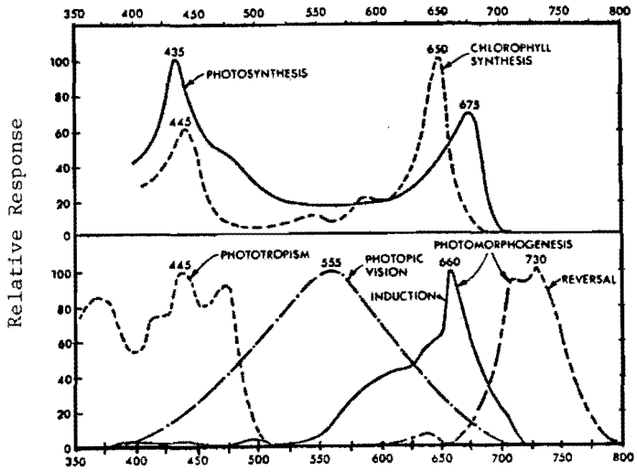

Source: 31, p. 25-3.

The action spectra of the five major photoresponses of plants show the utilization of energy in three spectral regions (400 to 500 nm, 600 to 700 nm, 700 to 800 nm), compared to photopic vision which utilizes energy in the 380 to 780 nm spectral region.

Figure 2. The standard (CIE) spectral luminous efficiency curve.

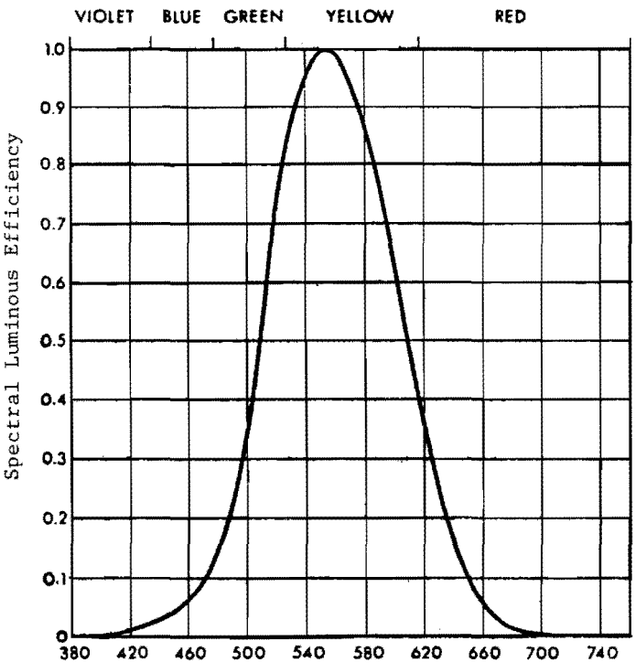

Source: 31, p. 2-5.

The standard (CIE) spectral luminous efficiency curve (for photopic vision) showing the relative capacity of radiant energy of various wavelengths to produce visual sensation. See Figure 1 for plant response curves to spectral radiant energy.

Figure 3. SED curves for solar radiation at several values of m.

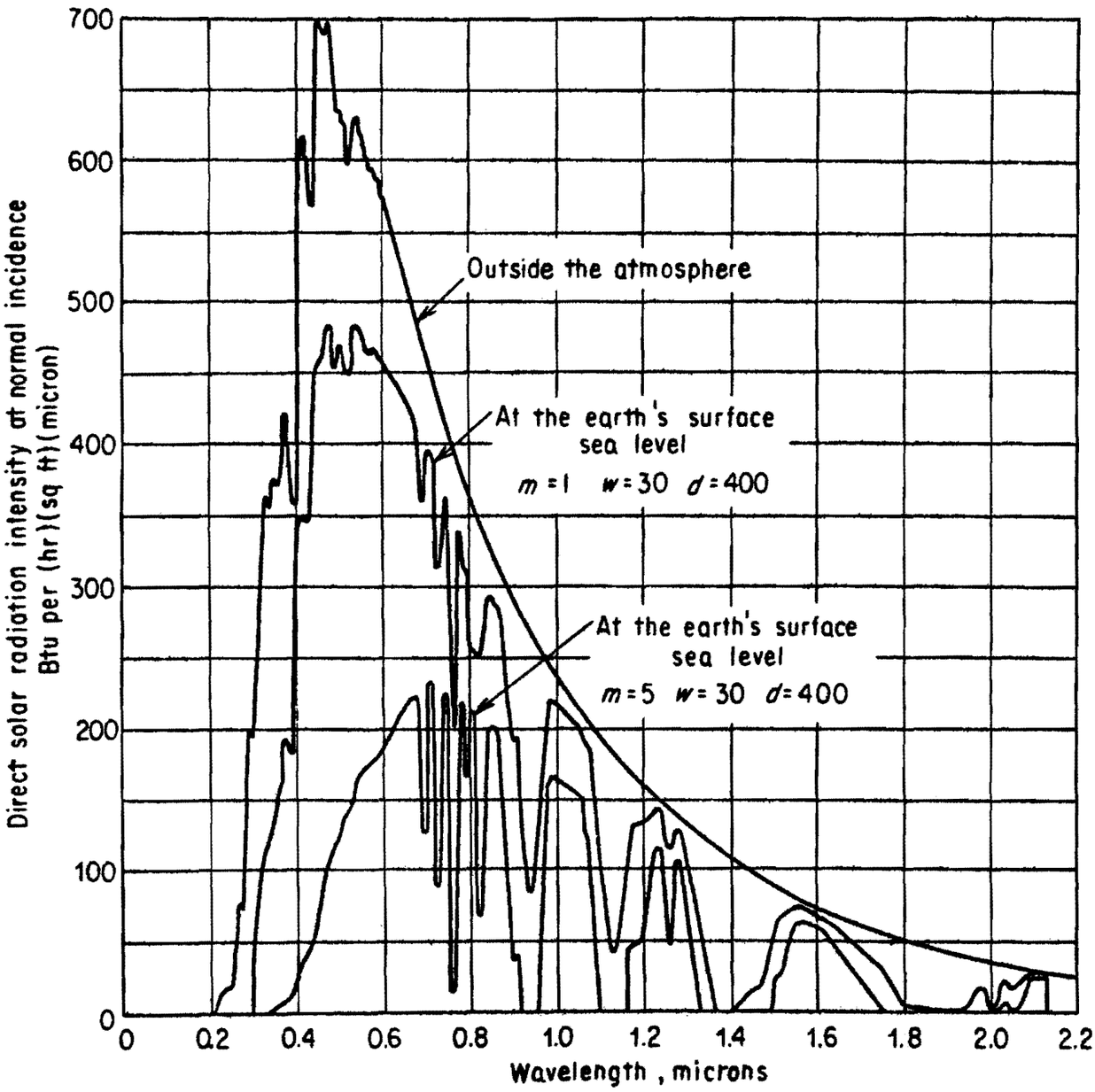

Spectral distribution of direct solar radiation intensity at normal incidence for the upper limit of the atmosphere and at the earth's surface during clear days.

Source: 59, p. 50.

Figure 4. The attenuation of solar radiation by airborn molecules.

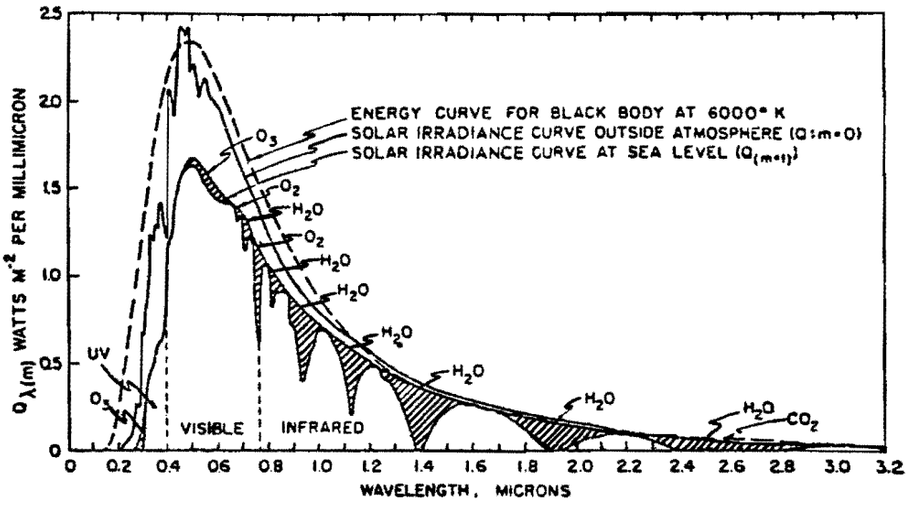

Solar spectral irradiance curves at sea level with varying optical air masses.

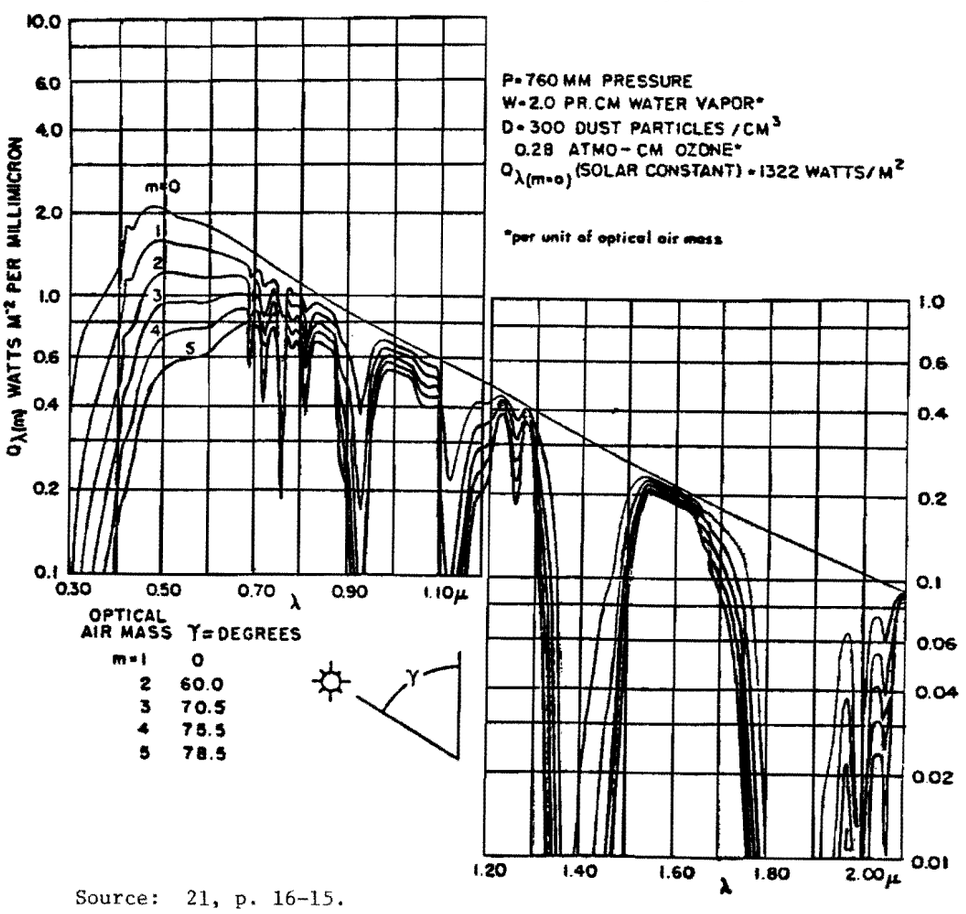

Source: 21, p. 16-15.

Figure 5. Solar radiation at noon at St. Paul, Minnesota.

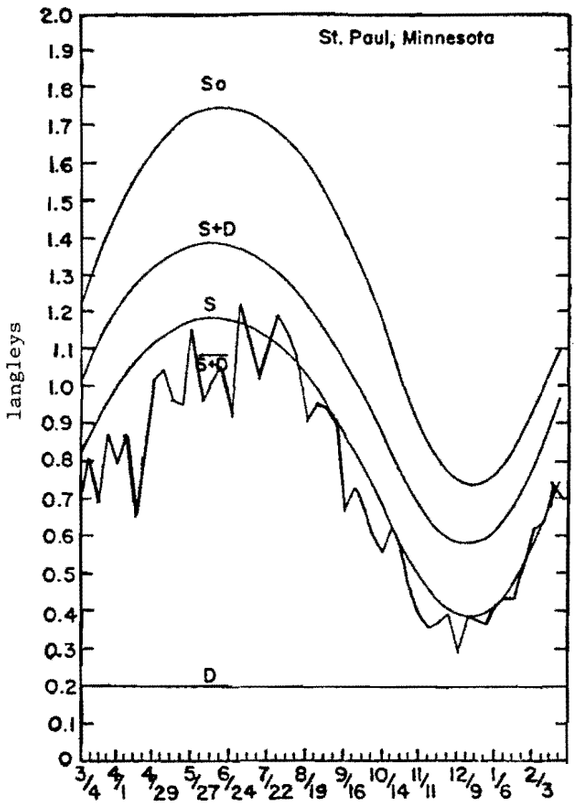

The annual march of the solar noon values of extraterrestrial radiation (So), clear-day direct plus diffuse radiation (S + D), clear-day direct radiation ($\underline{S}$), average-day direct plus diffuse radiation ($\overline{S + D}$), and clear-day diffuse radiation (D) at St. Paul.

Source: 3, p. 19.

Figure 6. Total daily solar radiation at St. Paul, Minnesota.

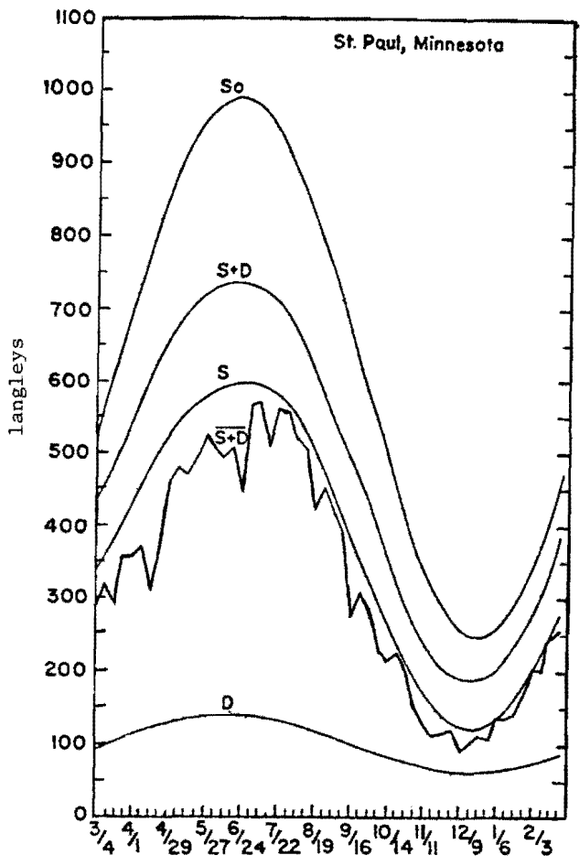

The annual march of the total daily values of extraterrestrial radiation (So), clear-day direct plus diffuse radiation (S + D), clear-day direct radiation ($\underline{S}$), average-day direct plus diffuse radiation ($\overline{S + D}$), and clear-day diffuse radiation (D) at St. Paul.

Source: 3, p. 19.

Figure 7. Photosynthetic response to reciprocal changes in the duration of light and darkness over a 2-second cycle compared to continuous irradiation.

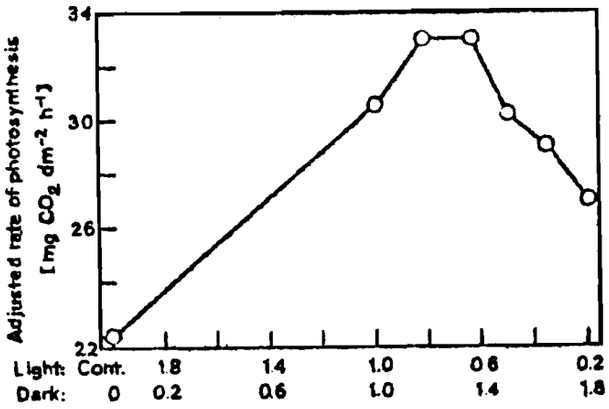

Source: 35, p. 21.

Figure 8. PAR response curve for photosynthesis under continuous compared to intermittent irradiation.

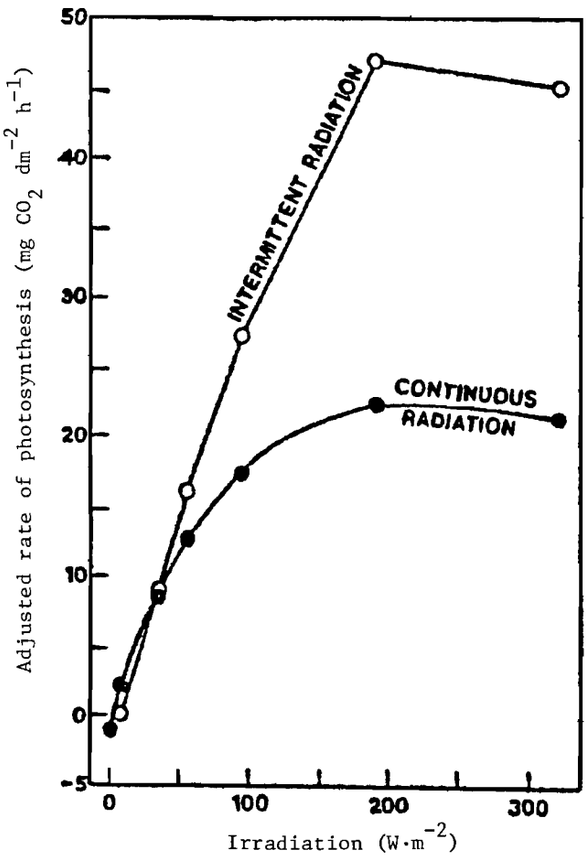

Source: 35, p. 22.

Figure 9. Area A projected on a horizontal surface by solar beam.

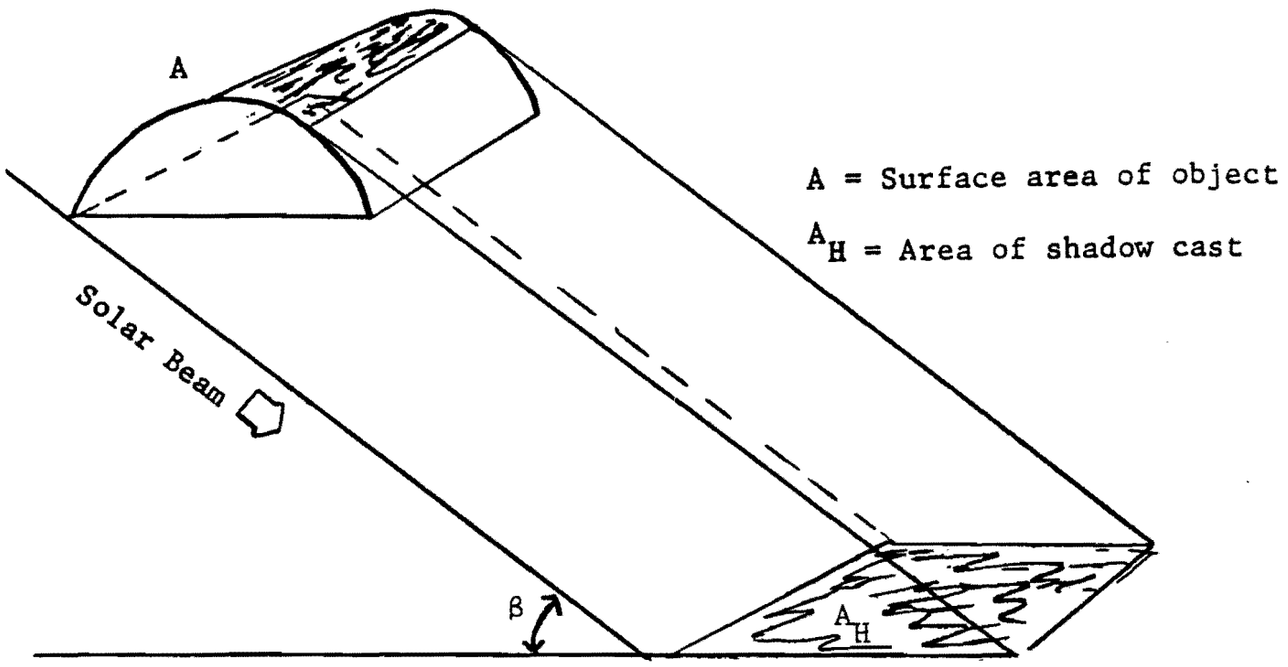

Figure 10. Projection of a cone on a horizontal plane.

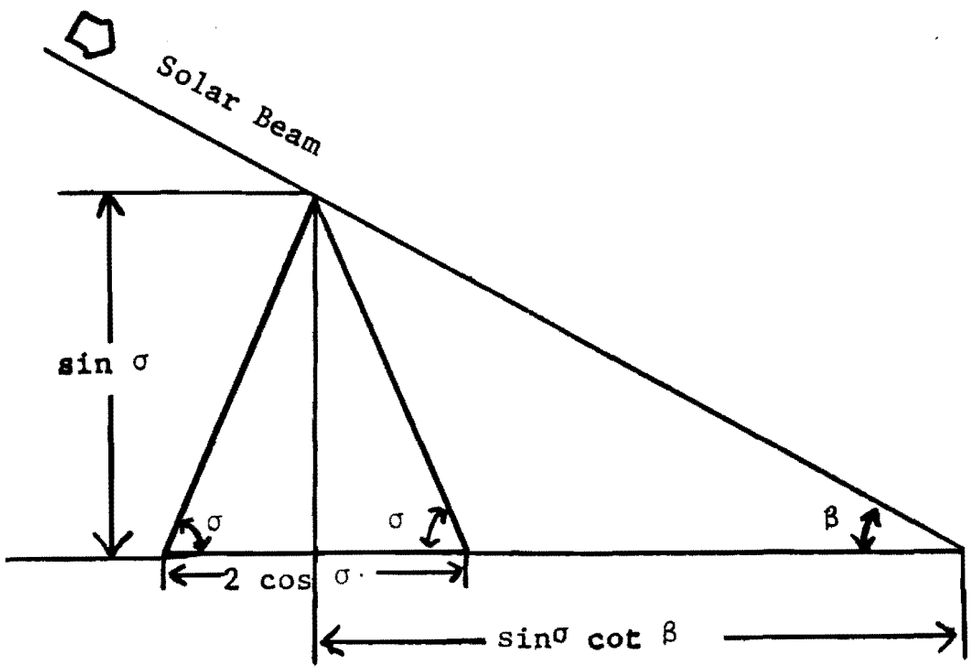

Figure 11. The occurrence of solar noon at CEVCO (~93°11' West) in terms of Central (local) Standard Time.

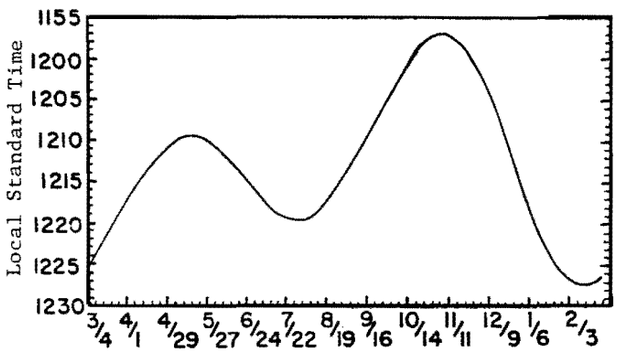

Source: 3, p. 4.

Figure 12. Latitude, hour angle, and solar declination.

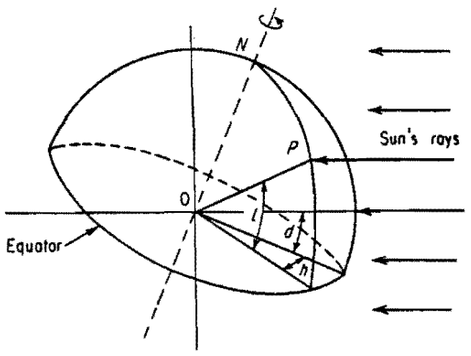

Source: 58, p. 284.

Figure 13. Schematic celestial sphere showing apparent path of sun and solar declination angle.

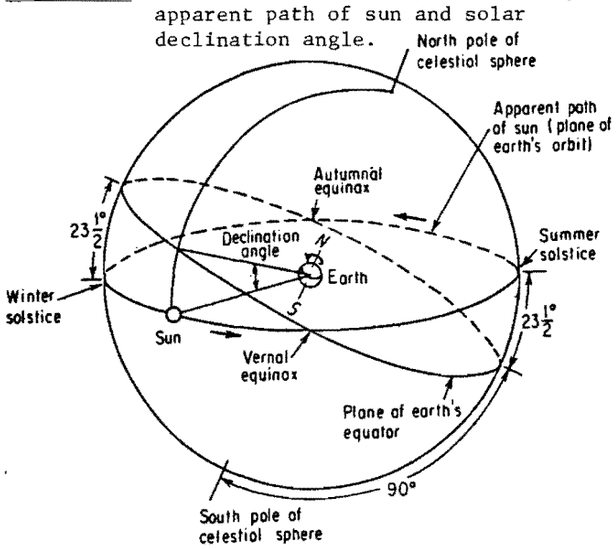

Source: 58, p. 284.

Figure 14. Definition of solar zenith, altitude, and azimuth angles.

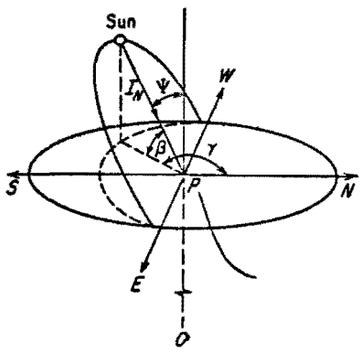

Source: 58, p. 288.

Figure 15. Relation of a point on Earth's surface to solar rays.

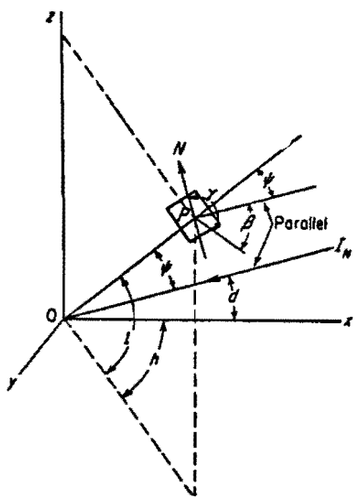

Source: 58, p. 288.

Figure 16. CEVCO house dimensions.

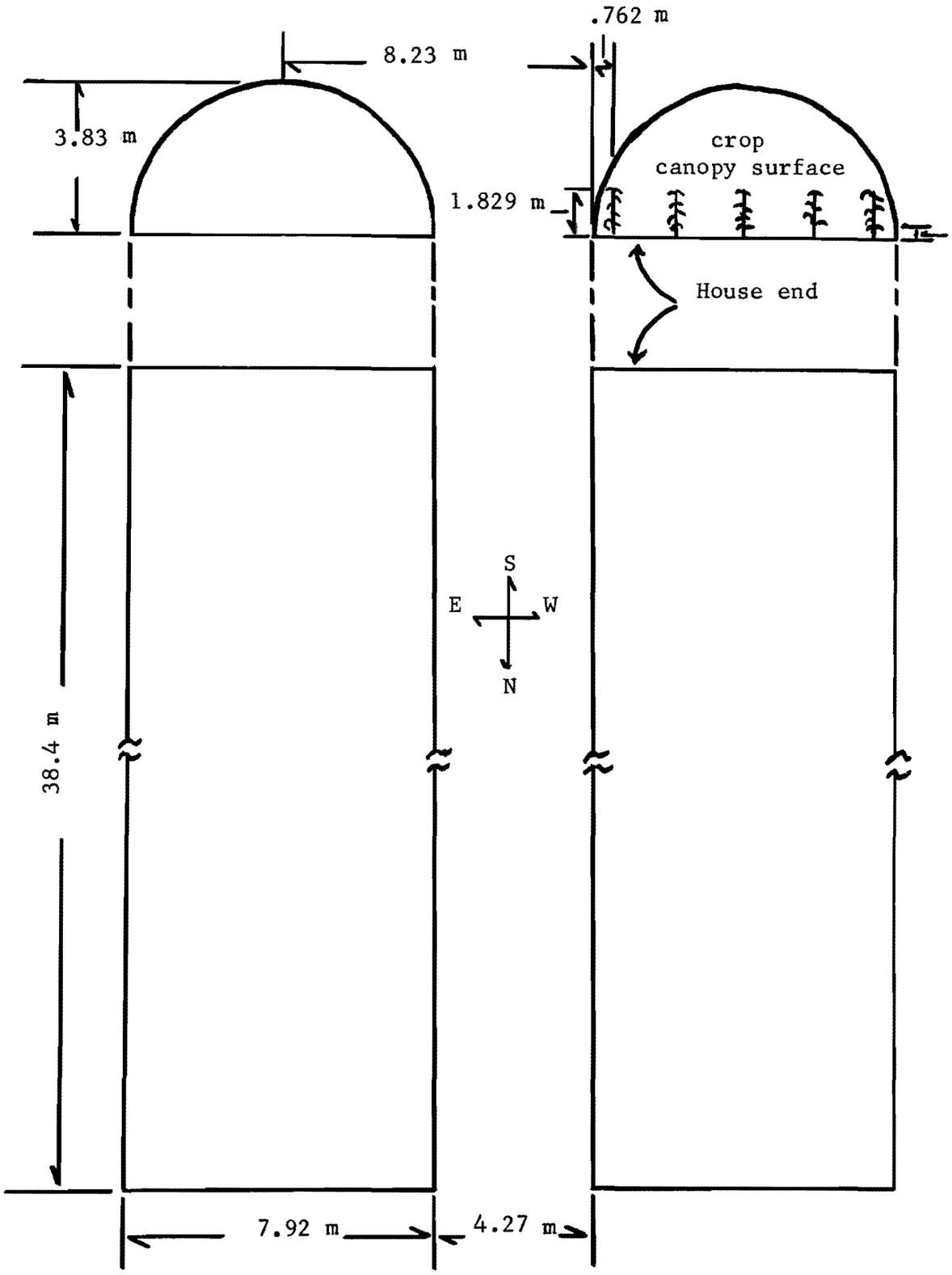

Figure 17. Time of sunrise and sunset at CEVCO (≈93° 11' West) and duration of longest and shortest days of the year.

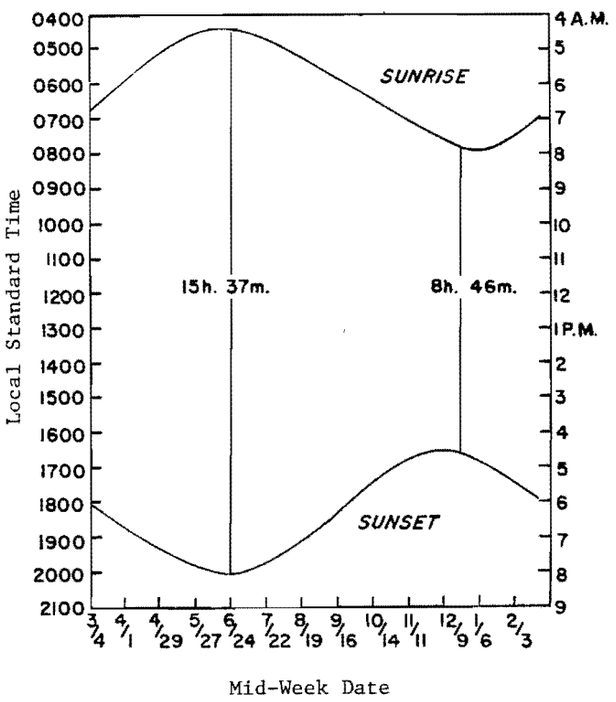

Source: 3, p. 4.

Figure 18. The apparent path of the sun in the sky during selected dates at 45° North latitude.

Solar Altitude and Azimuth

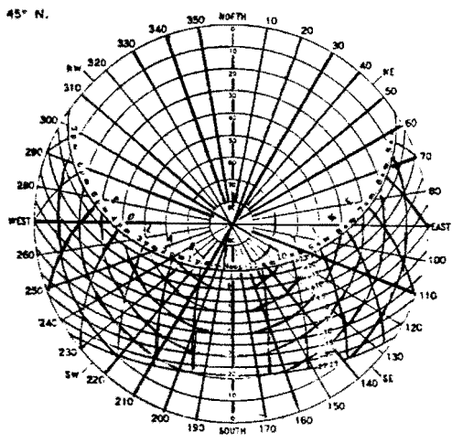

Declination	Approximate dates
+23°27'	June 22
+20°	May 21, July 24
+15°	May 1, August 12
+10°	April 16, August 28
+ 5°	April 3, September 10
0°	March 21, September 23
- 5°	March 8, October 6
-10°	February 23, October 20
-15°	February 9, November 22
-20°	January 21, November 22
-23°27'	December 22

Source: 36, p. 502.

Figure 19. Geometric relationships of direct solar radiation incident upon a N-S oriented vertical plane (i.e., a surrogate for a CEVCO house).

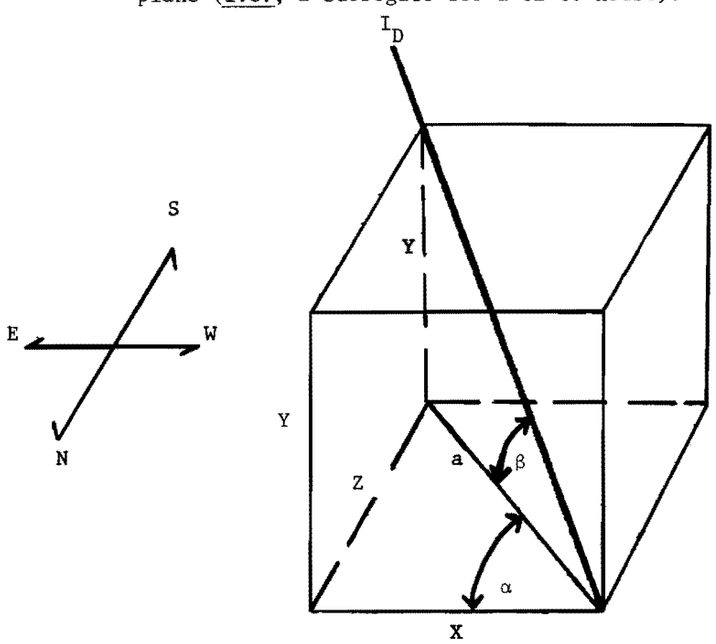

$$a = \frac{Y}{\tan \beta} \qquad \cos \alpha = \frac{X}{a} \qquad X = \frac{Y \cdot \cos \alpha}{\tan \beta}$$

Where:

I_D = incidence of direct solar radiation upon a surface, X = distance between center of shading house and east bed of shaded house, Y = height of house - .5 m, β = solar altitude angle, and α = wall-solar azimuth angle,

$\sin \alpha = \frac{Z}{a}$ and $Z = \frac{Y \cdot \sin \alpha}{\tan \beta}$.

Figure 20. East-West versus North-South house orientation effects upon shading and house spacing on December 22 at 45° N latitude.

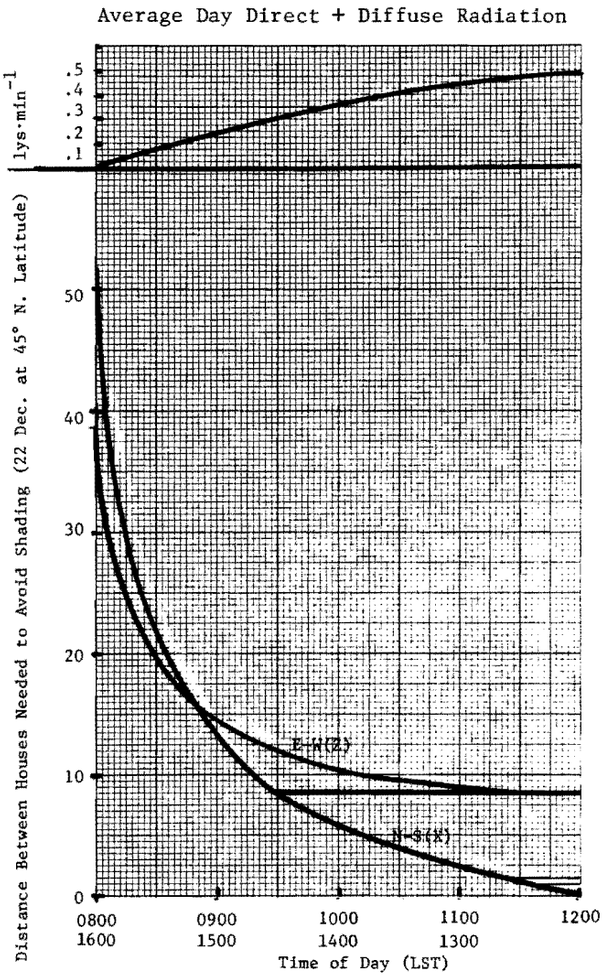

Figure 21. Solar reflectivity for various ground surfaces.

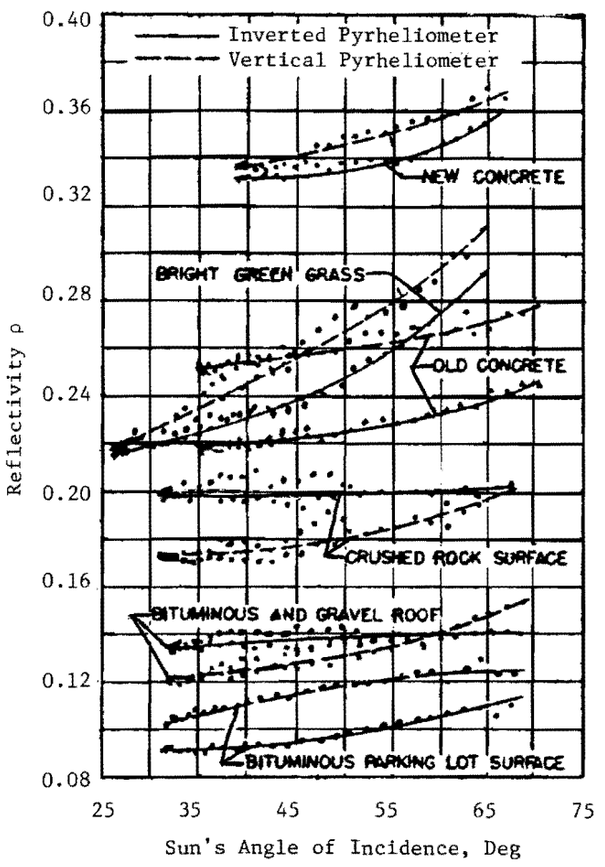

Material	Reflectance in percent)
Asphalt (free from dirt)	7
Earth (moist cultivated)	7
Granolite pavement	17
Grass (dark green)	6
Gravel	13
Macadam	18
Slate (dark clay)	8
Snow	
new	74
old	64
Vegetation (mean)	25

Source: 57, p. 31; 31, p. 7-10.

Figure 22. Relation of a small surface, dA_2, to a diffusely reflecting large surface, A_1.

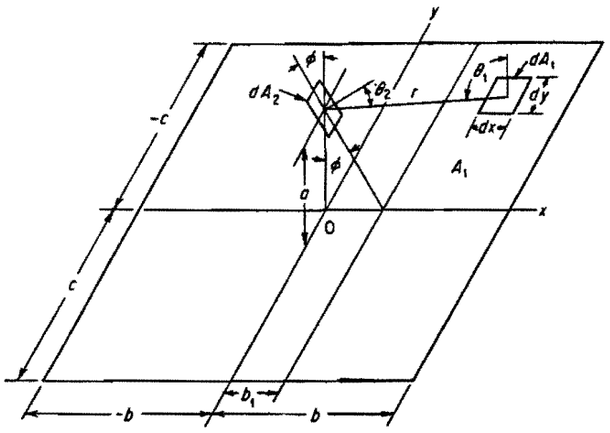

Source: 58, p. 329.

Figure 23. Reflected radiation upon a house from adjacent surfaces.

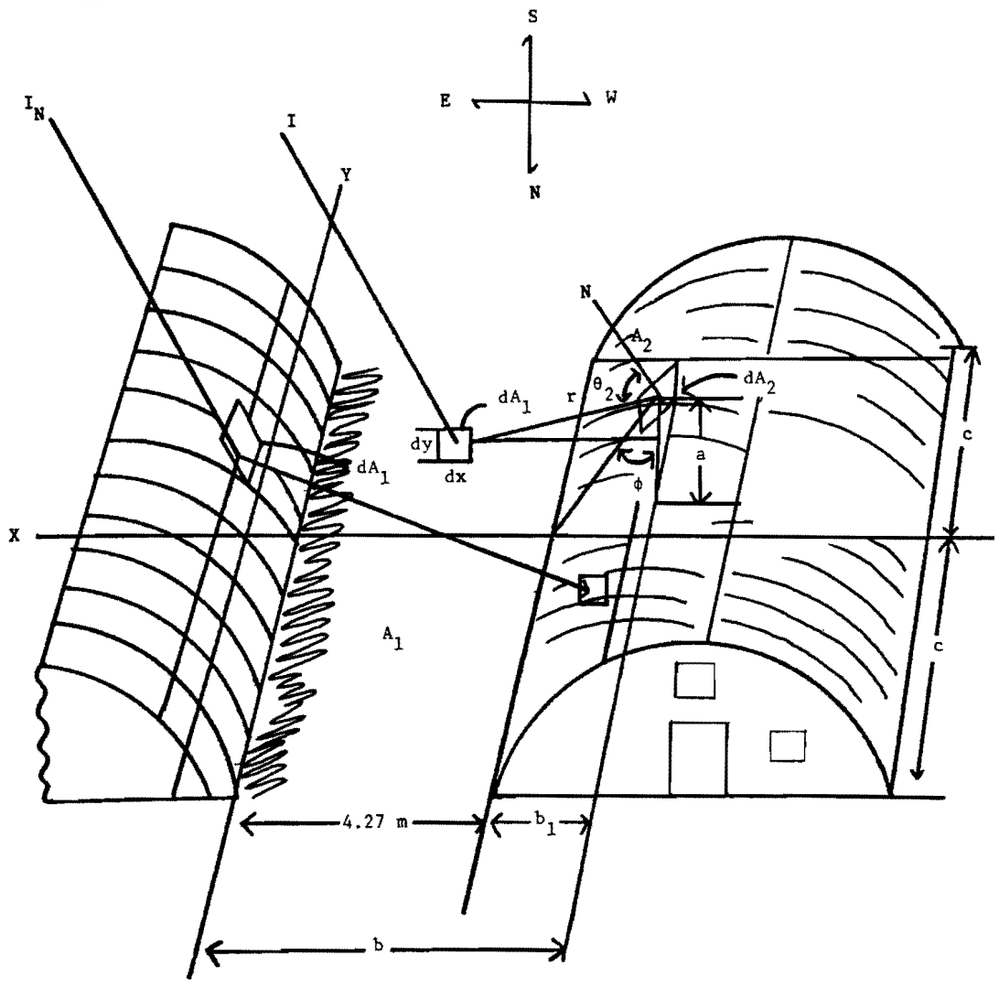

Figure 24. Values of F for values of ϕ on a CEVCO house.

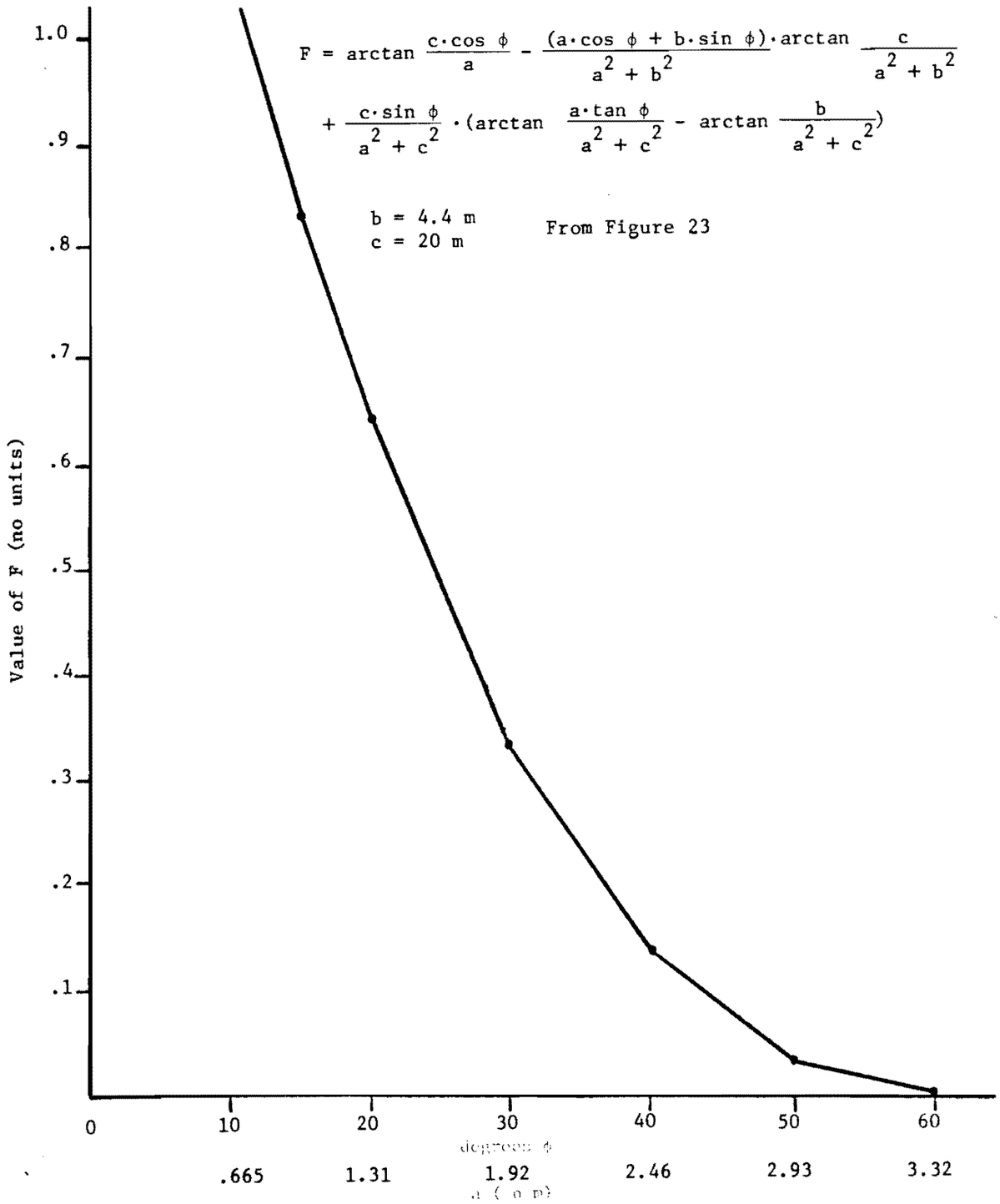

Figure 25. Relationship of I_R from adjacent house cover upon a small area of a CEVCO house cover.

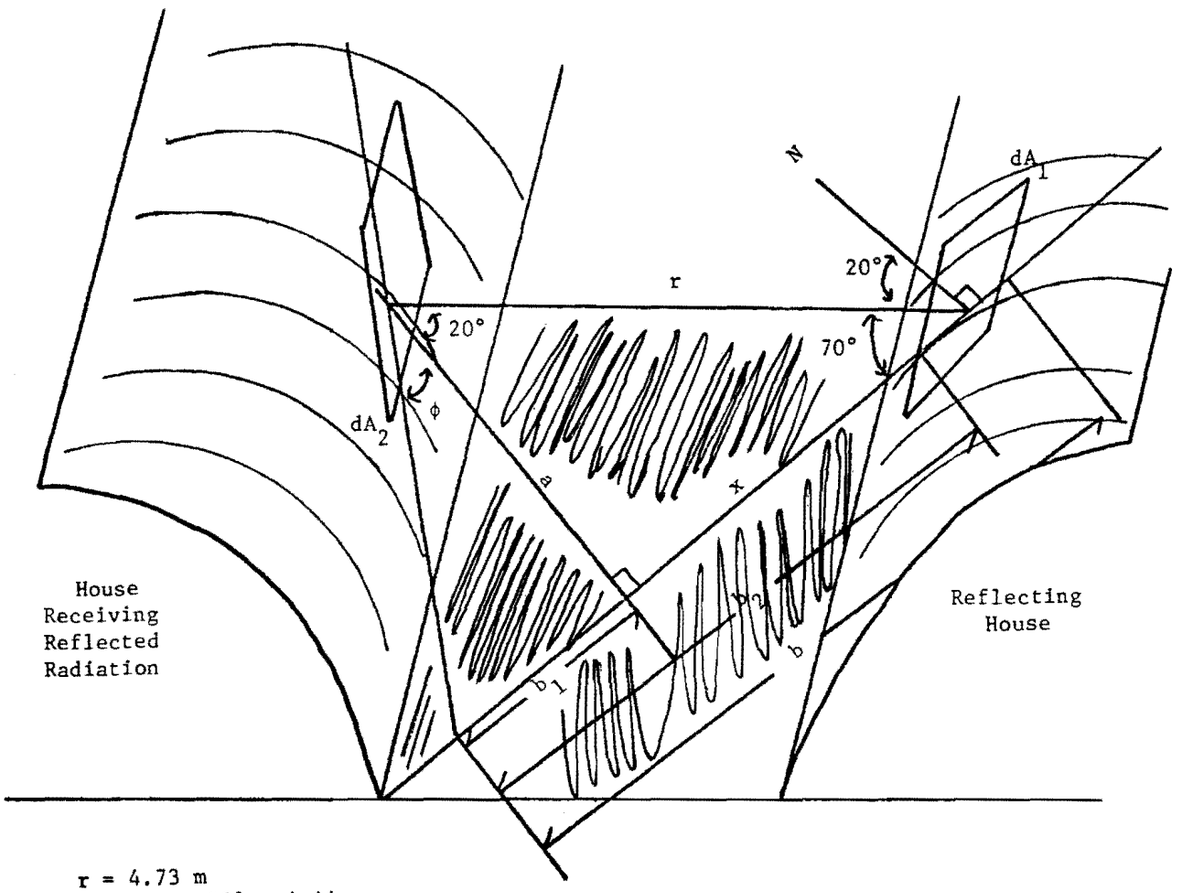

r = 4.73 m
a = r·sin 70° = 4.44 m
x = r·cos 70° = 1.62 m
b_1 = a·tan -50 = -5.29 m
ϕ = -50°
Dimensions of A_1 are:

$b-b_2$ = 3.05 m
c = 19.5 m (see Figure 22)
b_2 = 5.38 m
b = 8.43 m

Figure 26. Relation of a small segment, dA_2, of house cover to large surface, A, between houses.

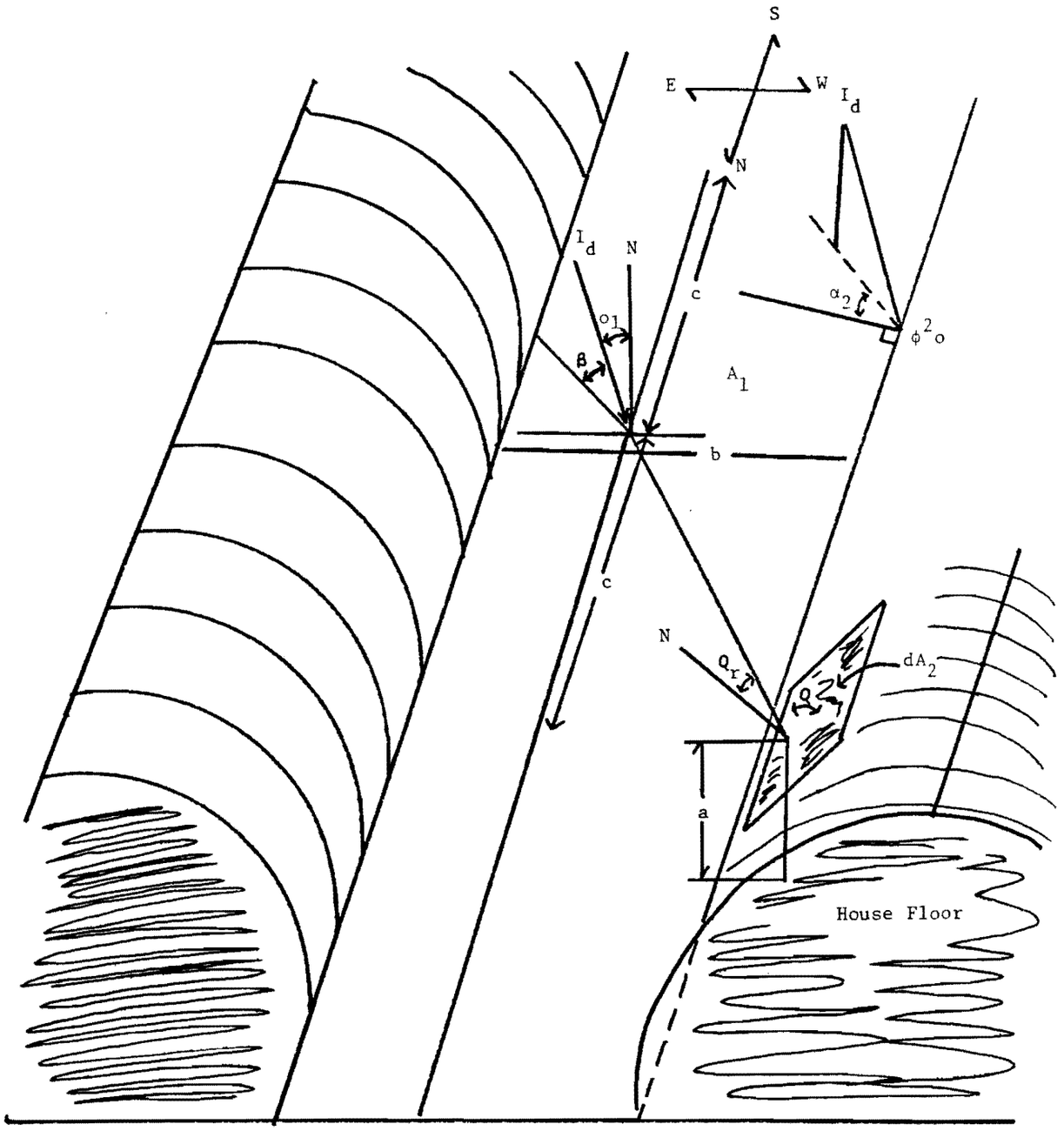

The same relationships exist for an east-west oriented house, except that dimension b changes to match the altered house spacing.

Figure 27. Angles for direct solar radiation striking a CEVCO house.

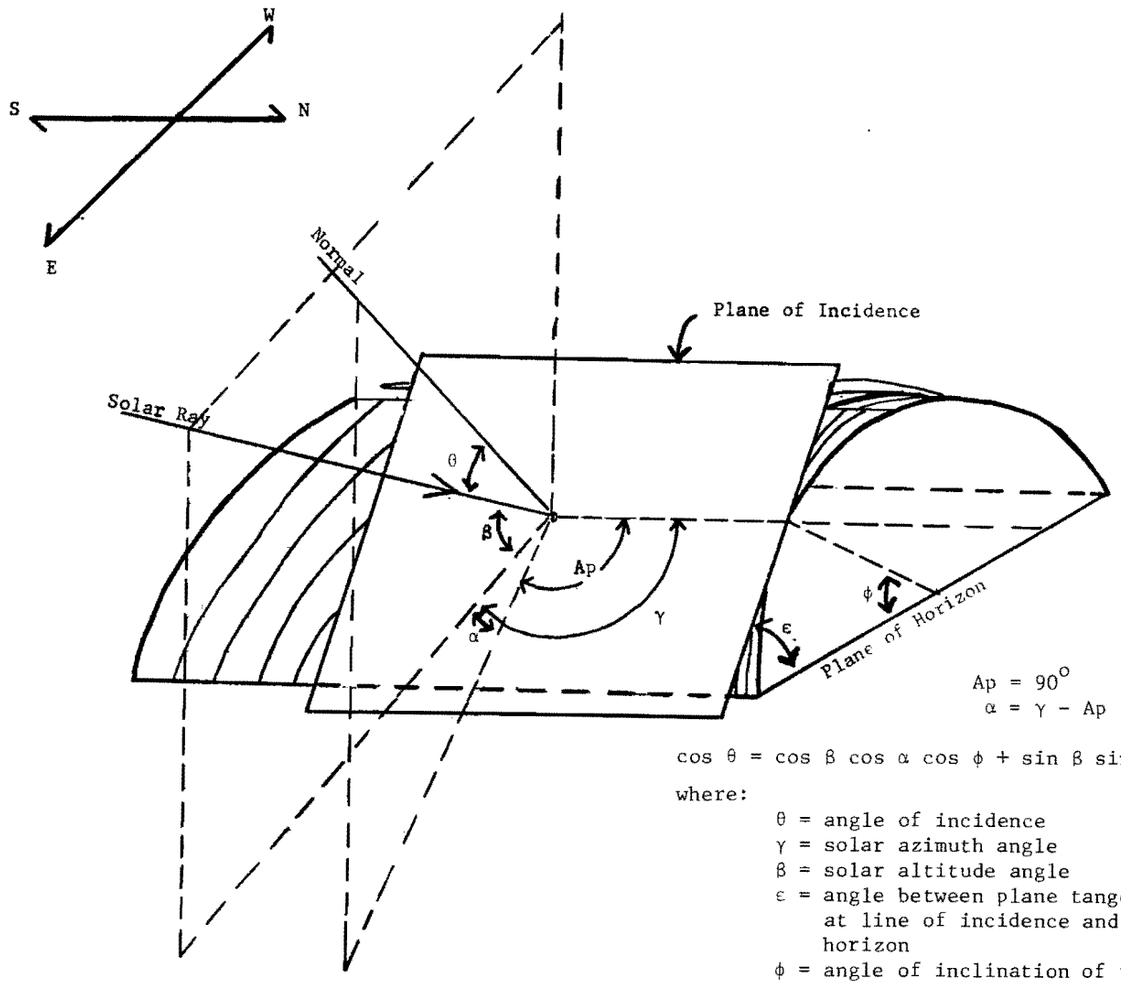

$Ap = 90^{o}$

$\alpha = \gamma - Ap$

$\cos \theta = \cos \beta \cos \alpha \cos \phi + \sin \beta \sin \phi$

where:

θ = angle of incidence
γ = solar azimuth angle
β = solar altitude angle
ε = angle between plane tangent to house at line of incidence and plane of horizon
ϕ = angle of inclination of the plane of incidence from vertical position

Figure 28. Transmittance of outdoor exposed acrylic, modified, general purpose, fiberglass panels.

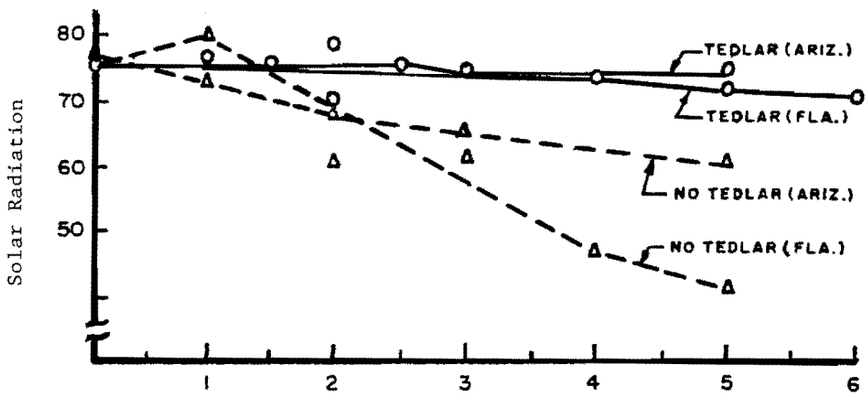

Source: 10, p. 5.

Figure 29. Spectral energy distribution of weathered polyester fiberglass (66 months) when cleaned and refinished.

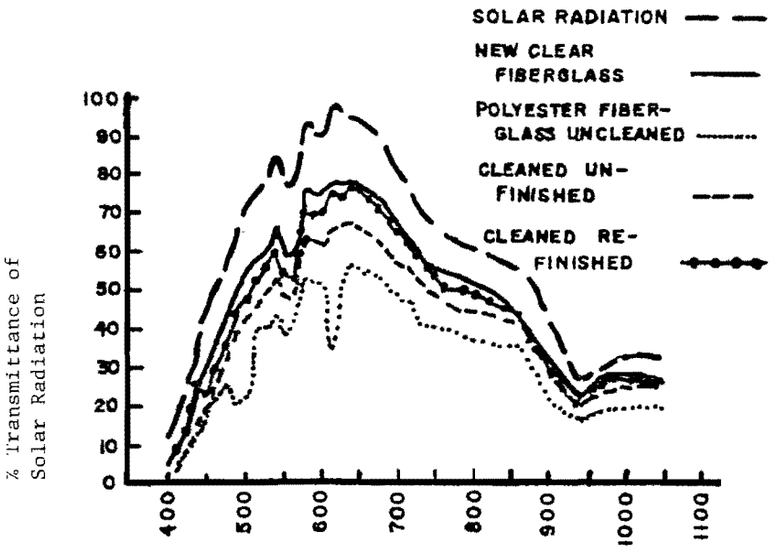

Source: 10, p. 5.

Figure 30. Direct solar irradiation geometry of the west bed of a CEVCO N-S oriented house.

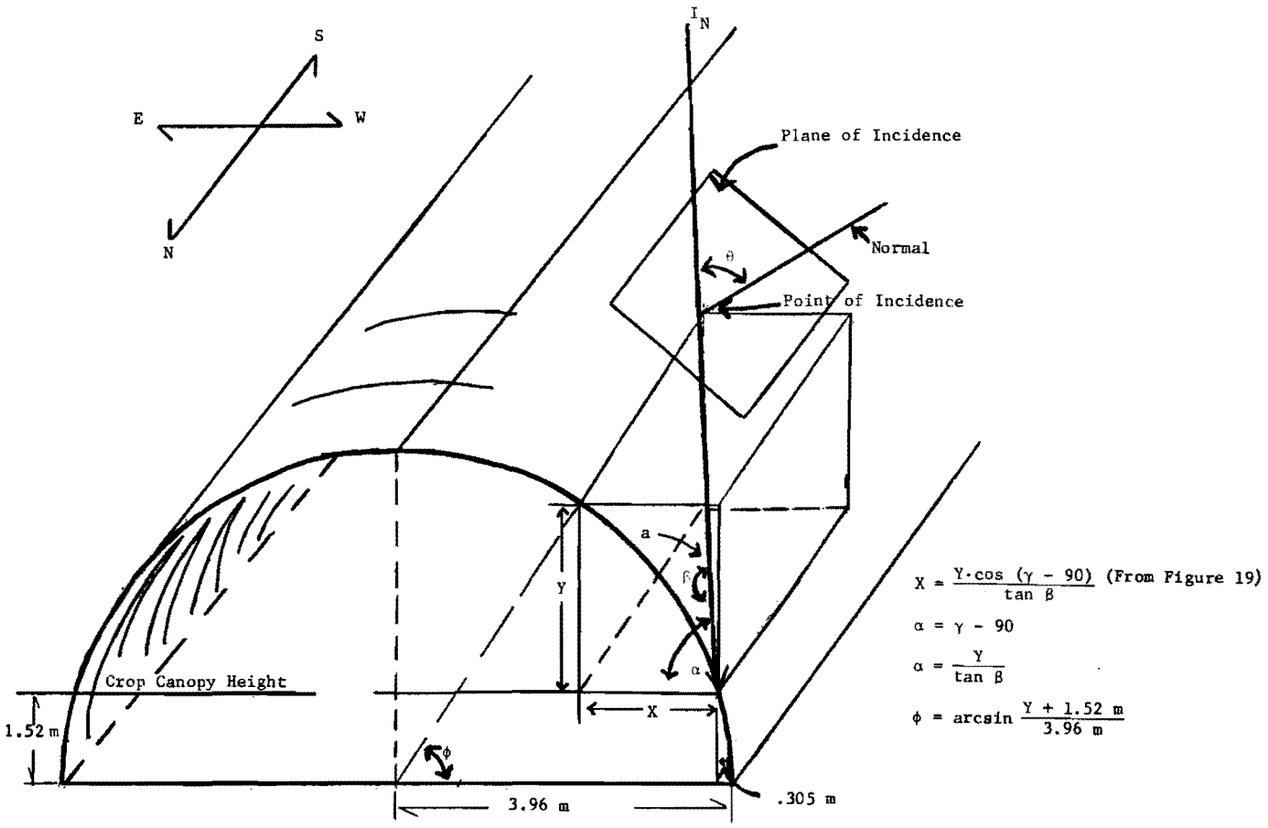

$$X = \frac{Y \cdot \cos(\gamma - 90)}{\tan \beta} \text{ (From Figure 19)}$$

$$\alpha = \gamma - 90$$

$$\alpha = \frac{Y}{\tan \beta}$$

$$\phi = \arcsin \frac{Y + 1.52 \text{ m}}{3.96 \text{ m}}$$

Figure 31. Values and ratio of X and Y fixed by house dimensions.

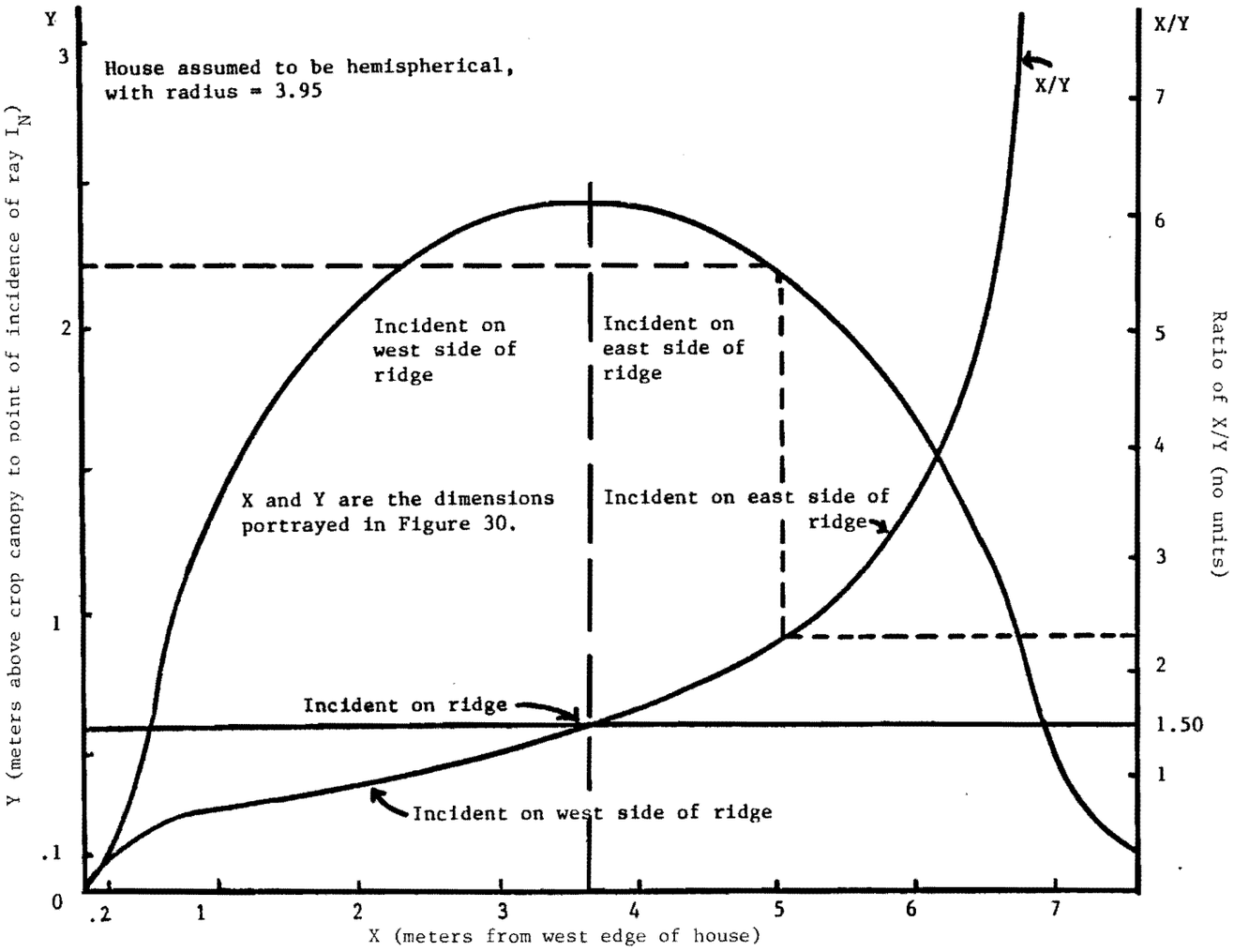

Figure 32. OARDC artificial lighting experiment with tomato cultivar W-R25.

Sown November 13

November 25

Received normal solar irradiation in a greenhouse.
Temperature: 21-24°C day; 16-17°C night.

November 25

Growth chamber using F96T12/CW/VHO + 40 W incandescent lamps on 12 hrs·day^{-1} at 67 W·m^{-2}.
Temperature: 24°C day; 16°C night.

Transplanted 10 January

(1) Received normal solar irradiation for duration of experiment.

(2) From 0300-0800 hours received 215 W·m^{-2} from FR96T12/GRO/VHO/WS for 2 weeks. Received normal solar irradiation each day.

(3) From 0300-0800 hours received 215 W·m^{-2} from FR96T12/GRO/VHO/WS through February 28. Received normal solar irradiation each day.

All plants pulled July 1

Source: 33.

Figure 33. Fluorescent lamp lumen maintenance curves.

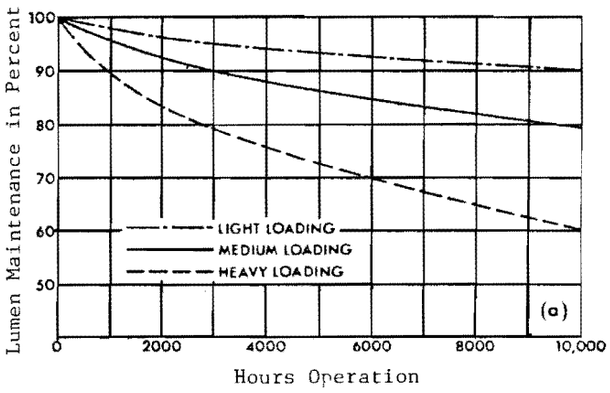

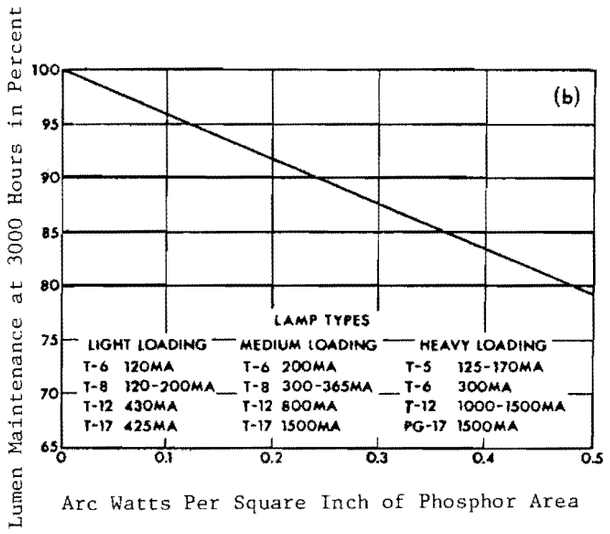

Source: 31, p. 8-25.

Figure 34. Efficacy of typical fluorescent lamps as a function of bulb diameter.

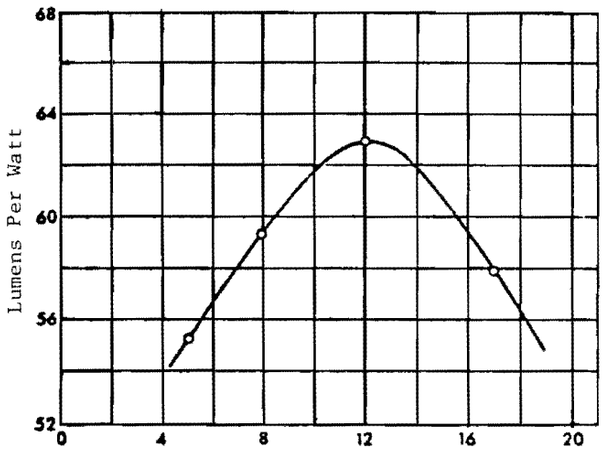

Source: 31, p. 8-23.

Figure 35. Efficacy of typical fluorescent lamps as function of lamp length.

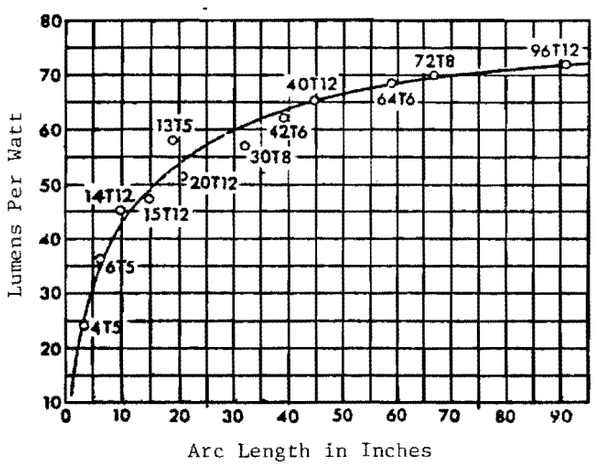

Source: 31, p. 8-23.

Figure 36. The effects of heat upon the light output of fluorescent lamps.

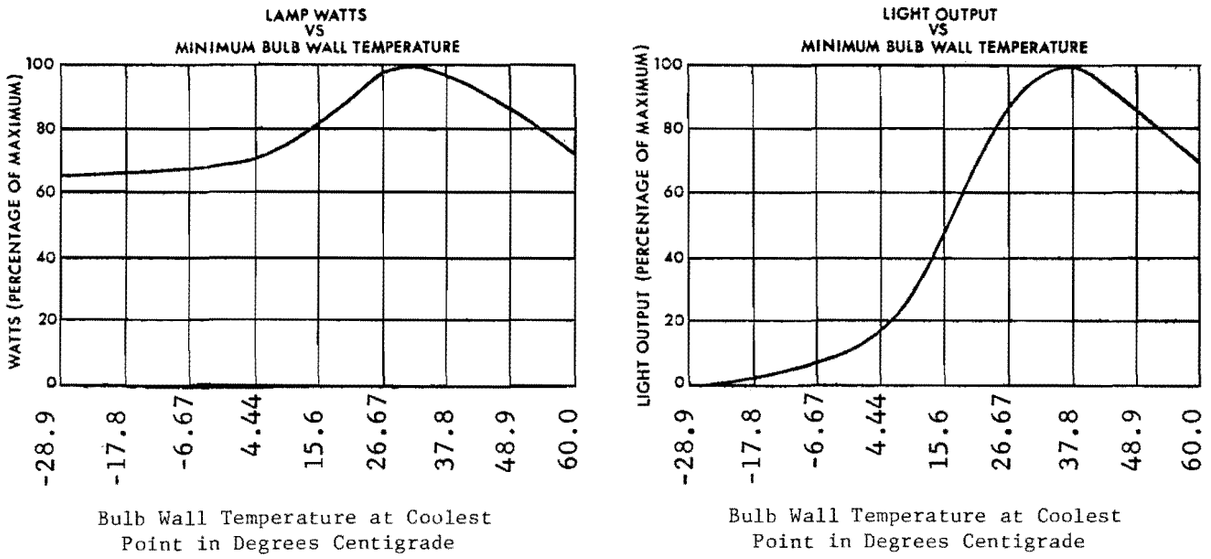

Typical fluorescent lamp temperature characteristics. Exact shape of curves will depend upon lamp and ballast type; however, all fluorescent lamps have curves of the same general shape, since this depends upon mercury vapor pressure.

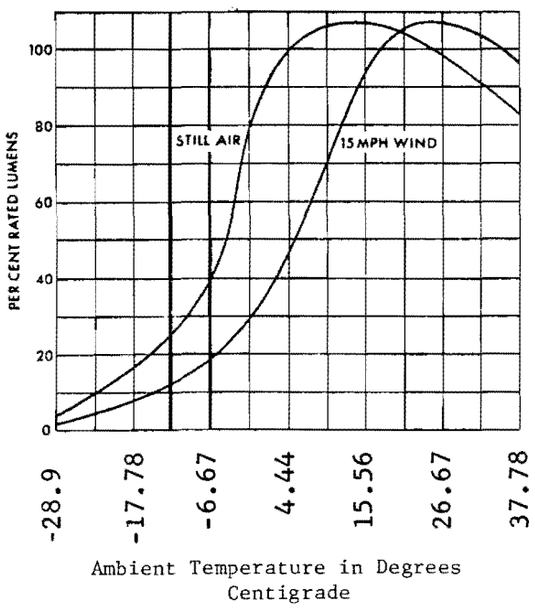

Light output vs. ambient temperature. F96T12/HO fluorescent lamp. Light output falls to low values at temperatures below freezing. Loss in light at high ambient temperatures is much less.

Source: 31, p. 8-26.

Figure 37. Light output versus ambient temperature for open and enclosed fluorescent lamps.

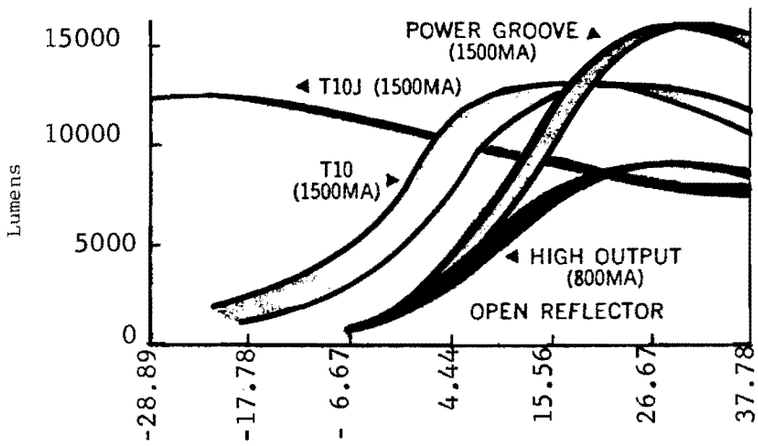

Under the exposed operating conditions of the test, the T10J is the only lamp that maintains output in sub-freezing conditions. The other lamps produce satisfactory results if temperature does not drop below -1°C (T10), 4.4°C (high-output), or 10°C (Power Groove).

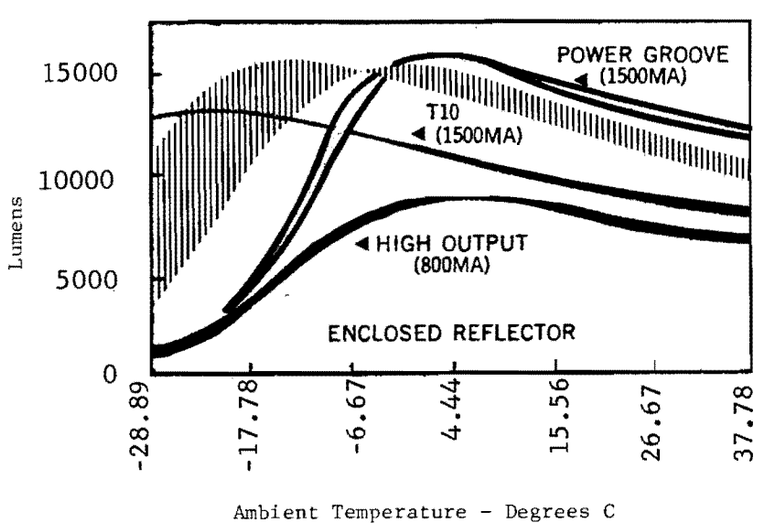

The T10 lamp in an enclosed fixture performs much like the T10J when all fixture openings are sealed. The effect of luminaire design on output is shown by the shaded curve which includes several types of multi-lamp, enclosed units, designed for Power Groove lamps. The general shapes of the curves are the same. Curves shift right or left depending on the degree of protection provided by the luminaire.

Source: 19, p. 19.

Figure 38. Spectral energy distribution curves for typical "white" fluorescent lamps.

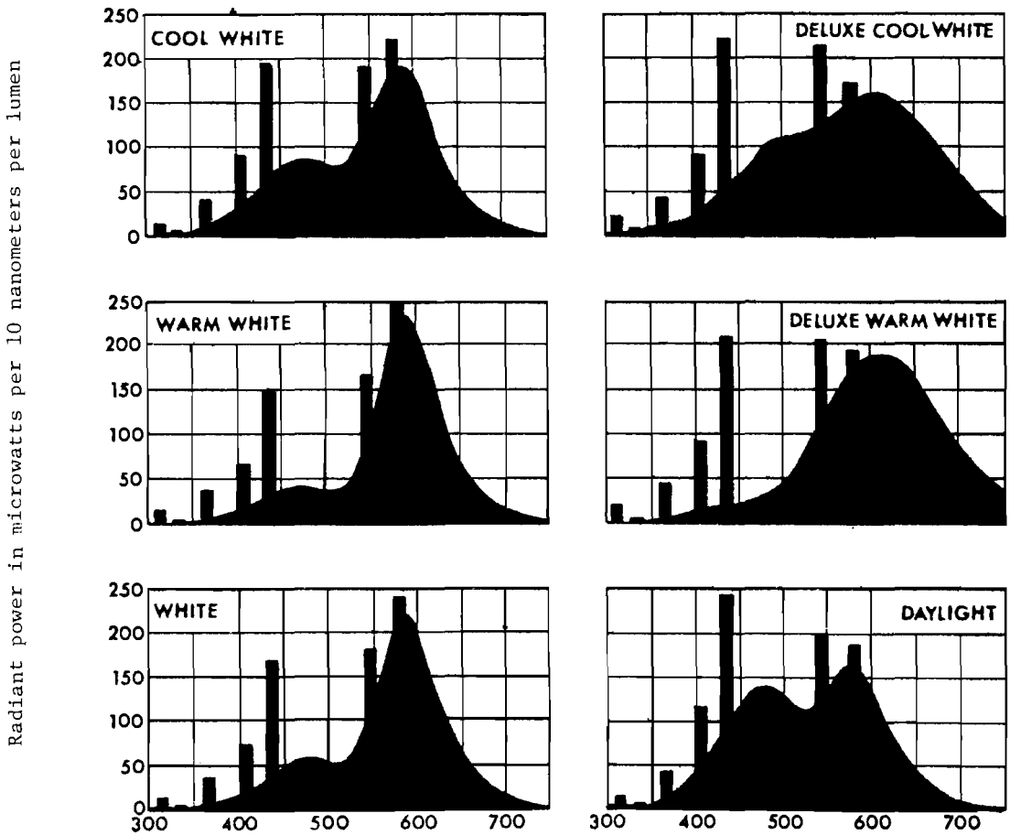

Source: 31, p. 8-19.

Figure 39. Spectral energy distribution curves for fluorescent and incandescent lamps.

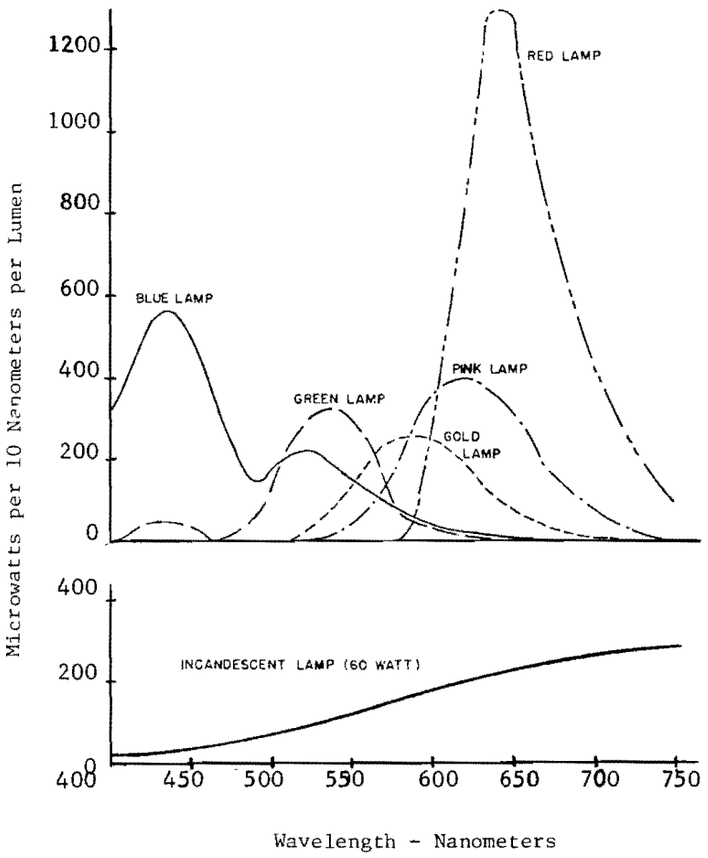

Source: 11, p. 307.

Figure 40. Spectral energy distribution curves for Sylvania Gro-Lux and Gro-Lux wide-spectrum lamps.

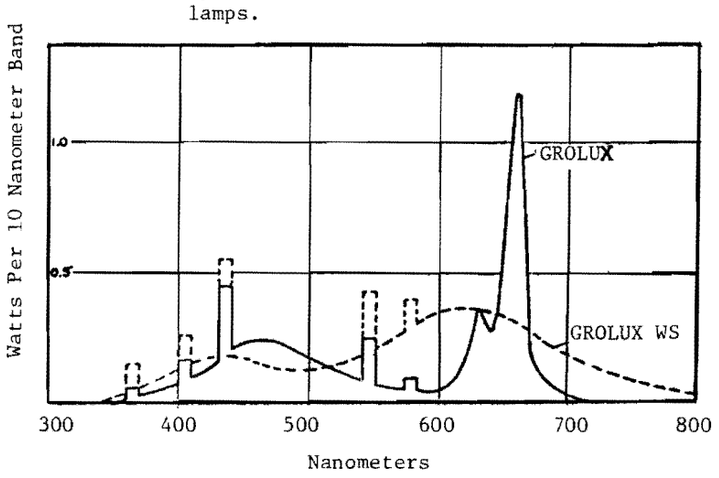

Source: 50, p. 1.

Figure 41. Comparative efficiencies of different categories of lamps.

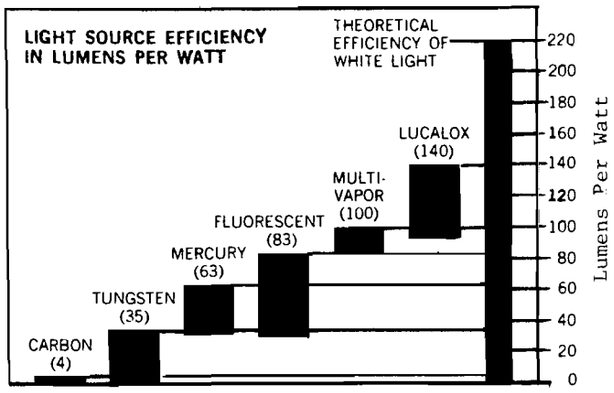

Source: 18, p. 3.

Figure 42. Mercury lamp ballasts: Effect of line voltage on lamp watts.

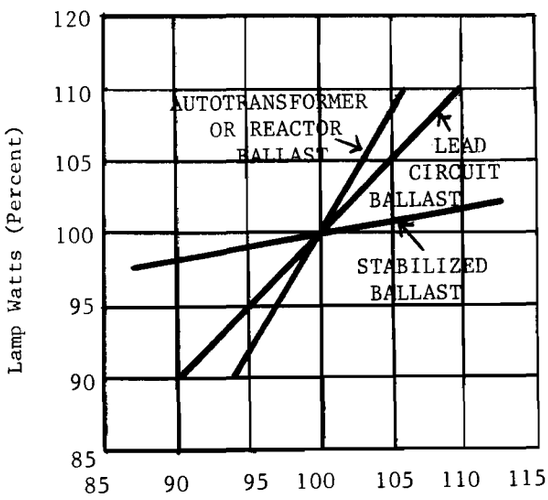

Source: 18, p. 19.

Figure 43. High-pressure sodium ballasts: Effect of line voltage on lamp watts.

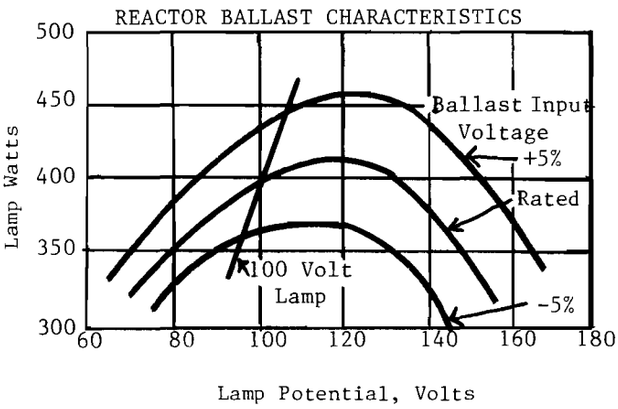

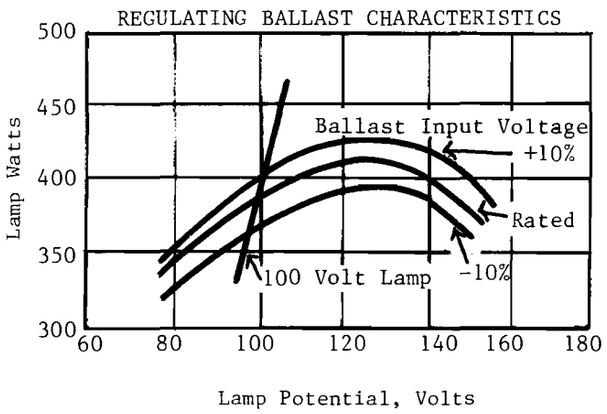

Source: 18, p. 34.

Figure 44. Ambient temperature vs. rated life for integrally ballasted high-intensity discharge lamps.

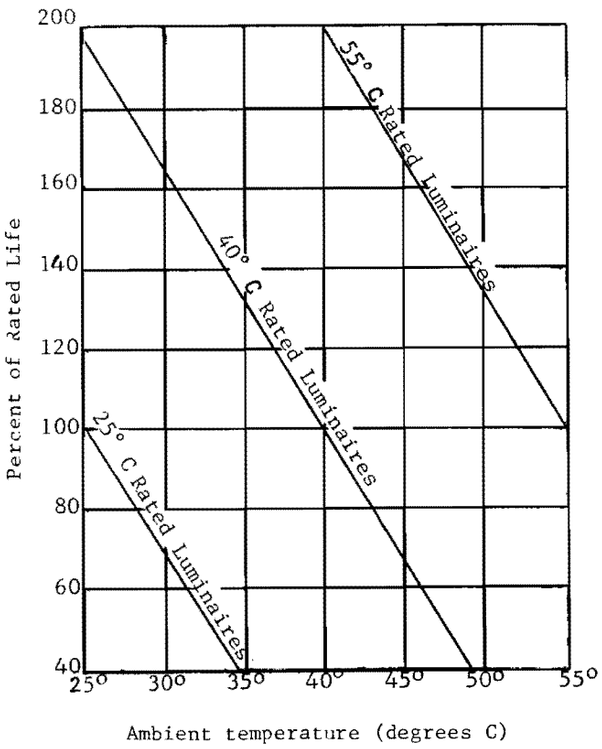

Source: 29, p. 3.

Figure 45.

Mortality Curves of 400-Watt HID Lamps

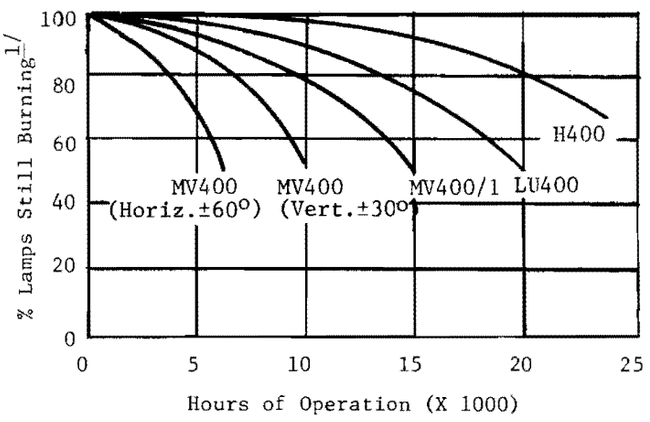

Mortality Curves of 1000-Watt HID Lamps

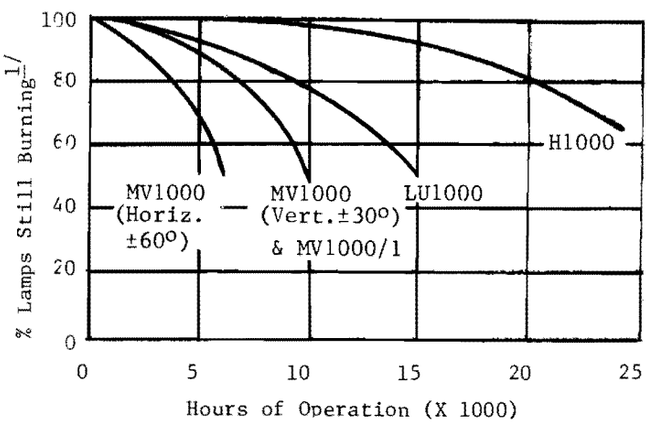

1/ At 10 hours/start

Horizontal operation metal halide lamp life is 6000 hours.

Source: 18, pp. 36-37.

Figure 46.

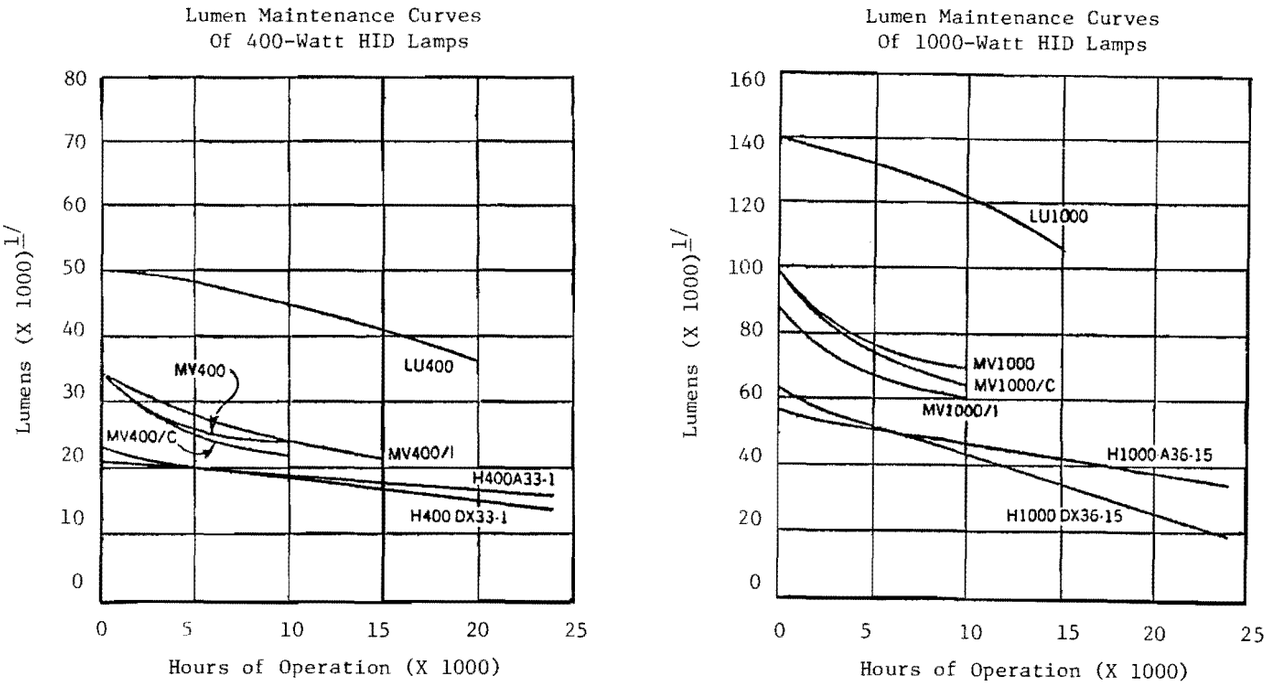

1/ At 10 hours/start

Source: 18, pp. 36-37.

Figure 47. Spectral energy distribution curve for a high-pressure sodium lamp.

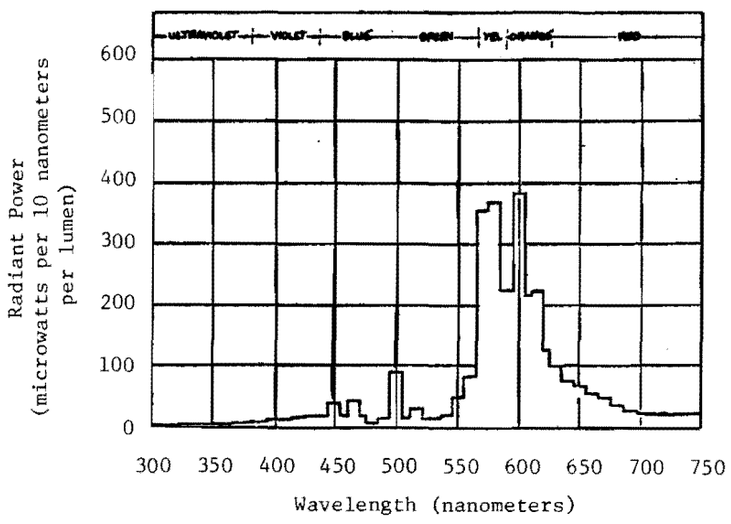

Source: 18, p. 31.

Figure 48. Spectral energy distribution curve for a deluxe white mercury lamp.

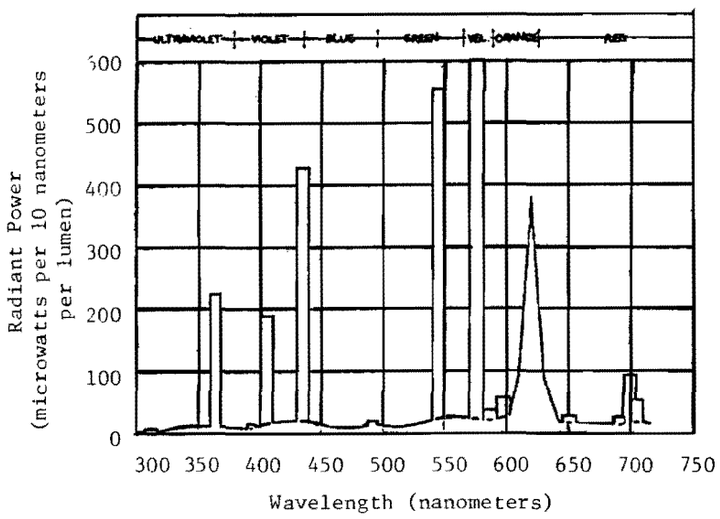

Source: 18, p. 13.

Figure 49. Spectral energy distribution curve for a clear standard metal halide lamp.

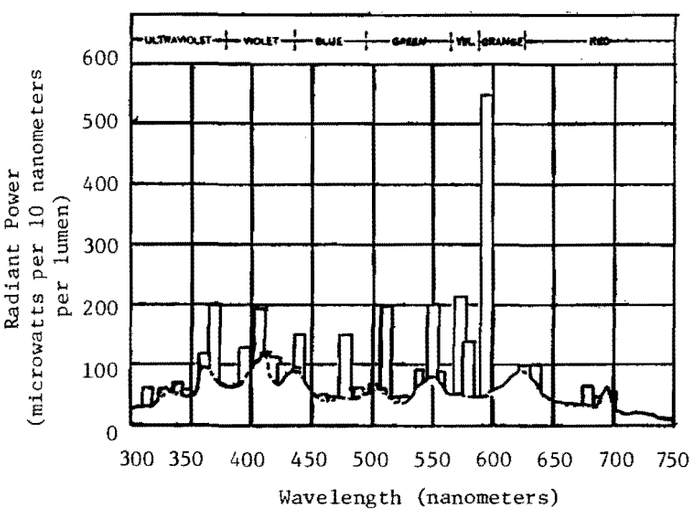

Source: 18, p. 24.

Figure 50. Ceiling and room cavities of a CEVCO house.